Surveillance of patients post endovascular aneurysm repair: How does duplex ultrasound compare with computed tomography (CT)?

Thesis submitted for MD (Res) to Queen Mary, University of London

Under the supervision of

Dr Malcolm Birch

Director of Clinical Physics

Barts Health NHS Trust

Honorary Senior Research Fellow

Queen Mary University of London, and

Mr Constantinos Kyriakides

Consultant Vascular and Endovascular Surgeon

Barts Health NHS Trust,

Honorary Senior Lecturer

Queen Mary University of London

Paritosh Mohan Sharma

MBBS, MRCS

Table of contents

List of figures

List of tables

Declaration

The work presented here, is my independent work under the guidance of Mr Kyriakides and Dr Birch, my supervisors.

Acknowledgements

I would especially like to express my gratitude towards my supervisors Mr Constantinos Kyriakides and Dr Malcolm Birch who have helped me throughout the course of this MD starting from the conception of this project, designing the phantom and of course with the supervision of my thesis. I would also like to thank Mr Mark Brewin, Ms Abigail Thrush and all the members of the clinical physics department who have helped me enormously and especially the engineering staff who devoted their time and expertise in helping with the design and construction of the phantom.

I would also like to acknowledge Ms Helen Dawson, Mr Mustafa Azzam, Ms Bridget Boyle, Ms Jackie Trant and Mr Vish Ramoutar without whose help and support I would not have been able to complete my experiments.

A special word of thanks for my wife Manjeet who has been extremely patient with me during these last few years despite all the difficulties and has helped me finally realise this long cherished dream. You have been a great source of support. Finally, I would like to acknowledge the contribution of my parents and grandparents, for their encouragement and unwavering support over the years.

Also, a word of thanks for my examiners who have helped shape the final version of this thesis with their helpful comments and suggestions.

Abstract

Endovascular aneurysm repair (EVAR) has become increasingly popular over the last few years, but is associated with complications such as endoleaks, graft fracture and migration (Ouriel, Clair et al. 2003), which prompt urgent intervention. This has necessitated lifelong follow up of patients with CT scans at regular intervals, which has significant cost implications and exposes patients to a large radiation dose. Duplex ultrasound has been proposed as an alternative (Henao, Hodge et al. 2006, Sandford, Bown et al. 2006), but substantial variation has been reported in the literature in terms of its sensitivity and specificity for detecting complications.

The aim of this research project was to assess the limitations of duplex ultrasound and to establish whether its sensitivity and specificity in routine clinical imaging for the surveillance of patients post EVAR could be improved to the same level as CT. Novel ultrasound blood and tissue mimicking phantoms were used to assess the limits of ultrasound, and the effects of operator experience, in detecting complications (Ramnarine, Nassiri et al. 1998, Teirlinck, Bezemer et al. 1998, Madsen, Dong et al. 1999, Surry, Austin et al. 2004).

The study was divided into a clinical arm and a laboratory-based arm. The clinical arm compared results from CT and Duplex ultrasound for patients post EVAR. In the laboratory, novel tissue and blood mimicking ultrasound phantoms with known geometry, material and blood flow parameters were used to assess the limitations of duplex ultrasound, independent of the operator. The effect of operator experience on the reliable detection and classification of complications was also assessed. In

addition, machine dependent parameters were studied to optimise the sensitivity of duplex ultrasound in EVAR evaluations.

The results of our laboratory experiments demonstrated that endoleak detection with duplex ultrasound proved more difficult with increasing depth of the endoleak from the viewing position and when the endoleak was in a plane distal to the aortic flow. Our results also demonstrated an increasing trend toward flow detection with increasing flow rates of the endoleak. Our clinical arm corroborated the findings of the laboratory arm with endoleaks that were missed on DUS being identified as slow flow endoleaks located posteriorly and in direct apposition with the stent graft.

Although our results did not unequivocally demonstrate the superiority of DUS compared to CT, there was a clear trend towards diagnosis of all endoleaks that required intervention. Our experiments support the use of DUS for the surveillance of patients post EVAR in a complimentary role to CT, thus reducing the substantial radiation exposure for these patients and the associated cost burden to health providers.

INTRODUCTION

Abdominal aortic aneurysms

An aneurysm is defined as an excessive localized enlargement of an artery, caused by a weakness of its wall, by at least half of its original diameter (Sakalihasan, Limet et al. 2005, Norman S Williams, Bulstrode et al. 2008). They can affect any artery in the human body but the majority are seen in the abdominal aorta.

The aorta is the main artery of the human body that originates from the left ventricle of the heart and terminates by dividing into the common iliac arteries that are responsible for blood supply to the pelvis and legs. Anatomically the aorta is classified into the thoracic and abdominal parts, which as the names suggest, are present in the chest and abdominal cavities respectively. The thoracic aorta is further classified into the ascending aorta, the arch of the aorta and the descending aorta.

The abdominal aorta supplies blood to the abdominal organs and is the predominant artery to be affected by aneurysm formation. Abdominal aortic aneurysms are traditionally classified according to their anatomical relationship with the origin of the renal arteries into supra renal, juxta renal and infra renal varieties. Supra and infra renal aneurysms affect parts of the aorta above and below the origins of the renal arteries, whilst juxta renal aneurysms involve the origins of the renal arteries. Most abdominal aortic aneurysms are infra renal and usually terminate proximal to the aortic bifurcation into the common iliac arteries.

Aneurysms have also been classified as follows (Norman S Williams, Bulstrode et al. 2008)

a. True and False: True aneurysms involve all the three layers of the arterial wall namely intima, media and adventitia. False aneurysms are predominantly traumatic in origin and do not involve all the layers of the arterial wall.
b. Congenital or acquired: Berry aneurysms affecting the intracranial circulation are inherited aneurysms, though they usually manifest in adult life.
c. Based on aetiology: Aneurysms have been divided into atherosclerotic, mycotic, syphilitic, inflammatory, traumatic and congenital. Atherosclerosis is thought to be the underlying process in most aneurysms. Mycotic aneurysms occur as a consequence of an infective process leading to the destruction of the arterial wall. Tertiary syphilis is associated with thoracic and abdominal aneurysms. Inflammatory aneurysms are a distinct entity and are so named due to the presence of an intense peri-aortic inflammatory response.
d. Based on anatomical location: Aneurysms can be classified on the basis of their anatomic location into intra-cranial, thoracic, abdominal or peripheral aneurysms.
e. Based on morphology: Aneurysms can also be classified according to their shape into the more common fusiform type, which have a uniform shape with symmetrical and circumferential involvement of the aortic wall, or the saccular type that are more localised dilatations and appear as an out pouching of only a portion of the arterial wall. Dissecting aneurysms occur as a result of deficiency of the arterial media as occurs in syphilis, Marfan's syndrome and Erdheim's cystic medial necrosis.

Pathophysiology

Aortic walls are made up of concentric layers of smooth muscle cells and the proteins elastin and collagen. Together, these elements are responsible for the visco-elastic properties of the arterial wall. Remodelling is a process by which tissues continually regenerate; older tissue components are replaced by newer ones. In normal aortic tissue, remodelling is a result of a balance between proteolytic enzymes such as metalloproteinases, cathepsins, chymase and tryptase; and their inhibitors such as tissue inhibitors of metalloproteinases (TIMP).

Aneurysm formation is a complex process that involves destructive remodelling of aortic tissues throughout the affected segment of the aorta. Aneurysms are characterised by increased local production of proteolytic enzymes and reduced expression of their inhibitors, thus causing degradation of elastin and collagen in the media and the adventitia of vessel walls. This is also accompanied by the loss of medial smooth muscle cells, thinning of vessel walls and transmural infiltration by lymphocytes and macrophages.

The exact mechanisms of aneurysm formation are still poorly understood, however, the recruitment of inflammatory cells into the adventitial and medial layers of the aortic wall is thought to be an early step in their development. The trigger for this influx of inflammatory cells is as yet unknown. It has been postulated that molecular mimicry might play a role in this initial lymphomonoytic response (Hirose and Tilson 2001). Various factors such as vascular injury, elastin degradation and infections particularly with organisms such as Chlamydia pneumonia have been implicated in bringing about the inflammatory influx (Kuivaniemi, Platsoucas et al. 2008).

Recruitment of inflammatory cells is associated with increased levels of cytokines and interleukins that are responsible for the activation of proteolytic enzymes and reduced expression of their inhibitors. Cells within the inflammatory exudate have also been recognised to produce Fas ligand and Fas associated phosphatase-1 (FAP-1). Within aneurysmal aortic tissue, Fas and FAP-1 have been associated with the regulation of apoptosis of vascular smooth muscle cells and other lymphocytes. Apoptosis of these cells is thought to contribute to aneurysm formation (Hirose and Tilson 2001, Curci and Thompson 2004, Lindholt and Shi 2006). Fas ligand is a transmembrane protein that is thought to regulate apoptosis of medial smooth muscle cells. FAP-1 is a tyrosine phosphatase that interacts with the cytosolic pool of Fas. Expression of FAP-1 has been postulated to be coexistent with attenuation of Fas export to the cell surface and subsequent reduction in Fas related cytotoxicity (Ivanov, Lopez Bergami et al. 2003).

Imbalances in remodelling bring about proteolytic fragmentation of elastic fibres and a progressive loss in the concentration of elastin in the media of vessel walls until rupture. In the absence of elastic fibres, the adventitia with predominant collagen is responsible for aortic vessel resistance. It has been postulated that collagen degradation is the ultimate cause of aneurysm rupture (Dobrin and Mrkvicka 1994).

Atherosclerosis and abdominal aortic aneurysms

The aneurysmal aorta is usually associated with the presence of atherosclerotic changes. Atherosclerotic plaques have been associated with medial thinning and compensatory arterial enlargement. It has been postulated that segments of the

abdominal aorta afflicted with atherosclerotic plaques may predispose to aneurysm formation. Traditionally, aneurysmal change has been regarded as a consequence of atherosclerosis. However, this association has been challenged in recent years. A second theory suggests that the development of AAA and atherosclerosis is independent. Some recent authors have postulated that both AAA and atherosclerosis might develop individually but may stimulate the development of the other. Other studies have suggested that both occlusive and aneurysmal disease may have similar origins but the natural progression is divergent (Golledge and Norman 2010, Johnsen, Forsdahl et al. 2010).

It is still poorly understood as to why atherosclerotic plaques lead to aneurysmal change in certain individuals and occlusive disease in others. Autopsy studies have demonstrated that the abdominal aortic diameter increases with increasing atherosclerotic plaque, that is in turn associated with medial thinning and loss of native aortic architecture. Xu et al (Xu, Zarins et al. 2001) suggested that a balance between plaque stability and progression might decide upon which path the aorta takes – occlusive or aneurysmal. In cases where plaques demonstrate repeated progression and erosion, the consequential wall thinning renders the aortic wall incapable of sustaining wall stresses and resulting in aneurysmal dilatation. In cases of stable plaques however, the result is occlusive disease.

Epidemiology and Risk Factors

Abdominal aortic aneurysms affect 4-10% of people older than 60 years of age (Hellmann, Grand et al. 2007). The prevalence of these aneurysms increases with age and varies between 1.3 – 8.9% in men and 1 – 2.2% in women.

Age

The prevalence of abdominal aortic aneurysms tends to increase with increasing age. Most studies describe a sharp rise in the prevalence of AAA's after the age of 60. Under the age of 60, its prevalence is thought to be of the order of 1%, and above the age of 80 this appears to plateau.

Sex

Abdominal aortic aneurysms are three to four times more common in men as compared to women. In women, these aneurysms are associated with a far worse prognosis than men. The UK small aneurysm trial reported a 4-fold higher incidence of rupture in women compared to men (2002). Also, ruptures tend to occur at a smaller aneurysm diameter in women than in men.

Race

Evidence to date suggests that Abdominal Aortic Aneurysms tend to affect the Northern European and North American population more than Asians or Africans (Blanchard 1999).

Smoking

By far the strongest association of abdominal aortic aneurysms is with smoking. The relative risk for current smokers is at least 2. Also, the association of ever smoking with AA is 2.5 times greater than for Coronary Artery Disease (CAD). Continued

smoking has also been associated with increased AAA expansion, increased rupture rates and generally a worse prognosis (Blanchard 1999).

Family History

Approximately 1% to 5% of patients with abdominal aortic aneurysms have a positive family history. Patients with a family history of abdominal aortic aneurysms have also been related to a higher risk of aneurysm rupture (Sakalihasan, Limet et al. 2005).

Hypercholesterolemia

Elevated serum cholesterol levels were found to be associated with the presence of AAAs in several studies (Blanchard 1999, Sakalihasan, Limet et al. 2005). This has been explained as a connection with atherosclerosis, although some studies do suggest a direct inflammatory effect.

Hypertension

Hypertension has been shown to have a weak association with the presence of AAA's (Sakalihasan, Limet et al. 2005).

Natural History

The vast majority of patients affected by abdominal aortic aneurysms remain asymptomatic, most patients being diagnosed either incidentally or by aneurysm screening programmes. Symptoms that have been attributed to the presence of abdominal aortic aneurysms include low back pain and chronic vague abdominal pain. Some patients can present with complications such as distal embolisation, aorto-enteric or aorto-caval fistulation, and symptoms of compression of abdominal viscera or with rupture of the aneurysm.

Aneurysm rupture carries a high risk of mortality. Despite improvement in surgical mortality rates for elective abdominal aortic aneurysm repair, the operative mortality rates for ruptured AAA's has remained high. The operative mortality rates for ruptured abdominal aortic aneurysms have been quoted at approximately 50% (Bown, Sutton et al. 2002), although both the incidence of ruptured AAA (Anjum, von Allmen et al. 2012) and operative mortality (Bown, Sutton et al. 2002) have been declining over the years. Combined pre-hospital and operative mortality rates from ruptured AAA's approaches 80%. The risk of aneurysm rupture is directly proportional to the size of the aneurysm. Aneurysms < 4 cm in size carry an annual rupture risk of 0.3%, those between 4.0 and 4.9 cm aneurysm are associated with a 1.5% annual risk of rupture, those with a 5.0 to 5.9 cm aneurysm carry an annual rupture risk of 3%. The annual risk of rupture approaches 25% for aneurysms greater than 8 cm in size. Heavy smokers, patients on steroids for COPD, patients with poorly controlled hypertension; those with a strong family history of aneurysms and those with very eccentric shaped aneurysms are also at an increased risk of rupture (Lederle, Nelson et al. 2003, Sakalihasan, Limet et al. 2005).

Rapid expansion of aneurysms is thought to precede rupture and has been observed in aneurysms independent of their initial size. Factors other than aneurysm size, thus, have also been thought to be responsible for rupture. Increasing serum levels of MMP-9, α1-antitrypsin and avid FDG uptake on PET scanning have been suggested as tools by some authors to predict aneurysm rupture (Sakalihasan, Limet et al. 2005).

Aneurysm growth rates vary between 0.3 and 0.57 cm per year. Large aneurysms (>5 cm in size) grow more rapidly than smaller ones. Current guidance advises surgical repair in patients with an aneurysm size greater than 5.5 cm or those with an expansion rate of more than 1 cm/year.

Investigators have assessed the risk benefit ratio of intervention for small sized aneurysms. The UK small aneurysm trial (The UK small aneurysm trial participants 1998) randomly assigned 1090 patients with asymptomatic, infra renal abdominal aortic aneurysms 4 - 5.5 cm in size, to either on-going surveillance or early elective open surgery. Their results did not reveal any overall survival advantage in patients undergoing early surgery as opposed to being on ultrasonic surveillance. Similar results were also obtained by the North American ADAM trial (Lederle, Wilson et al. 2002) that randomised 1136 patients with aneurysms 4 - 5.5 cm in size to surveillance or surgery. There was no reported difference in the primary outcome measure of all cause mortality between the two groups. These studies were responsible for the accepted current practice suggesting operative intervention for suitable patients with aneurysms of 5.5 cm and above or with expansion rates of more than 1 cm/year.

The inflammatory abdominal aortic aneurysm

Approximately 3-10% of patients with abdominal aortic aneurysms have been identified as being afflicted with the inflammatory variety. This distinct category was first identified by Walker et al in 1972 (Walker, Bloor et al. 1972). These aneurysms are characterised by three pathologic features: (1) a thickened aneurysm wall, (2) periaortic and retroperitoneal fibrosis, and (3) extensive adhesions involving adjacent structures. The expansion of the aneurysm wall is predominantly noted to be in the adventitia of the aortic wall. This expansion is secondary to an extensive inflammatory reaction brought about by plasma cells, lymphocytes, macrophages and up regulation of inflammatory cytokines including interleukins 2, 4, 1α and adhesion molecules. The periaortic fibrosis associated with inflammatory aortic aneurysms tends to involve the anterior and lateral walls of the aneurysm; the posterior wall is usually spared. This feature of inflammatory aneurysms helps to distinguish them from other causes of retroperitoneal fibrosis such as bladder malignancies.

The association of smoking and male sex, risk factors for abdominal aortic aneurysms, is even stronger for inflammatory abdominal aortic aneurysms (Pennell, Hollier et al. 1985, Hellmann, Grand et al. 2007, Palmisano and Vaglio 2009). There appears to be a stronger familial clustering but the risk of rupture associated with these aneurysms appears to be less than for the non-inflammatory variety (Hellmann, Grand et al. 2007). Patients with these aneurysms also tend to be younger and usually are symptomatic with back and abdominal pain.

Some authors have reported on the non-operative management of inflammatory abdominal aortic aneurysms with corticosteroids or immunosuppressant agents such as methotrexate, cyclophosphamide and azathioprine (Hellmann, Grand et al. 2007,

Palmisano and Vaglio 2009). However there is generalised agreement in that these approaches do not alter the long-term progression and risk of rupture of this variety of aneurysms. Surgical management of these aneurysms is the same that of the non-inflammatory type; repair being recommended when ≥5.5 cm in size.

Operative options

Surgery has been the mainstay of treatment of aneurysms. Options available for surgical repair of abdominal aortic aneurysms include

1. Conventional open repair
2. Endovascular repair
3. Laparoscopic repair

Open surgery involves replacement of the aneurysmal segment of the aorta with a synthetic graft utilising either a midline/transverse laparotomy or a retroperitoneal approach. The choice of graft used (either a straight graft or a trouser graft) depends upon the involvement of the iliac arteries with the aneurysm. In cases where the aneurysm involves the iliac arteries, a bifurcated (trouser) graft may be used; the waist of the graft being suture to the aorta proximal to the origin of the aneurysm and the trouser ends being sutured to the iliac arteries. If the aneurysm does not involve the iliac arteries, a straight graft can be used, replacing the aneurysmal segment of the aorta.

Abdominal aneurysm repair is a major surgical undertaking, associated with a 2-5% mortality rate. Other significant complications associated with open surgery include chest infection, myocardial infarction, renal failure, bowel ischemia, bowel obstruction, incisional hernias, limb ischemia, amputation, wound infections and paraesthesia.

Endovascular and laparoscopic aneurysm repair are minimally invasive alternatives to open surgery. Endovascular repair involves insertion of a stent-graft across the

aneurysm from within. This excludes the aneurysm from the circulation. The aneurysm is accessed though the common femoral arteries either through groin incisions or percutaneously. A stent-graft is then deployed across the aneurysm, excluding it from the circulation. In cases where the femoral or iliac arterial diameter is too small to introduce the stent-graft, a surgical conduit fashioned on to the iliac artery may be used to deploy the device. This conduit is usually sutured onto either the common or external iliac artery utilising a retroperitoneal approach. As described subsequently, not all patients though, would be suitable for endovascular repair. The anatomy of the aneurysm neck is the most important determinant of suitability for EVAR.

Laparoscopic repair involves the replacement of the aneurysmal aorta with either a tube or bifurcated graft using either hand-assisted laparoscopic surgery (HALS) or total laparoscopic surgery (TLS). For HALS, apart from small incisions for the laparoscope and instruments, a mini midline laparotomy wound is used to assist the repair, whereas for TLS the whole repair is achieved laparoscopically.

Endovascular and laparoscopic repair are associated with reduced in-patient length of stay and recent trials have reported similar or better results compared to open surgery (EVAR trial participants 2005, EVAR trial participants 2005).

Endovascular abdominal aortic aneurysm repair

Endovascular Aneurysm Repair (EVAR) was first introduced by Parodi et al (Parodi, Palmaz et al. 1991) in 1989 and has gained popularity over the years. The procedure involves placement of a stent-graft across the aneurysm from within the circulation. The EVAR device is placed into the aorta through the femoral arteries that can be accessed by means of a surgical cut down or by utilising percutaneous access. The EVAR device forms a seal with the aorta proximal to the aneurysm and the iliac arteries distal to the aneurysm – the proximal and distal seal zones.

The evidence for EVAR

Intuitively, EVAR is a less invasive procedure as compared to standard open surgery; however, patients with abdominal aortic aneurysms are complex and often have multiple co-morbidities that makes aneurysm repair, open or endovascular, a high-risk procedure.

Several large trials have compared outcomes between endovascular and open repair of aneurysms (Prinissen, Verhoeven et al. 2004, EVAR trial participants 2005, Lederle, Freischalag et al. 2009, EVAR trial participants 2010). The UK EVAR trial was a large multicentre randomised controlled trial that evaluated outcomes related to mortality, durability, health related quality of life and cost benefits between patients undergoing endovascular and open repair of their abdominal aortic aneurysms. 1252 patients >60 years of age with aneurysms >5.5 cm in size and with suitable anatomy, were randomised to either open or endovascular repair. 30-day operative mortality

was 1.8% in the EVAR group and 4.3% in the open repair group (p=0.02). However, by the end of the follow up period, this early aneurysm-related death benefit had been lost (p=0.73). This was partly blamed upon endograft related ruptures. Also, there was no difference in all cause mortality between the 2 groups (p=0.72). Kaplan-Meier analysis revealed the 2 curves for all cause mortality converging at 2 years and for aneurysm related mortality converging at 6 years. There was a significantly higher re-intervention rate in the endovascular group (3-4 times higher in the EVAR group compared to the open group) that also translated to higher costs being ascribed to endovascular aneurysm repair as opposed to open repair.

The DREAM triallists have reported similar results, (Prinissen, Verhoeven et al. 2004, De Bruin, Baas et al. 2010) with the initial survival benefit from EVAR being lost at long-term follow up (cumulative survival rates 69.9% for open repair and 68.9% for endovascular repair at 6 years). Re-intervention rates, again, followed precedents from other trials with rates being significantly higher in the endovascular group.

The OVER trial, a large North American trial, published their 2-year follow up results comparing open and endovascular approaches for abdominal aortic aneurysm repairs in 2009 (Lederle, Freischalag et al. 2009). Long-term results were published in 2012 (Lederle, Freischlag et al. 2012). As with the other trials, their primary outcome was all cause mortality with secondary outcome measures being procedural failure, short-term morbidity, length of hospital stay, health related quality of life and erectile dysfunction. They reported a sustained peri-operative mortality reduction with endovascular repair up to a period of 3 years post EVAR; survival benefits being the same in both groups thereafter. An interesting finding from this trial was the reported higher long-term survival in younger patients who had undergone endovascular repair compared to older patients.

All the large comparative EVAR trials have identified a peri-operative mortality reduction with endovascular aneurysm repair. Long-term results however suggest that this benefit is lost by about 2-3 years time, with survival rates being similar in both arms. Endovascular repair has also been associated with higher costs overall due to a higher re-intervention rate.

Suitability for EVAR - Anatomical requirements

Not all aneurysms are suitable for endovascular repair. Several anatomic criteria have been described to assess suitability of aneurysm morphology for endovascular repair. These include aneurysm neck length, diameter, angulation, thrombus burden; iliac landing zone length, diameter and iliac vessel tortuosity.

Neck morphology

The neck of the aneurysm is the length of normal calibre aorta distal to the lowermost renal artery and the commencement of the aneurysm. This is the proximal attachment area of the EVAR stent-graft (proximal sealing zone). Most manufacturers recommend a minimum aneurysm neck length of 1 – 1.5 cm for the device to be able to achieve an adequate seal with the aortic wall (Cook Inc. , Endologix Inc. , Medtronic Inc. , Vascutek Inc. , W L Gore Inc.). Apart from the actual diameter of the aneurysm neck the shape of the neck itself is also important. The aneurysm neck has been described in the literature as parallel, conical (tapered), flared (reverse tapered), barrel, irregular and hourglass shaped (McDonnell, Halak et al. 2006). Intuitively, the parallel configuration is the most amenable to providing a good proximal seal zone and the flared configuration the most unfavourable. A long, parallel proximal aortic neck is a favourable feature for EVAR planning.

The recommended proximal aortic diameters that can be treated by endovascular means, range from 18 mm – 32 mm. To achieve an appropriate proximal seal between the endograft and the aortic wall, manufacturers recommend oversizing the proximal endograft by 10-20% to aortic neck diameter (Cook Inc. , Endologix Inc. , Medtronic

Inc. , Vascutek Inc. , W L Gore Inc.). There is some evidence to suggest that oversizing the proximal endograft by up to 25% reduces the incidence of proximal endoleaks, however with oversizing of >30% there is increased folding of the proximal aorta and also some evidence suggesting increased migration of the device (Sternbergh, Money et al. 2004, van Prehn, Schlosser et al. 2009, Lin, Kratzberg et al. 2012).

The angle of the aneurysm neck is an important consideration whilst planning. Angulation of the neck has an impact on the seal achieved and has also been linked to device migration. The two angulations to be considered are:

1) Angle with the supra-renal aorta: this is the angulation between the supra-renal aorta and the immediate infra renal (neck) aorta. Manufacturers recommend that this angle should be less than 45°. (Angle 'a' Figure 1)
2) Angle with long axis of the aneurysm: This is the angulation between the infra renal neck and the long axis of the aneurysm. General recommendations form the device manufacturers suggest a maximum limit of 60°. (Angle 'b' Figure 1)

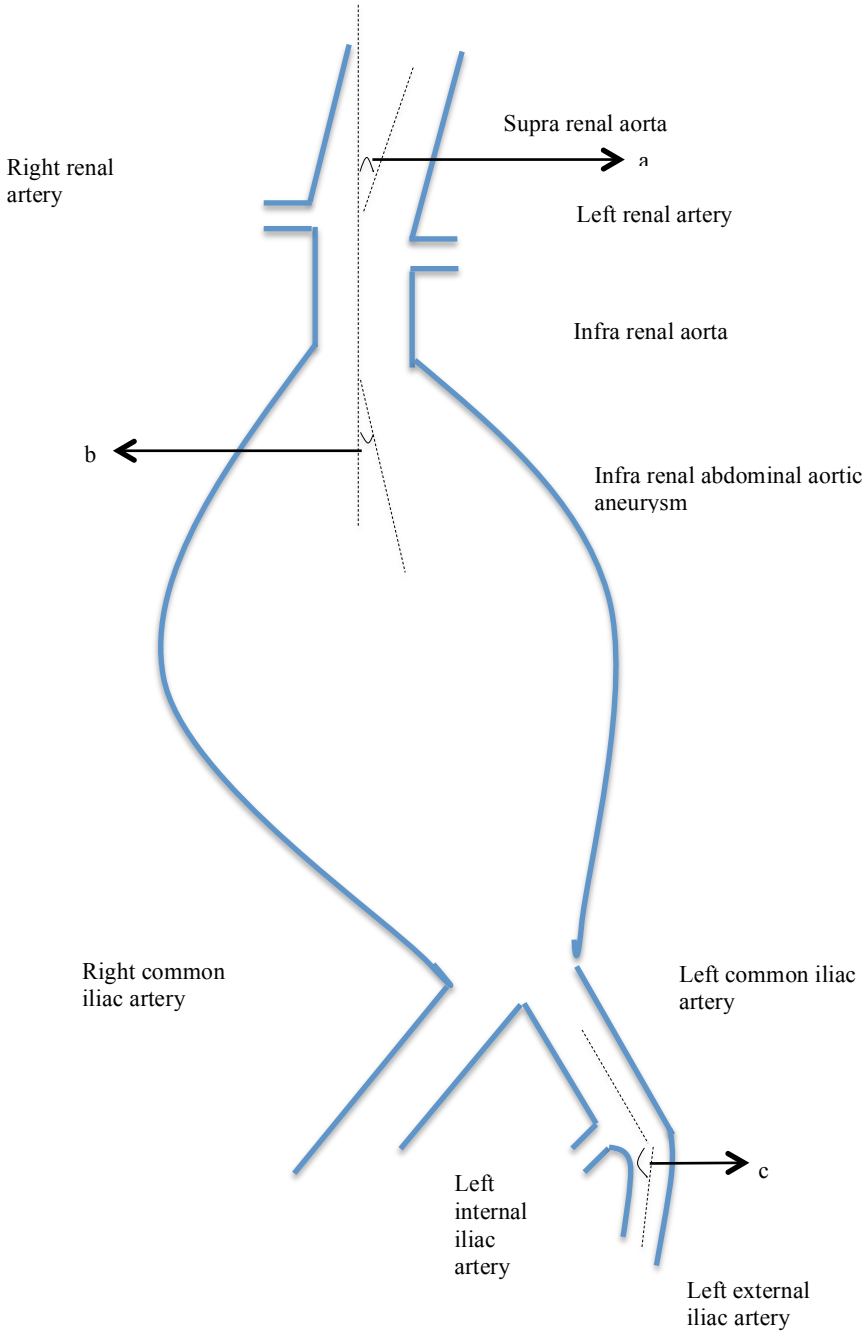

Figure 1: ***Schematic showing a typical infra-renal abdominal aortic aneurysm. Angle (a): angulation between supra-renal aorta and infra-renal 'neck', angle (b): angulation between infra-renal neck and long axis of the aneurysm, angle (c): maximum iliac angulation***

Several authors have assessed the impact of thrombus burden and calcification in the proximal aortic neck and outcomes following endograft implantation (Chaikof, Fillinger et al. 2002, Walker, Kalva et al. 2010, Bastos Goncalves, Verhagen et al. 2012). >50% circumferential calcification or thrombus (>2 mm thick) is regarded as an adverse feature for endovascular repair and has been associated with a higher incidence of inadequate proximal sealing.

Iliac morphology

Analogous to the proximal aortic neck, the iliac arteries provide the distal landing (sealing) zone for the endograft. The iliac vessels also provide access to the aneurysm for the endograft. Iliac vessel diameter, tortuosity and the presence of any stenosis will, therefore, have an impact on the procedure. The length and diameter of the iliac landing zone also influences the adequacy of distal sealing. The minimum recommended length of the iliac sealing zone varies between 10 – 15 mm for the commonly used devices (Cook Inc. , Endologix Inc. , Medtronic Inc. , Vascutek Inc. , W L Gore Inc.). Minimum iliac diameter required for the device to be able to pass through the iliac arteries is 7-8 mm. Iliac arterial diameters between 7 – 20 mm can be treated, larger or smaller arteries will require alternative sealing zones or other treatment modalities. As for the proximal neck, the device manufacturers recommend an oversize of 10 – 15 % (Cook Inc. , Endologix Inc. , Medtronic Inc. , Vascutek Inc. , W L Gore Inc.). To achieve adequate distal sealing, some patients would require the device to land in the external iliac arteries. In these cases, the internal iliac artery (if patent) can be embolised. However, it is important to try and keep at least one internal iliac artery in circulation (by deploying the iliac limb proximal to the internal iliac artery) to prevent complications such as bowel ischaemia and spinal cord ischaemia.

As discussed subsequently special iliac branch devices may be considered in selected cases. Increased tortuosity of the iliac arteries increases the technical difficulty associated with the procedure. Iliac tortuosity is measured as an index (τ); this is a ratio of the centre-line length to straight-line length from the aortic bifurcation to the common femoral artery. A (τ) of >1.6 or c (Iliac angle in schematic, maximum iliac angulation) < 90 are adverse features for endovascular repair (Chaikof, Fillinger et al. 2002, Walker, Kalva et al. 2010).

Device types and characteristics

EVAR grafts are composed of a metallic outer skeleton (stent) and a fabric graft. The metallic stent provides structural support to the device. Commonly used materials for these stents are nitinol (Nickel Titanium alloy) and stainless steel. The metallic exoskeleton scaffold encloses a fabric cylindrical or bifurcated trouser graft. These grafts are commonly made using expanded polytetraflouroehylene (ePTFE), fluorinated ethylene propylene (FEP) and polyester (polyethylene terephthalate, PET). The fabric of the device allows for exclusion of the aneurysm from the circulation.

The principle of EVAR involves forming a proximal and distal seal with the aortic and iliac wall. The proximal seal with the aortic wall is achieved either by means of positive fixation (hooks or barbs that attach to the aortic wall) or by radial force. The distal seal is usually achieved by radial force.

Devices attach to the aortic wall either at the supra or infra renal levels. EVAR devices utilising supra-renal fixation incorporate a short proximal bare metal stent (area devoid of fabric graft) that sits across the origins of the renal arteries. Devices with infra-renal fixation attach to the infra-renal aorta. Most devices tend to employ a combination of positive fixation with hooks or barbs and radial force (achieved by oversizing the graft by 15 – 20%).

The supra-renal aortic wall is thought to be more resistant to post repair aneurysmal change. These devices are therefore thought to provide better fixation in cases with challenging or difficult anatomy (Robbins, Kritpracha et al. 2005). However, other reports have suggested that in the absence of other unfavourable features, patients with short neck lengths achieve similar results with both supra and infra renal fixation

(Hager, Cho et al. 2012). Deployment of bare metal stents used for supra-renal fixation across the origins of the renal arteries, also does not seem to have an impact on long-term renal function (Lau, Hakaim et al. 2003, Parmer, Carpenter et al. 2006).

All EVAR devices have a modular design allowing for customisation based on the individual patients' anatomy. There are three main types of devices

1. Aorto-uni-iliac systems: These have stent-graft body that is deployed from the aorta into one common iliac artery. The contra lateral iliac artery (if patent) is usually occluded by means of an occluder device. This procedure is generally combined with the formation of a surgical femoro-femoral cross over graft to ensure blood flow into the contralateral leg.
2. Bifurcated devices: These comprise a bifurcated main body with a 'gate' for docking of the contra-lateral iliac limb. Limb extensions are then placed as appropriate to customize the graft to the individual patient.
3. Unibody endoprosthesis: These are positioned to sit on the aortic bifurcation. Modular pieces are then attached for proximal and distal extension.

Complex Endografts

Approximately 20% of patients with abdominal aortic aneurysms will have unfavourable anatomical features for standard infra renal EVAR (Malina, Resch et al. 2008). Endograft technology has evolved over the last decade such that branched and fenestrated endografts are now available for consideration of treatment in this patient group.

Fenestrated EVAR

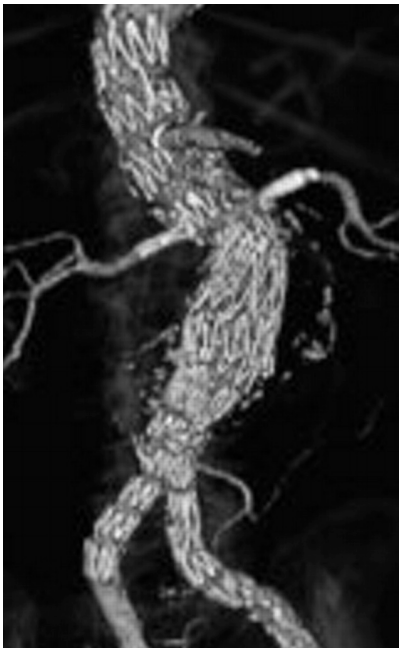

Figure 2: ***Fenestrated EVAR***

Fenestrated devices have special ports ("fenestrations") built into the device through which visceral arteries can be cannulated and appropriate stents placed (bare metal or covered). These fenestrations in the graft material are reinforced with stent rings sutured to the graft material to provide strength to the device and prevent collapse of the visceral stent. The fenestrations usually come in three configurations: large

fenestrations, small fenestrations and scallops (incomplete fenestration at the end of the stent graft). The fenestrations allow for the entire stent graft to cover part of the supra-renal aorta without compromising the visceral arteries thereby enabling endovascular repair of juxta-renal aneurysms.

Branched EVAR

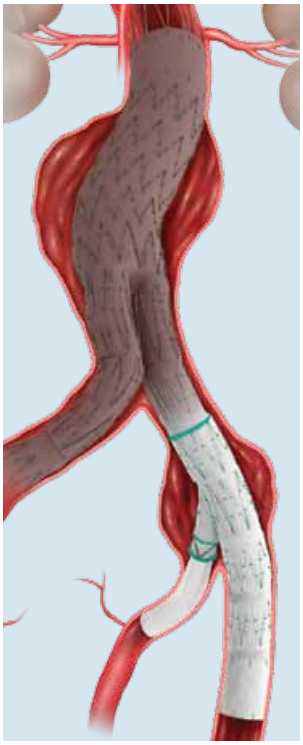

Figure 3: ***Iliac branched EVAR © Cook Medical***

As for the fenestrated devices, branched EVAR devices have branches (small stent grafts) that are extensions from the main body of the device. These stent-graft branches are carefully manoeuvred into the visceral arteries during the procedure. Branched devices are particularly useful in cases where the aneurysm involves the

visceral vessels. Branched devices have also been used to treat aneurysmal iliac arteries where the aneurysms involve the origins of the internal iliac arteries.

Chimneys and Periscopes

Besides the techniques and newer grafts described above, standard grafts can be deployed alongside visceral stents, the proximal ends of which sit proximal (chimney technique) or distal (periscope technique) to the main endograft. The bodies of these visceral stents lie outside the main endograft body. This type of device placement is associated with a typical phenomenon called gutter endoleaks whereby blood tends to track alongside the visceral stents.

Complications

EVAR is associated with potential complications, including graft migration, kinking and fracture, endoleaks and limb outflow impairment. These complications may necessitate further interventions to prevent mortality and morbidity through aneurysm rupture and distal ischaemia (Table 1). Thus, post EVAR patients undergo surveillance with serial scans to enable early detection of complications.

Table 1: ***EVAR complications table***

Immediate	**Early**	**Late**
Deployment Failure	Endoleaks	Device migration
Incorrect device placement	Endotension	Device disruption
Endograft kinking	Endograft kinking	Endograft kinking
Aneurysm rupture	Wound Infections	Graft thrombosis/stenosis
Conversion to open	Device fracture	Endoleaks
Endoleaks	Outflow compromise	Infection
Haemorrhage	Visceral ischaemia	Aneurysm rupture
Ischaemic complications (Legs, Spinal cord, Bowel, Kidneys)	Renal impairment (incorrect device placement or contrast nephropathy)	
Mechanical obstruction, thrombosis, embolism		

Endoleaks are defined as areas of persistent blood flow outside the graft, but within the aneurysm sac (Veith, Baum et al. 2002). Reports suggest that endoleaks can affect up to 20% of patients undergoing EVAR (EVAR trial participants 2005). They are thought to be responsible for most treatment failures beyond the first year. Endoleaks have been classified into 5 types depending upon the origin of the leak (Table 2).

Types I and III endoleaks are a result of inadequate seals at the proximal, distal sealing zones of the endograft and modular disruption respectively. These endoleaks typically have high flow rates with patients being at significant risk of continued sac pressurisation and subsequent rupture. Data from the EUROSTAR registry suggests that types I and III endoleaks are associated with a higher intervention rate compared to type II endoleaks. Patients with these types of endoleaks are also at significantly higher risk of aneurysm rupture compared to patients without endoleaks (van Marrewijk, Buth et al. 2002). Type II endoleaks are a result of back flow from patent inferior mesenteric or lumbar arteries. Compared to types I and III, they are typically slower, with recorded flow velocities at the origins of the endoleak vessels being in the range of 75 – 200 cm/sec (Arko, Filis et al. 2003).

Arko et al (Arko, Filis et al. 2003) assessed whether intra-sac flow velocities could predict sealing of type II endoleaks. The followed up 265 patients that had been treated with the AneuRx® and Talent® (Medtronic Inc, AVE, Santa Rosa, California, USA) and found type II endoleaks in 23% patients at discharge. Spectral velocities were measured at the entrance of the feeding vessel at the sac. They found that patients with type II endoleaks that sealed spontaneously had velocities significantly lower than those in whom these endoleaks persisted. Persisting type II endoleaks had flow rates in excess of 100 cm/sec. The aneurysm sac diameter also responded to

sealing of endoleaks with sac diameters reducing after spontaneous sealing of endoleaks.

Types I and III endoleaks usually require intervention, whereas type II endoleaks in the absence of associated increase in aneurysm sac size are usually managed conservatively. Re-intervention rates after EVAR have been reported to be as high as three to four times that of open repair (EVAR trial participants 2010).

Table 2: ***Classification of endoleaks***

Endoleak	Description (origin of flow)
Type I	Attachment site leaks
A	Proximal
B	Distal
C	Iliac Occluder
Type II	Branch Leaks
A	Simple (1 patent branch)
B	Complex (2 or more patent branches)
Type III	Graft defect
A	Junctional leak or Modular defect
B	Fabric Disruption (Midgraft Hole)
Type IV	Fabric Porosity (within 30 days of procedure)
Type V	Endotension
A	With no endoleak
B	With sealed endoleak
C	With Type 1 or 3 endoleak
D	With Type 2 endoleak

Type IV endoleaks are representative of porosity of the fabric of the endograft. By definition they occur within 30days of the procedure. The old Gore Excluder endoprosthesis® (W. L. Gore Inc., Newark, DE, USA) had specifically been associated with reduced shrinkage of the aneurysm sac after deployment compared to other devices (Bertges, Chow et al. 2003, Haider, Najjar et al. 2006). This was explained on the basis of porosity of the graft to serous fluid that moved across the expanded PTFE graft material. This device was substituted for a low permeability alternative in July 2004.

Type V endoleaks are leaks that cannot be classified on imaging. Sub-classification is based on subsequent classification at open surgery.

Predictors of complications post EVAR

Continued pressurisation of the aneurysm sac post endovascular repair usually results in enlargement of the sac size. Several studies have evaluated this enlargement with a view to identifying factors that would help predict such an outcome (Fairman, Nolte et al. 2006, Lalka, Greenberg et al. 2009, Schanzer, Greenberg et al. 2011). Fairman et al studied 351 patients who had undergone EVAR with the Zenith modular bifurcated device (Cook, Inc, Bloomington, Ind., USA). They identified presence of an endoleak and pre procedural aneurysm neck thrombus/calcification as factors predictive of sac size change. Their study population was selected for the Zenith AAA multicentre trial with favourable neck anatomy with only 6% of patients with circumferential neck thrombus/plaque. Despite their reported identification of the presence of neck thrombus and plaque the authors therefore argued that they had potentially underestimated the value of achieving an adequate proximal seal and its impact on subsequent complications. The authors also identified that all cases with sac enlargement were associated with the presence of an endoleak.

Schanzer et al evaluated CT scans of 10228 patients who underwent EVAR in the United States between 1999 and 2008. Pre and post-operative scans were assessed to identify anatomical features that would be able to predict post endograft implantation abdominal aortic aneurysm sac enlargement. They also assessed these scans to ascertain the compliance with the device manufacturers' instructions for use (IFU). They identified presence of an endoleak, age > 80 yrs., aortic neck diameter > 28 mm, aortic neck angle > 60 and common iliac artery diameter > 20 mm as independent predictors for AAA sac enlargement post EVAR (Table 3). Interestingly, they also found that only 42% of patients met the most conservative definition for IFU and 69%

the most liberal definition. The authors also identified that the rate of aneurysm sac expansion was significantly higher in patients who underwent EVAR outside of the device manufacturers IFU.

Table 3: Predictors of sac enlargement (Schanzer, Greenberg et al. 2011)

Predictors of AAA sac enlargement
Age >80
Conical aortic neck
Aortic neck diameter > 28 mm
Aortic neck angle > 60
Common iliac artery diameter > 20 mm
Anatomy outside IFU
Presence of an endoleak during follow up

One of the criticisms of this study by Schanzer et al has been the selection bias introduced by using the M2S database, which has been recognised to be non consecutive and may comprise selected and potentially more complex cases. No data was supplied to ascertain the time lapse between the baseline CT scan and EVAR; the enlargement in aneurysm sac size may have been pre-EVAR. Another point of not about this study was that the baseline AAA diameter for 59% of patients was <5.5 cm, the generally accepted size for intervention. M2S data included patient operated upon for reasons other than aneurysmal disease (aortic ulcer, iliac disease, pseudo aneurysms etc.) that may have confounded results. Schanzer et al utilised the pre procedural sac size rather than the immediate post procedural CT scans as their baseline AAA sac measurements that gain may have impacted upon the results. Nonetheless, the M2S database is a large database of patients that have undergone

endovascular repairs and is at least partly if not completely representative of changes that occur in the aneurysm sac post repair.

These studies associating pre operative anatomy with the continued sac pressurisation illustrate the importance of adequate planning prior to undertaking endovascular interventions. Adherence to the instructions for use and judicious planning reduces the risk of developing complications such as endoleaks, device migration and late aneurysm ruptures that are associated with treatment failure.

Surveillance of patients post endovascular abdominal aortic aneurysm repair

Post EVAR, patients routinely undergo imaging at regular intervals to detect complications. Computed tomography (CT) scanning has been widely regarded as the best current method for this surveillance (Veith, Baum et al. 2002). Duplex scanning has been proposed as an alternative to CT, but its use has not become commonplace due to the reported variation in its sensitivity and specificity in detecting these complications compared to CT (Wolf, Johnson et al. 2000, Raman, Missig-Carrol et al. 2003, Elkouri, Panneton et al. 2004, Sandford, Bown et al. 2006).

Currently available imaging options

Computed Tomography (CT)

CT angiography is widely regarded as the current modality of choice for surveillance of patients post EVAR. It has been demonstrated to be superior to conventional catheter angiography in detecting endoleaks (Armerding, Rubin et al. 2000). CT angiography delivers comprehensive vascular and non-vascular imaging and is convenient for patients due to its relatively quick scan acquisition time and widespread availability.

Commonly employed CT surveillance protocols recommend regular scans at 3, 6 and 12 months post implantation and at yearly intervals thereafter. CT surveillance scans have evolved from a single arterial phase protocol to biphasic (arterial and a delayed scan) and triphasic protocols (an initial non contrast scan followed by an arterial first

pass scan and a delayed scan). Traditionally, a triphasic protocol has been preferred for post EVAR surveillance. The non-contrast scan helps in the identification of high-density materials. This enables differentiation between true endoleaks and areas of calcification or high attenuation that mimic endoleaks (pseudo-endoleaks) (Rozenblit, Patlas et al. 2003). The arterial first pass scan is followed by a delayed scan that aids in the detection of slow flow endoleaks which might have been missed on the first pass scan (Rozenblit, Patlas et al. 2003, Iezzi, Cotroneo et al. 2006).

Following scan acquisition, the images are viewed on a CT workstation that has capabilities for multi-planar reconstruction (MPR). The entirety of the abdominal aorta is imaged, evaluating the proximal and distal sealing zones and comparing neck and iliac diameters with previous imaging. The aneurysm sac size is measured and the maximal size is compared to previous imaging. Areas of contrast enhancement outside of the stent-graft but within the aneurysm sac are investigated with a view to confirming endoleaks and ascertaining their origin. The integrity of the endograft is also evaluated and any impending complications commented upon.

The prolonged nature of post EVAR surveillance subjects patients to a substantial radiation dose and has significant cost implications. The triphasic protocol (initial non-contrast scan, arterial first pass scan and delayed phase scan) exposes patients to a large radiation dose at every sitting. Some authors have suggested employing a biphasic protocol (unenhanced and arterial first pass scans), but others have argued about their reliability in detecting slow flow endoleaks (Golzarian, Dussaussois et al. 1998, Rozenblit, Patlas et al. 2003, Iezzi, Cotroneo et al. 2006). Some centres perform initial non-contrast scans only at the first scan opportunity. Subsequent scans are performed to a biphasic protocol, which are then compared with the initial non-contrast scan, thus minimising radiation exposure to patients.

A standard triphasic post EVAR surveillance CT scan can expose patients to a radiation dose of approximately 20-30 milliseiverts (mSv), which is roughly equivalent to 300-400 plain X-rays. Such a dose has been associated with a theoretical lifetime risk of radiation induced fatal cancer in about 1 in 2000 patients (0.05%) (International Commission on Radiological Protection 2000).

Contrast agents traditionally used for CT angiography comprise iodinated compounds that have been associated with an increased risk of anaphylaxis and nephropathy. Currently employed agents for post-EVAR CT angiography are organic (non-ionic), low osmolar compounds such as Iohexol (Omnipaque) and Ioversol (Optiray). These agents are more hydrophilic and less chemotoxic when compared to older contrast agents (McClennan 1987, McClennan 1990, Spring and Quesenberry 1991, Sovak 1994, Dawson 1996, Cohan and Ellis 1997).

CT contrast agents have been associated with anaphylactic reactions and are potentially nephrotoxic, thereby precluding their use in elderly patients with impaired renal function. A significant proportion of the patient population with abdominal aortic aneurysms is elderly and often present with mild to moderate impairment of renal function. These potential drawbacks have prompted investigators to explore other imaging modalities for surveillance of patients post EVAR.

Magnetic Resonance Angiography (MRA)

MRA is an alternative imaging modality for EVAR surveillance and can provide imaging comparable, if not superior, to conventional CT scanning. A recent study, comparing the sensitivities of MRA and CT angiography for endoleak detection after EVAR, found MRA to be very sensitive in detecting slow flow endoleaks (van der Laan, Bartels et al. 2006). MR offers an advantage over CT scanning as it is free from radiation and does not employ iodinated contrast media.

The scanning protocol commonly employed for MR scanning of this patient group, involves axial and/or coronal spin echo T1-weighted sequences and a contrast enhanced angiogram. Several synchronous phases are acquired beginning with the arterial phase and extending into the equilibrium and venous phases (Ayuso, de Caralt et al. 2004, Hellinger 2005, van der Laan, Bartels et al. 2006). This protocol maximises the chances of detecting complications.

MR scanning, although reported to be very accurate in detecting slow flow endoleaks (van der Laan, Bartels et al. 2006), is associated with its own set of potential problems. Apart from the high costs involved, patients with stainless steel stent grafts are not suitable for MR scanning due to excessive artefact susceptibility. Cardiac pacemakers, intracranial aneurysm clips or any other ferromagnetic implants are contraindications for MR scanning. The images obtained with MR scanning also have a lower spatial resolution than CT and may less reliably detect calcification. MR scan acquisition also takes longer than for CT. Claustrophobic patients often require sedation prior to MR scanning.

Newer open MR scanners, provide weaker magnetic fields, and have not been preferred for post EVAR scanning. They provide less detailed imaging compared to standard tunnel scanners and have an even longer scan acquisition time.

MRA employs organic gadolinium compounds as contrast agents. These agents utilise the inherent paramagnetic properties of gadolinium to alter magnetic fields around tissues. This alteration of magnetic fields provides for improved visualisation of vascular structures that helps in the detection of complications post EVAR.

MR contrast agents, although considered to be safer than CT contrast agents in patients with mild renal impairment, have recently been found to be associated with Nephrogenic Systemic Fibrosis (NSF) in patients with severe renal impairment. Current MHRA (Medicines and Healthcare products regulatory Agency) guidance advises careful consideration prior to administering these contrast agents in patients with severe renal impairment (GFR [glomerular filtration rate] <30mL/min/1·73m2 or in patients who have had, or who are awaiting, liver transplantation) (Medicines and Healthcare products regulatory Agency 2007).

Duplex ultrasound (DUS)

DUS has increasingly been used for surveillance of patients post EVAR. Widespread availability and relatively low cost association of DUS have made it popular with researchers. Yet, its use has not become commonplace. This has been attributed to a lack of universal reproducibility of highly specific and sensitive results in detecting complications post EVAR (Wolf, Johnson et al. 2000, Raman, Missig-Carrol et al. 2003, Elkouri, Panneton et al. 2004, Sandford, Bown et al. 2006). Its operator dependent nature, difficulties in visualising abdominal viscera in patients of large body habitus and bowel gas interference have all been thought to be responsible for this variation.

For a standard post EVAR surveillance duplex, the aorta is scanned in both longitudinal and transverse planes using B-mode imaging to determine the extent of the stent-graft and to ascertain the maximum aortic sac diameter. Colour Doppler is then used to scan the aorta from the diaphragm or origin of renal arteries down to the common femoral arteries, evaluating the stent for integrity and kinking. Special attention is paid to the proximal and distal stent-graft attachment sites and to the origin of the inferior mesenteric and lumbar arteries to detect endoleaks.

Vastly improved endoleak detection rates have been reported by some recent studies employing contrast-enhanced ultrasound (Bendick, Bove et al. 2003, Giannoni, Palombo et al. 2003, Napoli, Bargellini et al. 2004, Henao, Hodge et al. 2006). Second generation contrast agents, preferred nowadays, including Sulphur Hexafluoride (Sonovue) and Galactose / Palmitic Acid (Levovist) are gas-filled, stable micro bubbles that have a high degree of echogenicity. These micro-bubbles

cause an increase in backscatter, which is detected by ultrasound, and aids in the identification of endoleaks.

These results, although encouraging, have not been uniform (McWilliams, Martin et al. 1999, McWilliams, Martin et al. 2002, Bendick, Bove et al. 2003, Giannoni, Palombo et al. 2003, Napoli, Bargellini et al. 2004, Henao, Hodge et al. 2006). In 1999, a study conducted by McWilliams et al, comparing contrast enhanced duplex with arterial phase CT found duplex to be very sensitive and specific and questioned whether endoleaks identified by duplex and missed by CT were not, in fact, true endoleaks (McWilliams, Martin et al. 1999). A further study by the same group published in 2002, this time comparing contrast enhanced duplex with biphasic CT could not reproduce the same results and found CT to be a better tool (McWilliams, Martin et al. 2002). Henao et al, using a continuous infusion technique and comparing contrast-enhanced duplex to biphasic CT, found duplex to be comparable to CT and suggested its use as a primary surveillance modality (Henao, Hodge et al. 2006).

Intra-sac pressure monitoring

EVAR diverts blood flow through the stent graft, excluding the aneurysm from the circulation. This process is intended to prevent an increase in the intra sac pressure of the aneurysm. Endoleaks, especially types I and III are associated with an increase in sac pressures that can cause ruptures. There has been substantial interest in measuring intra-sac pressure as a means to carry out surveillance of patients post EVAR. Intra-sac pressures can be monitored either by using an implanted monitoring device or by performing a puncture of the aneurysm sac. Several implantable pressure monitoring devices have been trialled:

1. The Impressure AAA sac pressure sensor (Remon Medical Technologies, Caesarea, Israel). This system is ultrasound activated and communicates using ultrasound waves with an external monitor to provide pressure monitoring. On demand sac pressures can be obtained in an office setting.
2. The CardioMEMS Endosure wireless AAA pressure sensor (CardioMems, Atlanta, GA) uses radiofrequency (RF) to transmit pressure readings to an external module.
3. The TPS Telemetric pressure sensor (Helmholtz institute for biomedical engineering, RWTH, Aachen, Germany) uses a telemetric digital sensor and transmits data to an external monitoring station.

Direct measurement of sac pressures: The aneurysm sac can be punctured with guide wires mounted with pressure sensors to monitor intra-sac pressures. Several approaches have been described including translumbar sac puncture and transvenous transcaval puncture.

Aneurysm sac pressures tend to reduce following successful EVAR (Chuter, Ivancev et al. 1997, Sonesson, Dias et al. 2003, Dias, Ivancev et al. 2004). Types I and III endoleaks are associated with increased sac pressures. The APEX trial (Ohki, Ouriel et al. 2007) used a > 30% reduction in pulse pressure from the initial pressure to define a sealed sac and < 30% reduction to indicate a type I or III leak. However, type II endoleaks remain a diagnostic challenge as in cases of these endoleaks sac pressures may increase, decrease or remain the same. Sac pressures depend on the specific configurations of inflow and outflow channels; hence complex type II leaks are associated with variable pressure changes.

Authors continue to debate the clinical relevance of intra sac pressure measurements. Measuring sac pressures offers a physiological means of assessing the risk of rupture but it does not, currently, obviate the requirement for imaging. Further, sac pressure measurement depends upon the exact location of the measurement position within the sac. It has been demonstrated that pressures are higher within the endoleak channel as compared to elsewhere within the aneurysm sac (Dias, Ivancev et al. 2007). The dampening effect of thrombus may also affect pressure transmission. Concerns remain regarding this phenomenon that has been described as ‘compartmentalisation’ and the effects that this might have on the accuracy of intra-sac pressure monitoring. The consensus therefore remains that although intra-sac pressure monitoring remains a valuable adjunct to post EVAR surveillance, there is not enough evidence at present for it to be the sole surveillance modality.

Surveillance Costs

Patients post endovascular aneurysm repair need lifelong surveillance to detect associated complications. Current surveillance protocols employing regular CT scans have implied a high cost association with EVAR. Typical post EVAR CT and MR scans cost approximately £750-1000 ($1500 – 2000)* and £1000 – 1300 ($ 2000 – 2600)* respectively. Typical post EVAR surveillance duplex, in comparison, cost approximately £300 - 400 ($600 - 800)* (*Indicative costs referenced from 2 independent UK hospitals at the time of the original research, likely to have reduced over the years). Surveillance costs for both these modalities are likely to become cheaper with widespread use of both CT and DUS.

Surveillance programmes need to be both clinically sound and cost effective. Post EVAR surveillance has traditionally been carried out with regular CT scans that have been responsible for the high costs associated with it. A clinically proven surveillance programme incorporating duplex ultrasound would offset some of these costs.

The ideal imaging modality for surveillance of patients post EVAR, would be inexpensive, widely available, provide universally reproducible results and subject patients to little or no radiation.

Every imaging modality used for this surveillance, has been associated with its own set of advantages and disadvantages. DUS is inexpensive, does not use iodinated contrast media and is relatively easy to perform. These advantages would make duplex the ideal surveillance modality but for its reliability in producing highly sensitive and specific results, which remains to be proven.

Ultrasound phantoms

Ultrasound phantoms are specially designed objects that when scanned provide consistent results similar to scanning human tissue. They contain one or more materials that simulate the interaction of tissues with ultrasound and have traditionally been used to provide quality assurance and as simple calibration tools for imaging modalities. However they are now also being increasingly employed for the provision of medical training by simulating anatomic and acoustic representations of events that occur within the human body.

Ultrasound phantoms can now be used to simulate conditions and events as diverse as abdominal aortic aneurysms to foetal development. Current applications for ultrasound phantoms include quality assurance of ultrasound systems, training for performing ultrasound guided biopsies, foetal developmental monitoring; and aneurysm surveillance and detection.

Phantoms are constructed using materials that mimic the ultrasonic characteristics of human tissue or tissue mimicking materials (TMM), and usually contain a target or test object. The entire structure is housed within a casing, which prevents damage to the TMM by handling and desiccation. This casing could vary from being a simple film to an entire housing frame with windows that allow for transmission and reception of ultrasound waves.

Tissue mimicking materials

Tissue mimicking materials simulate the acoustic properties (i.e. speed of sound, attenuation coefficient, backscatter coefficient, elasticity and thermal properties) of human soft tissue. These properties of the TMM are either known or are established as a standard prior to the phantom being employed (Teirlinck, Bezemer et al. 1998, Madsen, Dong et al. 1999, Ramnarine, Anderson et al. 2001). TMMs could be a slab of homogenous tissue or may contain other objects with known shape, size, depth and ultrasonic parameters.

Commonly employed tissue mimicking materials include agar, urethanes, epoxies and other natural materials such as vegetable oil. Table 8 provides the physical properties of the tissue mimicking material that was used as part of our study.

Blood mimicking materials

Blood mimicking fluids used in ultrasound phantoms mimic the acoustic and hemodynamic properties of blood. Typically these materials consist of particles suspended in a fluid. Historically particles such as sephadex, starch, nylon, polystyrene microspheres and hardened red blood cells have been used. For a solution to be employed as a blood mimic, its physical and ultrasonic properties should be similar to human blood (Ramnarine, Nassiri et al. 1998). Specifically, the suspended particulates should be of a similar size, shape to red blood cells and should remain buoyant even at low velocities. The ultrasound backscatter of the fluid should also be comparable to that of flowing human blood. Table 9 provides the physical properties of the blood mimicking fluid employed for our study.

ORIGINAL RESEARCH

DUS and CT for post EVAR surveillance: Literature review

A literature review was performed to identify the existing knowledge base regarding surveillance of patients post EVAR, comparing Duplex ultrasound and CT. MEDLINE and Embase databases were searched using medical subject headings (MeSH terms) (Table 4) with the Boolean operatives AND or OR. Additional studies were included through review of abstracts presented at various vascular surgical conferences.

Table 4: ***MeSH terms used for literature review***

MeSH terms
Aortic aneurysm
Blood vessel prosthesis
Implantation
Stents
Endovascular procedures
Surveillance
Doppler ultrasound imaging
Ultrasonography
Angiography
Computed tomography
Contrast media

The search included all papers published between 1996 and 2006. Abstracts for all studies were reviewed. Twenty-one studies published in English were identified that directly compared CT and DUS for surveillance of patients post endovascular

aneurysm repair; these formed the basis for our literature review (**Table 5**). Inclusion criteria were defined as provision of adequate patient data, assessment of concurrent CT and either DUS or contrast-enhanced DUS scans, publication in English language journals and availability of full text for review. Primary outcome measures were defined as the sensitivity and specificity of Duplex ultrasound for the detection of endoleaks.

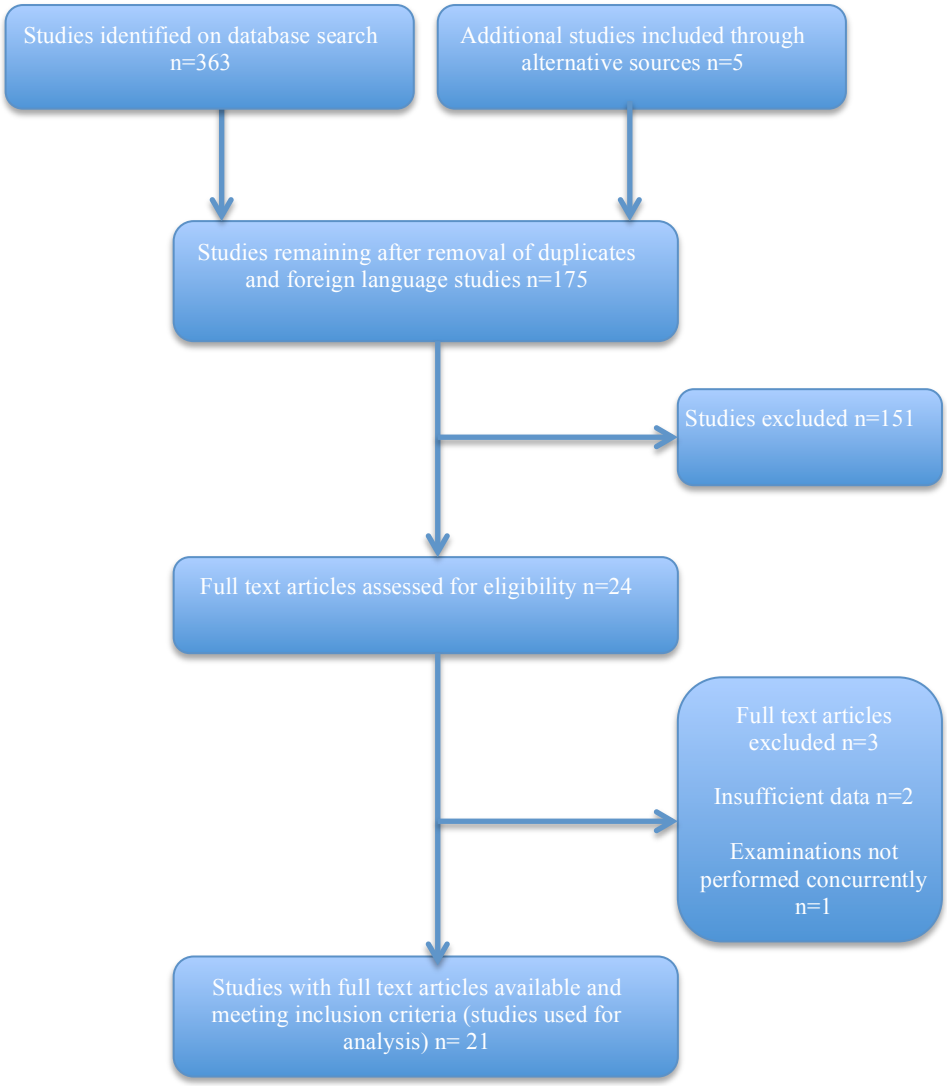

Figure 4: ***PRISMA flowchart for literature review***

Table 5: ***Studies included in review of literature comparing CT and DUS for post EVAR surveillance***

Study	Year
Heilberger et al (Heilberger, Schunn et al. 1997)	1997
Sato et al (Sato, Goff et al. 1998)	1998
Thompson et al (Thompson, Boyle et al. 1998)	1998
McWilliams et al (McWilliams, Martin et al. 1999)	1999
Wolf et al (Wolf, Johnson et al. 2000)	2000
Zannetti et al (Zannetti, De Rango et al. 2000)	2000
d'Audiffret et al (d'Audiffret, Desgranges et al. 2001)	2001
Pages et al (Pages, Favre et al. 2001)	2001
Golzarian et al (Golzarian, Murgo et al. 2002)	2002
Greenfield et al (Greenfield, Halpern et al. 2002)	2002
McWilliams et al (McWilliams, Martin et al. 2002)	2002
Parent et al (Parent, Meier et al. 2002)	2002
McLafferty et al (McLafferty, McCrary et al. 2002)	2002
Bendick et al (Bendick, Bove et al. 2003)	2003
Raman et al (Raman, Missig-Carrol et al. 2003)	2003
Giannoni et al (Giannoni, Palombo et al. 2003)	2003
Napoli et al (Napoli, Bargellini et al. 2004)	2004
Elkouri et al (Elkouri, Panneton et al. 2004)	2004
AbuRahma(AbuRahma, Welch et al. 2005)	2005
Sandford et al (Sandford, Bown et al. 2006)	2006
Henao et al (Henao, Hodge et al. 2006)	2006

Endovascular abdominal aortic aneurysm repair necessitates serial follow up of patients to diagnose complications that could lead to potentially life threatening events such as aneurysm rupture. Typical surveillance protocols have been based on regular CT scanning post EVAR. Several researchers have attempted to devise a surveillance protocol for these patients based on Duplex ultrasonography with variable success Table 5.

Protocols for imaging and surveillance

Patients post EVAR are usually maintained in a registry and undergo regular surveillance scans usually with CT. Studies evaluating alternative imaging modalities have involved concurrent or paired imaging alongside regular CT scans. Most studies included in this literature review comparing DUS and CT for EVAR surveillance have analysed paired or concurrent DUS and CT examinations for patients (Wolf, Johnson et al. 2000, Zannetti, De Rango et al. 2000, Raman, Missig-Carrol et al. 2003, Sandford, Bown et al. 2006). These paired examinations have been performed within a specified time interval of each other to prevent inaccuracies in the study due to a time lag between the two imaging modalities. Surveillance protocols have involved scanning at 1 month, 3 months, 6 months, 1 year and at annual intervals thereafter unless complications were detected when departures have been made from the established protocol.

The protocol for CT examinations used for these studies has varied between using single phase CT scans (arterial phase scan) to complete triphasic scans (initial non contrast scan, arterial phase scan and delayed phase scan). Some studies have

employed a single arterial phase scan for EVAR surveillance to limit radiation exposure for these patients. The initial non-contrast scan performed prior to EVAR deployment was used as baseline for identifying calcification at subsequent scans. A delayed phase scan was performed only when a slow endoleak was suspected. Intravenous contrast was injected using a pump injector at a rate of 2.5 ml/s. The standard delay for the arterial phase was 28 sec and 60 sec after completion of the arterial scan for the delayed phase. The scanning parameters were similar for the studies utilising 5 mm collimation, 0.5 – 1 sec tube rotation, pitch of 2 and reconstruction every 3-5 mm.

The DUS protocol similarly remains largely uniform throughout these studies. A 2.0 to 3.5 MHz abdominal probe was used for the examination. Scanning began with identifying the limits of the stent graft in B-mode and assessment of its integrity, imaging the aorta from the coeliac artery origin down to the iliac bifurcation. Flow was confirmed within the aorta and iliac vessels and peak velocities compared to diagnose limb stenosis or kinking. The proximal and distal stent attachment sites were imaged, as were the origins of the inferior mesenteric, lumbar and renal arteries. Any flow seen in the peri-graft area was assessed closely to identify and classify endoleaks. Some researchers asked patients to be on a low residue diet the day before their scan, and to fast on the day of the scan to minimise bowel gas interference with scanning. For contrast-enhanced ultrasound, the agents used were Levovist and Optison, with either slow injection of the contrast agent through the ante-cubital fossa or through continuous infusion (Henao, Hodge et al. 2006).

Helberger et al (Heilberger, Schunn et al. 1997) were amongst the first to report the routine use of duplex ultrasonography for surveillance of patients post endovascular repair. They employed contrast-enhanced ultrasound using Levovist as the contrast agent for duplex. Although they did not report on the sensitivity and specificity of DUS compared to CT, they suggest that contrast-enhanced duplex was equivalent to CT in detecting major endoleaks and in fact was more sensitive in detecting slow flow type II endoleaks.

Duplex ultrasound

Sato et al (Sato, Goff et al. 1998) defined adequacy of duplex scans by four criteria, namely:

1. Satisfactory B-mode imaging of the AAA sac and the stent graft
2. Satisfactory colour Doppler imaging with no excessive overgain or undergain
3. Satisfactory colour Doppler assessment of the entire AAA sac in both longitudinal and transverse planes to screen for endoleaks
4. Spectral Doppler waveform confirmation of potential endoleaks

They retrospectively reviewed records from 117 concurrent CT and DUS examinations in 79 patients who had undergone EVAR. Despite reporting only 19% of their DUS scans to be adequate according to the above criteria, they found high sensitivity and negative predictive value for DUS (97% & 98% respectively) in diagnosing the presence of an endoleak post EVAR. They attributed their low specificity and positive predictive value (74% and 66% respectively) to the absence of

a standardised DUS protocol as their scans had been performed on patients across multiple sites using multiple DUS operators.

When comparing DUS and CT for detection and characterisation of endoleaks, Wolf et al (Wolf, Johnson et al. 2000) and Zannetti et al (Zannetti, De Rango et al. 2000), reported encouraging results for DUS. Specifically they have reported high specificity (95% and 98.4% respectively) and negative predictive values (90% and 99.4% respectively). Zannetti et al report good sensitivity for DUS (91.7%) in detecting the presence of endoleaks; however, when determining the source of the endoleak, this sensitivity drops to 66%. In their series, DUS failed to correctly classify two endoleaks as type 1, diagnosing them to be type 2 instead and failed to diagnose one endoleak seen on CT. They therefore conclude that although DUS could reduce the requirements for CT scanning, it could not completely replace CT for post EVAR surveillance. Wolf et al, however, report excellent results and conclude that DUS in experienced hands could provide results that are very similar to CT in detecting and classifying endoleaks. Their graft patency detection rates and aneurysm size measurements were also very similar for both modalities. They report that all endoleaks that DUS missed in their study were small, posterior endoleaks (Type 2 lumbar) and suggest that all leaks diagnosed on DUS and missed on CT were in fact true endoleaks associated with to-and-fro flow in the inferior mesenteric artery. They claim that both these classes of leaks were probably not clinically significant and suggest that DUS may be used for routine surveillance and follow up of patients post EVAR.

This theme is reproduced throughout the literature for proponents of DUS. Detractors, however point to the poor sensitivity and positive predictive value of DUS. Raman et al (Raman, Missig-Carrol et al. 2003) carried out retrospective reviews of 495 same-

day CT and DUS scans performed post EVAR and reported DUS to be 42.9% sensitive with a positive predictive value of 53.9% for detection of endoleaks. They suggest that these results could be attributable to being able to devote less time for individual DUS scans. They argue that as opposed to other studies reporting good results for DUS, they could only allocate approximately 20 minutes per scan and used older equipment and as such these technical factors might have had an impact on their results.

McLafferty et al (McLafferty, McCrary et al. 2002) have reported excellent endoleak detection rates (100% sensitivity, 99% specificity, 88% positive predictive value and 100% negative predictive value) for DUS as compared to CT, however, it has to be remembered that their methodology was different as compared to other series. As part of their on-going phase II and III trials evaluating the AneuRx stent graft, they carried out DUS surveillance one-month post stent graft placement. Their protocol did not include paired/concurrent CT and DUS scans; the DUS scan 1-month post EVAR was followed by a CT scan at 3 months if the DUS was positive for an endoleak, or a CT scan at 6 months if the DUS was negative for an endoleak. The sensitivity, specificity, positive and negative predictive values of DUS were calculated comparing DUS results at 1 month to the CT results at 3 or 6 months.

Contrast enhanced DUS

Several authors have evaluated contrast enhanced DUS as a modality of surveillance of patients post endovascular aneurysm repair (Heilberger, Schunn et al. 1997, McWilliams, Martin et al. 1999, McWilliams, Martin et al. 2002, Giannoni, Palombo et al. 2003, Napoli, Bargellini et al. 2004, Henao, Hodge et al. 2006). Heilberger et al

were among the first to employ contrast enhanced duplex for post EVAR surveillance. They used Levovist (D-Galactose and Palmitic acid) as an ultrasound contrast agent. As described previously, ultrasound contrast agents are made up of stable microbubbles that can be detected on ultrasound. Heilberger et al have reported excellent results with unenhanced DUS, detecting all major endoleaks except one that was thought to have been missed due to the presence of excessive bowel gas. Employing contrast enhanced DUS, they detected endoleaks that were not seen on either CT or catheter based angiography. As they did not consider CT to be their gold standard imaging modality, they argue that these leaks represent true endoleaks, thus reporting contrast enhanced DUS to be better at detecting endoleaks post EVAR. However, their results revealed that DUS was not as good as CT when evaluating graft integrity.

Using the same ultrasound contrast as Heilberger et al, McWilliams et al (McWilliams, Martin et al. 1999) performed a pilot study evaluating contrast enhanced DUS on 18 patients who also underwent single phase CT scans on the same day as the DUS. They found an increase in the sensitivity of duplex with the introduction of contrast, being able to diagnose all endoleaks visualised on CT. Further, they also diagnosed 6 false positive leaks on contrast-enhanced duplex, some of which were associated with an increase in the aneurysm sac size. They argued that these could in fact represent true endoleaks that were not visualised on single phase CT. A follow on study by the same group published in 2002 (McWilliams, Martin et al. 2002), compared unenhanced and contrast-enhanced duplex with biphasic CT. However, having followed up 53 patients with 96 scans, they could not replicate their earlier results. Although they reported the sensitivity of DUS to improve to 50% with the introduction of contrast (12% for unenhanced DUS), contrast enhanced ultrasound

missed 9 type 2 endoleaks in their series. They also reported 2 graft related leaks (types I or III), only one of these was diagnosed on ultrasound. The number of false positive endoleaks also increased with the introduction of ultrasound contrast; increasing from 4 on non-contrast DUS to 19 on contrast enhanced DUS.

Encouraging results were published by Giannoni et al (Giannoni, Palombo et al. 2003) employing Levovist for contrast-enhanced ultrasound. They found the sensitivity of DUS to improve to 100% with the introduction of ultrasound contrast. However, they too report a large number of false positives whilst detecting endoleaks. The overestimation of endoleaks with the introduction of ultrasound contrast is presumed to be a result of blooming of colour when the contrast agent reaches the site of investigation.

Contrast enhanced DUS using a second generation ultrasound contrast agent (Sonovue) was employed to further screen a group of 10 patients who were found to have enlargement of their post EVAR aneurysm sacs in the absence of endoleaks on CT and DUS by Napoli et al (Napoli, Bargellini et al. 2004). Contrast enhanced DUS detected endoleaks in all of these patients and these were confirmed in 8 patients on catheter angiography. The remaining 2 patients had unclassified leaks that were again confirmed on delayed CT. Napoli et al also subjected a further 20 patients to contrast enhanced DUS, 10 of whom had evidence of aneurysm shrinkage with no demonstrable endoleaks on either CT or DUS and a further 10 who had evidence of type 2 endoleaks on CT and DUS. These groups acted as controls for their study. Napoli et al employed low mechanical index 0.01-0.04 and real time tissue harmonic imaging for enhanced duplex ultrasound. These enhancements might explain their superior results.

Henao et al (Henao, Hodge et al. 2006) have again reported excellent endoleak detection rates with contrast enhanced ultrasound, albeit with a slightly different methodology. They used a second-generation ultrasound contrast media (Optison – Octafluoropropane and albumin) with a continuous infusion technique. Their DUS protocol was also modified to include harmonic imaging, reduced mechanical index of 0.4-0.5, compression of 1:3 and a focal zone positioned below the aorta to minimize microsphere rupture. They claim that these measures allowed for a longer scanning time. Though these measures have probably been responsible for their excellent results, their study also detected an additional 3 type 2 endoleaks that were not visualised on CT; these could be termed false positives when using CT as the gold standard.

DUS has been traditionally used for carrying out surveillance of patients known to have abdominal aortic aneurysms. Even though frequently used for this surveillance it has been acknowledged that DUS underestimates the size of abdominal aortic aneurysms as compared to CT (Lederle, Wilson et al. 1995). Specifically comparing these two modalities for estimation of AAA sac size post EVAR, there seems to be good correlation but poor agreement.

The general consensus therefore remains that DUS, although not at a stage to completely replace CT, can be a useful tool to reduce the number of CT scans that these patients have to undergo. The diagnostic accuracy of DUS does seem to increase with the introduction of contrast media; however, there is also a corresponding increase in the number of false positive endoleaks.

Conclusions

The common theme throughout most of these studies was that although Duplex is a relatively cheap imaging modality, its sensitivity in detecting complications in the post EVAR setting was low when compared to the gold-standard CT imaging. The specificity however was good as was its negative predictive value. The consensus view therefore was that Duplex remains an adjunct to CT for post EVAR surveillance. Its sensitivity in this patient group does not support its use a sole imaging modality.

Aims of the study

Our study has been designed to assess the existing limitations of duplex ultrasound for the surveillance of patients post endovascular repair of their abdominal aortic aneurysms. We propose to assess these limitations through the clinical arm of our study. We have introduced a surveillance protocol whereby patients post endovascular repair would undergo paired CT and DUS that would ideally be performed on the same day. CT scans would be reported by a team of vascular radiologists who would be blinded to the results of the Duplex scans. Similarly, a dedicated vascular laboratory with operators who have experience in ultrasonography of the post EVAR aorta would perform the Duplex scans. Similar to the vascular radiologists, the ultrasound operators would be blinded to the CT results.

In parallel, we have set up the laboratory experiment to ascertain the machine, operator dependant and independent characteristics of Duplex ultrasound that impact upon detection of complications in this setting. We propose to achieve this through the development and analysis of a non-anthropomorphic ultrasound phantom using novel tissue and blood mimicking materials to reproduce the acoustic events of the human aorta post endograft implantation. If successful, we would be able to ascertain whether the machine dependant parameters can be changed to improve the sensitivity of Duplex ultrasound to a level that would enable its use a sole surveillance modality for patients post EVAR.

Study design

EVAR has become an integral part of treatment protocols for abdominal aortic aneurysms, with many vascular surgical units across the UK now offering this minimally invasive approach for repair of abdominal aortic aneurysms. However, surveillance for patients post EVAR remains an important consideration. There has been a lack of consensus amongst vascular specialists for a standardised protocol for post EVAR surveillance and debate persists regarding the most appropriate imaging modality to carry out this surveillance (Heilberger, Schunn et al. 1997, Sato, Goff et al. 1998, McWilliams, Martin et al. 1999, Wolf, Johnson et al. 2000, Zannetti, De Rango et al. 2000, d'Audiffret, Desgranges et al. 2001, McWilliams, Martin et al. 2002, Giannoni, Palombo et al. 2003, Raman, Missig-Carrol et al. 2003, Elkouri, Panneton et al. 2004, Napoli, Bargellini et al. 2004, Henao, Hodge et al. 2006, Sandford, Bown et al. 2006).

Our study was designed to assess whether routine surveillance for patients post EVAR could be performed with Duplex ultrasound. CT based surveillance protocols have traditionally been favoured, CT scanning being regarded as gold standard imaging in major studies comparing different modalities (Heilberger, Schunn et al. 1997, Sato, Goff et al. 1998, McWilliams, Martin et al. 1999, Wolf, Johnson et al. 2000, Zannetti, De Rango et al. 2000, d'Audiffret, Desgranges et al. 2001, McWilliams, Martin et al. 2002, Giannoni, Palombo et al. 2003, Raman, Missig-Carrol et al. 2003, Elkouri, Panneton et al. 2004, Napoli, Bargellini et al. 2004, Henao, Hodge et al. 2006, Sandford, Bown et al. 2006). A significant proportion of post EVAR surveillance in the UK, including at our centre, has been dependant solely on CT scanning.

Our study was divided into a clinical and a laboratory arm. For the clinical part of our study, we organised for patients post EVAR who were previously being followed up

with regular CT scans, to have an additional DUS scan to be performed within a specified time period of the CT. For the laboratory part of the study, we designed a non-anthropomorphic ultrasound phantom that allowed us to assess the sensitivity of DUS when scanning patients post endovascular repair of their infra-renal abdominal aortic aneurysms. The aim of our study was to assess the sensitivity and specificity of DUS for the identification of endoleaks in the post EVAR setting as it currently stands and to ascertain the possibility of improving this through our non-anthropomorphic ultrasound phantom.

The laboratory arm

The laboratory arm of this project was designed to assess the limitations of Duplex ultrasound as a surveillance modality in the post EVAR setting. A novel ultrasound phantom was designed using tissue and blood-mimicking materials to simulate aspects of the blood flows and associated geometry of the abdominal aorta post endovascular aneurysm repair. The phantom was not an anthropomorphic depiction of the post EVAR aorta but enabled the evaluation of the key parameters of complications post EVAR. It also allowed for experimental control of the principal variables affecting ultrasonic imaging and measurement of the simulated blood flow of the post EVAR aorta. Also, the geometry of the phantom was such that key features determining the sensitivity of the ultrasound scanner could be assessed. A test protocol was formulated and various experimental set ups were evaluated by operators with varying levels of experience in vascular ultrasound.

Results were analysed to determine the limitations of duplex in detecting complications post EVAR. Inter-observer variations were analysed to determine the level of expertise required for accurate detection and classification of complications.

Phantom design

Endovascular repair of abdominal aortic aneurysms involves the placement of a stent-graft across the aneurysm from within the circulation. As discussed previously, major complications post EVAR include endoleaks, which have been thought to be responsible for most treatment failures beyond the first year. Endoleaks have been classified into 5 types depending upon their origin (Table 2). High flow and persistent low flow endoleaks can lead to continued pressurisation of the aneurysm sac that can result in its rupture. This and other potential complications such as graft fracture and migration have necessitated life long follow up of patients.

With ultrasound scanning, all endoleaks whether graft related or a result of back flow from the origins of other arteries within the aneurysm sac are visualised as flow separate from the aortic flow but within the aneurysm sac. This was used as the central theme when conceptualising the design of the phantom. The phantom consisted of a Perspex® (Lucite International, Memphis, Tennessee, USA) casing housing tissue mimicking material (TMM) i.e. the material has ultrasonic properties equivalent to human tissue. A stent-graft was placed centrally within the TMM and this simulated the ultrasound appearance of the abdominal aorta post EVAR. Flow channelled through this stent-graft depicted flow of blood through the aorta post endovascular repair. A second flow system, comprising of tubing of a significantly smaller diameter than the stent-graft, was used to simulate an endoleak. This second flow system ran obliquely along the length of the phantom and crossed the aortic stent-graft at its midpoint. Thus, the geometry of the smaller diameter flow system relative to the larger aortic flow allowed the opportunity to visualise their spatial relationships from different perspectives (Figure 5). This enabled the small flow to be

effectively ‘moved’ and hence be proximal or distal to the larger flow. A number of different endoleak scenarios could thus be repeatedly investigated.

Blood-mimicking fluid (BMF), that simulated the ultrasound properties of blood, was circulated in both the small ‘endoleak’ and large ‘aortic’ flow circuits. The flow rates in the two flow systems were different; BMF was pumped through the larger stent graft to simulate the appearance and flow characteristics of blood flowing through the abdominal aorta. BMF flow rates through the smaller endoleak flow were designed to simulate the typical range of clinical leaks and could be adjusted as an independent variable for each experiment.

The entire phantom could also be rotated along the axis of the large flow to enable the ultrasound operator to view the phantom from all sides. This arrangement gave a different view of the endoleak and the stent graft from each side of the phantom (Figures 1 & 2)

A test protocol evaluating various configurations of the geometrical and flow parameters was designed and used to evaluate the phantom by operators with varying levels of experience in vascular ultrasound.

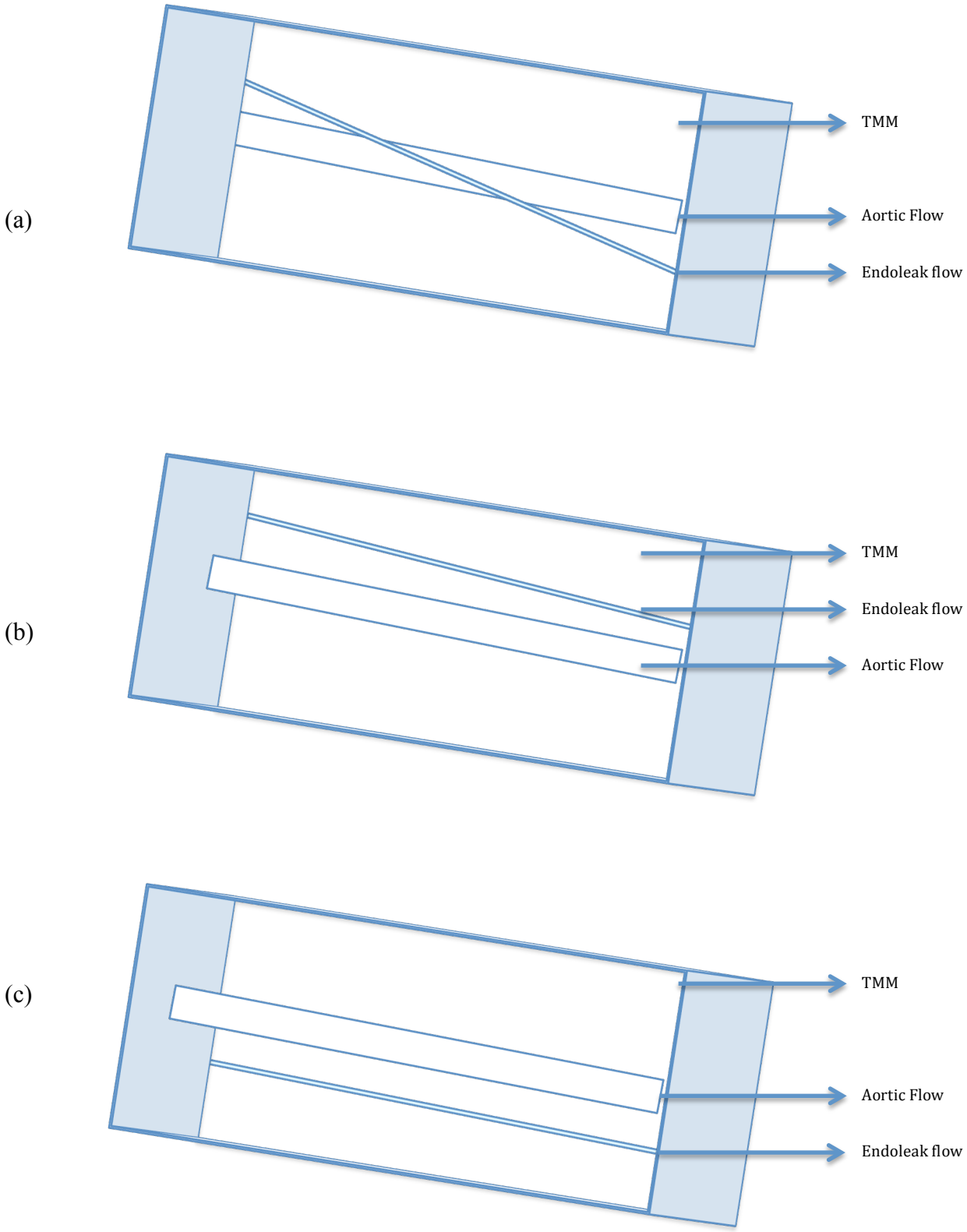

Figure 5: ***Schematic depicting the geometrical relationships of the small and large flows. (a) Tangential, (b) Proximal and (c) Distal planes. (For the purposes of depiction the small and large flow systems are some distance apart even though in the phantom they are exactly adjacent to each other at the point they cross each other.)***

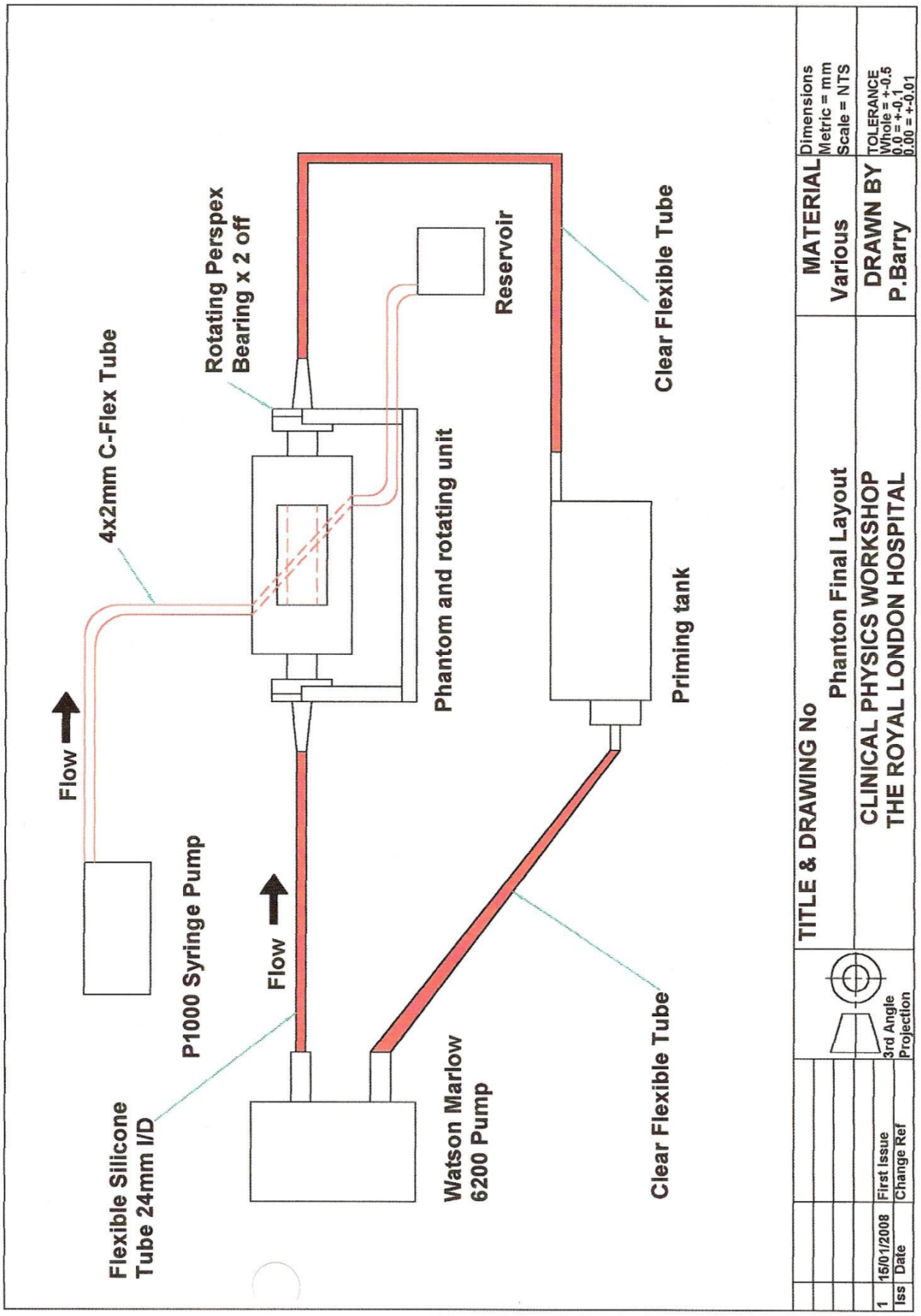

Figure 6: ***Schematic depicting the arrangements of the large (shaded) and small flow systems (unshaded)***

The Phantom

A custom-made 162 x 200 cm cuboidal Perspex box was used to house the ultrasound phantom. Perspex (methyl methacrylate) is a strong, lightweight acrylic material that has good impact strength and high environmental stability. A 24 mm inner diameter Medtronic Talent® (Medtronic Inc., Minneapolis, Minnesota, USA) aorto-uni-iliac stent graft was placed centrally within the Perspex box (Figure 7). When connected to the aortic flow, the ultrasonic appearance of this stent mimicked the human aorta post endovascular aneurysm repair. The centre of the aortic stent was equidistant at 81 mm from the viewing windows on all sides of the Perspex box.

A second flow system of a significantly smaller diameter, simulating an endoleak was placed obliquely across the aortic stent. The two flow systems were placed in such a way that they were exactly adjacent to each other at the point where they crossed over. A 2 mm inner diameter C-Flex® (Cole-Palmer, Walden, UK) tube was used for the smaller endoleak flow system.

C-Flex is a unique thermoplastic elastomer with a tensile strength that, at a diameter of 2 mm, resists collapse under pressure from tissue mimicking material. Its physical properties (good tensile and shear strength, good biocompatibility and chemical resistance with low gas permeability and a smooth surface) made it an ideal material to be used for our ultrasound phantom. C-Flex has been validated for use in Doppler flow phantoms with its reported speed of sound of being 1557 m/s with an attenuation coefficient of 24.1 dB cm^{-1} MHz^{-1} at a frequency of 5 MHz (Teirlinck, Bezemer et al. 1998, Browne, Watson et al. 2004, Brewin, Pike et al. 2008).

At the points of entry and exit of the small flow from the Perspex box, a 3mm stainless steel tube was used to connect the C Flex tubing within the phantom to the external circuit to prevent collapse of the second system and to make the phantom watertight (Figure 8).

Perspex has a high ultrasound attenuation coefficient making it difficult to be able to view the Doppler flow phantom with the ultrasound scanner. A low density polyethylene (LDPE) viewing window was therefore built into each side of the Perspex box for the operators to scan the phantom. LDPE is a thermoplastic polymer made from ethylene with a low ultrasound attenuation coefficient. It is a flexible but tough material that is largely non-reactive at room temperatures. Five viewing positions were marked on the LDPE viewing windows that corresponded to five geometrical combinations of the main aortic flow and the small flow.

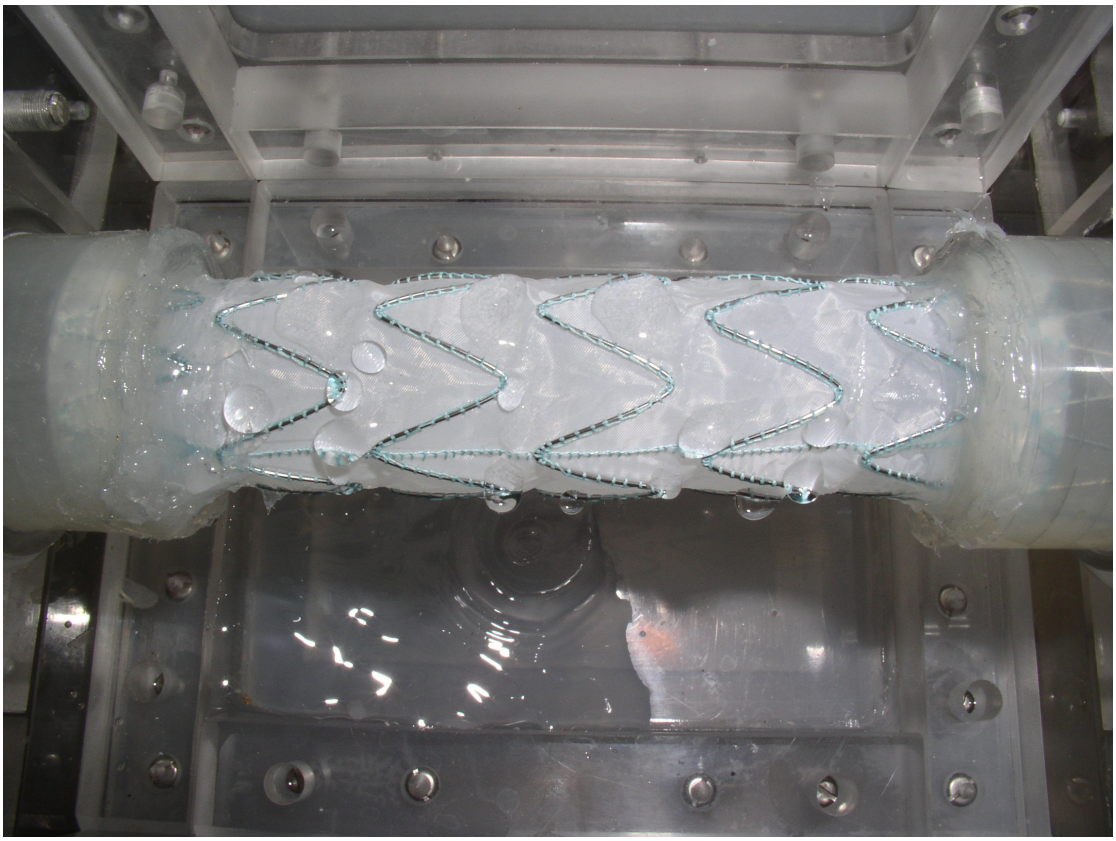

Figure 7: ***Photograph of the phantom in construction. EVAR graft deployed into the Perspex box.***

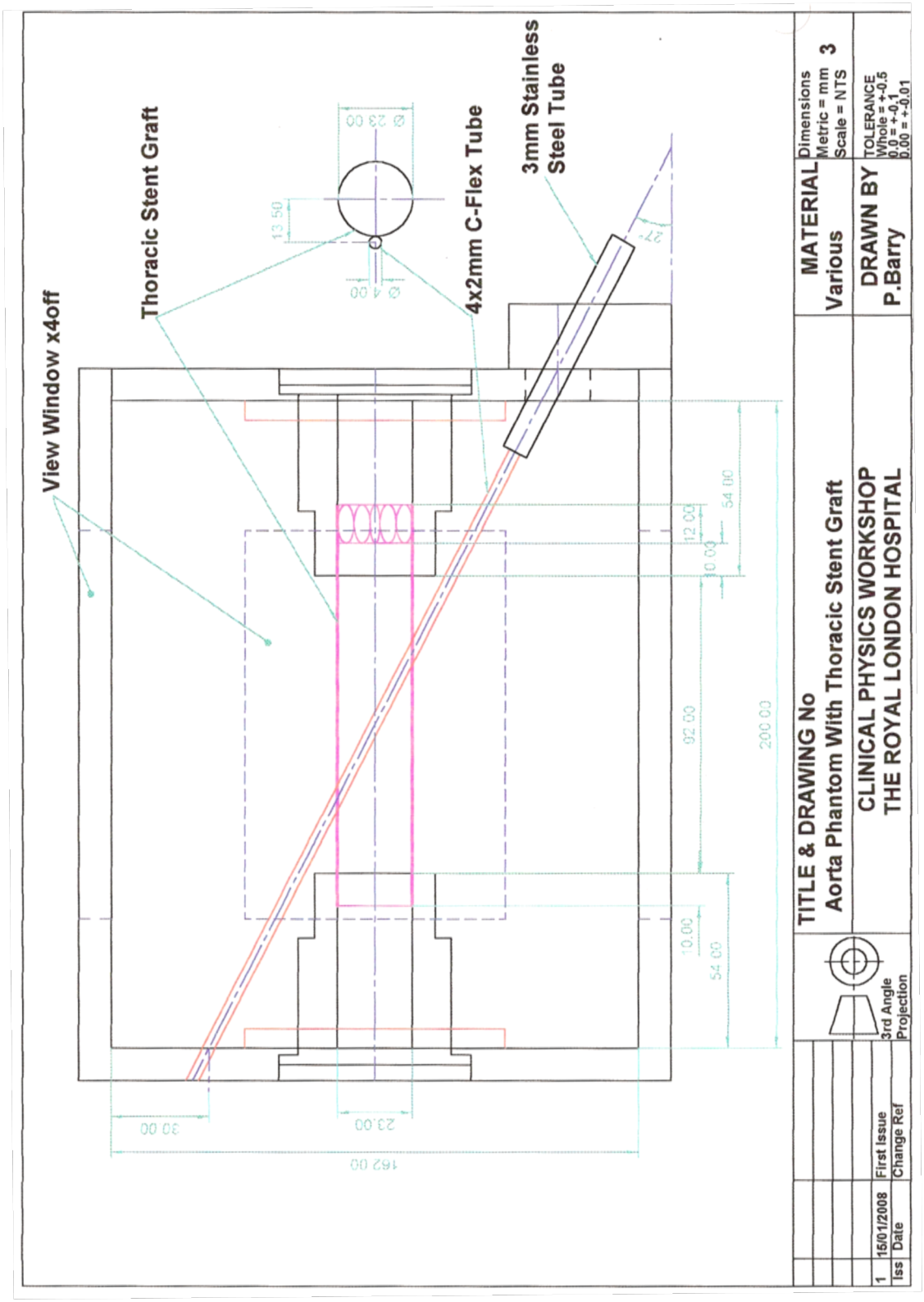

Figure 8: ***Schematic of the phantom depicting the Perspex casing, the aortic and "endoleak" flow geometry and the LDPE viewing windows.***

Assessments were performed in all the 3 planes [Proximal (second smaller flow proximal to the stent graft), distal (second flow distal to the stent-graft) and the tangential (second flow running tangentially across the stent-graft) planes] (Figure 9). To prevent the direction of endoleak flow from being perpendicular to the ultrasound beam in the proximal and distal planes, and to maintain the spatial arrangements at the specified viewing positions, the experiment was set up in such a way that the ultrasound transducer probe was placed at an arbitrary angle of 70° to the viewing window. A mobile visual guide was attached to the phantom that allowed the operators to align the ultrasound probe at the required angulation. For assessment of the tangential plane, the ultrasound probe was held perpendicularly to the LDPE viewing window. The visual guide could be moved to achieve this setting at all five viewing positions in all three planes. This arrangement corresponded to the cross sectional views as demonstrated in Figure 10.

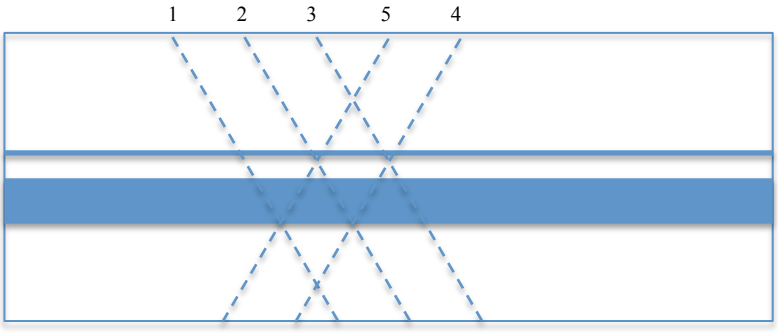

Proximal plane

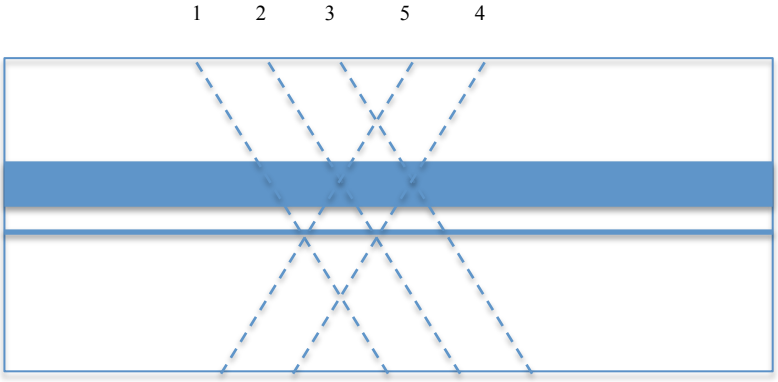

Distal plane

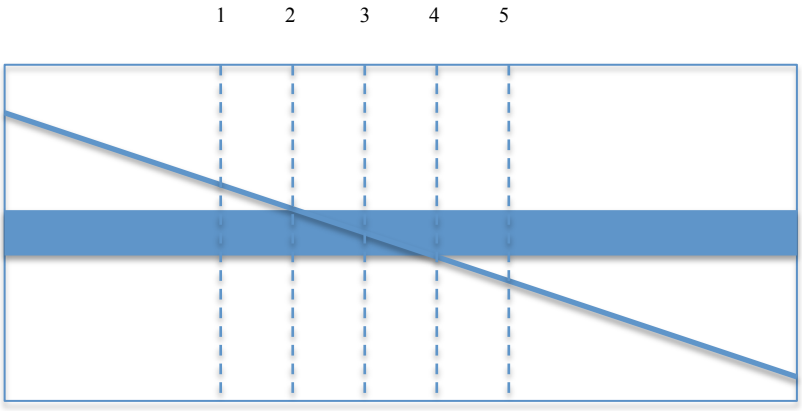

Tangential plane

Figure 9: ***Viewing position schematics for the three planes. For the proximal and distal planes, the probe was held at 70° to avoid the ultrasound beam being perpendicular to the direction of the small flow (numbers correspond to respective viewing positions).***

Proximal Plane

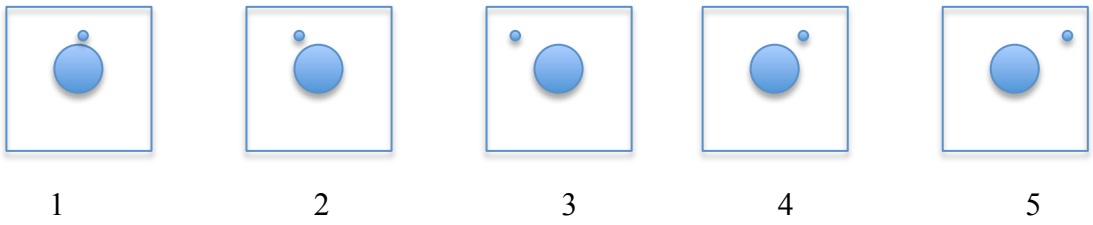

Distal Plane

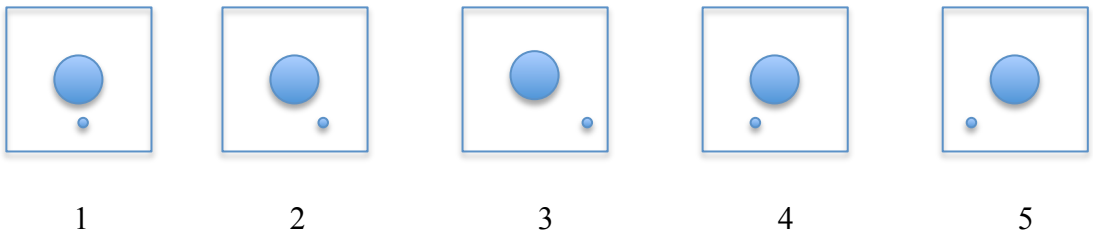

Tangential Plane

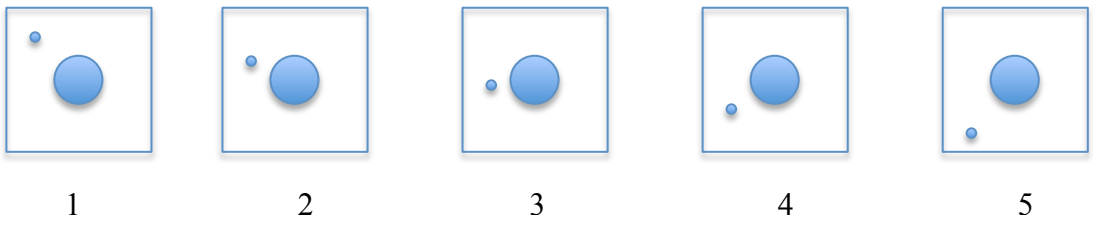

Figure 10: ***Cross sectional schematics corresponding to the viewing positions in all the planes. Large circle corresponds to large flow and small circle to small flow. Numbers correspond to the viewing positions. (For depiction purposes only, actual distances between the small and large flows are as in table 1)***

The distances between the two systems were predetermined and thus enabled experimental control (Table 6)

Table 6: ***Distances between large and small flows corresponding to the viewing windows for the three planes***

	Centre – Centre distance (mm) between large and small flows					Edge – Edge Distance (mm) between large and small flows				
Positions	1	2	3	4	5	1	2	3	4	5
Proximal	14.8	18.4	24.4	19.8	26.1	0.8	4.4	10.4	5.8	11.1
Distal	15.9	24.4	34.9	26.9	37.7	2.9	10.4	20.9	12.9	23.7
Tangential	22.8	16.6	14	16.6	22.8	8.8	2.6	0	2.6	8.8

The depth of the large flow from the viewing window was constant at 81 mm for all planes. The depth of the small flow from the viewing windows was the same for all viewing positions for the proximal and distal planes respectively. For the tangential plane, the depths were as tabulated in Table 7.

Table 7: ***Depths of the small flow from the viewing windows for the three planes***

Depth of small flow from viewing windows (mm)					
Positions	1	2	3	4	5
Proximal	67	67	67	67	67
Distal	95	95	95	95	95
Tangential	63	72	81	90	99

Stent Graft

A 24 mm inner diameter Medtronic Talent stent-graft was deployed within the TMM. The first reports of stent-graft deployment were by Parodi et al (Parodi, Palmaz et al. 1991). Those initial stent-grafts were custom-made, hand-sewn devices that comprised a balloon expandable metallic stent sutured to overlapping Dacron® grafts. Stent-grafts have evolved enormously since those early days and are now complex devices with advanced delivery mechanisms. Stent-grafts nowadays are commonly composed of nitinol stents with Dacron grafts. The metallic stent forms the skeleton of the device. The Dacron component is required for the device to be impervious to blood, thus excluding the aneurysm sac from the circulation. Attachment of the stent-graft to the aorta is by means of either hooks or barbs that attach it to normal aortic wall. Some devices attach to the aortic wall by means of radial force and polymer seals. Commonly used abdominal aortic stent grafts include the Medtronic Talent and Endurant® devices, the Gore® Excluder® device (W L Gore & Associates, Inc. Newark, Delaware, USA) and the Cook Zenith® device (Cook Group Inc., Bloomington, Indiana, USA).

Our Doppler flow phantom utilised a Medtronic Talent aorto-uni-iliac stent-graft with internal diameter of 24 mm. Endoleaks, as described previously, are areas of flow within the aneurysm sac but outside the stent-graft and are classified into several types depending upon their origin. From the point of view of Doppler ultrasound recognition of endoleaks, they could be considered to be a second flow visualised separate from the main aortic flow. This theme was used to design our phantom. A straight aorto-uni-iliac tube graft rather than a bifurcated stent-graft was therefore used in the phantom.

Pumps

The small and large flows pumped blood-mimicking fluid through the phantom at different rates utilising two separate pumps. The larger 'aortic' system required high velocities to mimic the flow of blood through the human aorta. Flow rates through the human aorta vary from 1.5 to 6 L/min from the resting to the post exercise state (Chandran 1993). We aimed to reproduce the natural pulsatility and flow characteristics of the abdominal aorta as far as possible with a commercially available pump and thus used a Watson-Marlow 620U IP31 NEMA2 peristaltic pump (Watson Marlow Pumps, Falmouth, Cornwall, UK). This pump provided constant, pulsatile flow that mimicked blood passing through the human abdominal aorta. The flow rate through our stent graft was maintained at 14.4 cm/s, 3900 ml/min.

The pump was set at 45 rpm that provided us with a simulated pulse rate of 90 beats per minute (Figure 10). As the pump revolutions increased, the maximum and minimum speeds started to diverge and the pulsatility of the flow became more apparent. At 45 rpm, the flow was pulsatile providing 90 beats per minute. At higher rpm's the pulsatility of flow was more evident however this lead to the introduction of artefacts and they were not representative of the human heart rate. The pump setting was therefore programmed at 45 rpm, providing pulsatile flow and being representative of the human heart rate.

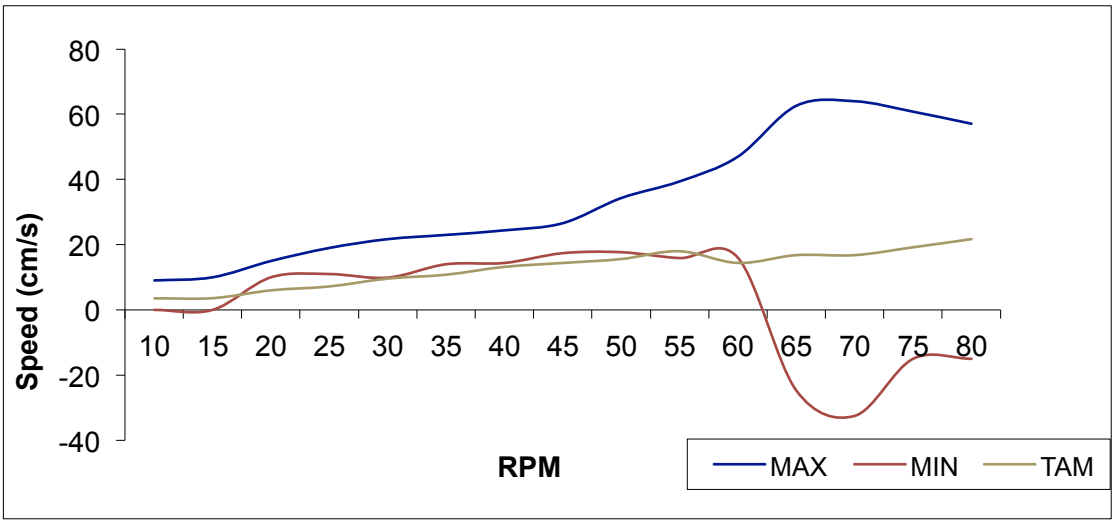

Figure 11: ***Graph to show blood flow speed in main flow against RPM of the pump (Maximum, minimum and time average mean)***

An IVAC 570 (CareFusion, San Diego, California, USA) infusion pump was used for the secondary flow. This pump provided a standard flow through the endoleak system and allowed the rate of flow to be experimentally manipulated. This enabled assessment of the impact of varying flow rates on determination of the presence of flow.

Tissue mimicking material

Tissue mimicking materials, as the name suggests, mimic the ultrasonic properties of tissue and are used in the development of ultrasound phantoms. Ultrasound phantoms and tissue mimicking materials have been in existence or a long time. Several different materials have been used as TMMs such as soft plastics (plastisols, urethane polymers), gels and other polymers. The TMM used in our phantom was an agar based. The recipe had been put forth by Teirlinck et al (Teirlinck, Bezemer et al. 1998) and conformed to the IEC 1685 draft specifications (International Electrochemical Commission) for flow Doppler test objects (International Electrotechnical Commission 2001). The composition of the TMM is detailed in Table 8.

Table 8: ***Composition of tissue mimicking material***

Component	**Wight composition (%)**
Distilled water	82.97
Glycerol	11.21
Silicon Carbide (≈ 37μm)	0.53
Aluminium oxide (3 μm)	0.94
Aluminium oxide (0.3 μm)	0.88
Rodalon (Benzalkonium Chloride)	0.46
Agar	3.0

The glycerol component of the TMM is responsible for providing the required speed of sound, the benzalkonium chloride prevents growth of microorganisms and the particulate matter composition (Al_2O_3 and SiC) modify the attenuation and backscatter (Ramnarine, Anderson et al. 2001, Brewin, Pike et al. 2008). The TMM is

prone to desiccation and degradation that necessitates careful handling and adequate housing. To overcome these potential problems, our phantom was placed inside a Perspex casing. A dedicated port was also built into the housing to maintain hydration of the TMM.

Blood mimicking fluid

A commercially sourced ATS 707 Doppler test fluid (ATS Laboratories Inc., Bridgeport, Connecticut, USA) was used as the blood mimicking fluid. Its physical properties are detailed in Table 9.

Table 9: ***Physical properties of blood mimicking fluid***

Speed of sound	1571 m/s ± 1%
Density	1.04 ± 0.01g/cc
Viscosity	1.66 ± 0.1 centistokes
Particulate size	30 ± 3 μm mean diameter
Particulate concentration	$1.7 \pm 0.1 \times 10^4$ particles/cc

The same blood mimicking fluid was circulated through both the aortic and endoleak flow systems care being taken to avoid any air bubbles to enter the system.

Independent flow systems

Two independent flow circuits were established, a large flow system with the aortic pump mimicking blood flow through the abdominal aorta and a small flow system representing the endoleak. The "heart" of the system was the aortic pump. Blood mimicking fluid draining from the aortic phantom was collected into a reservoir, from where it was cycled back into the inflow of the aortic pump (Figures 2 & 7). (needs updating)

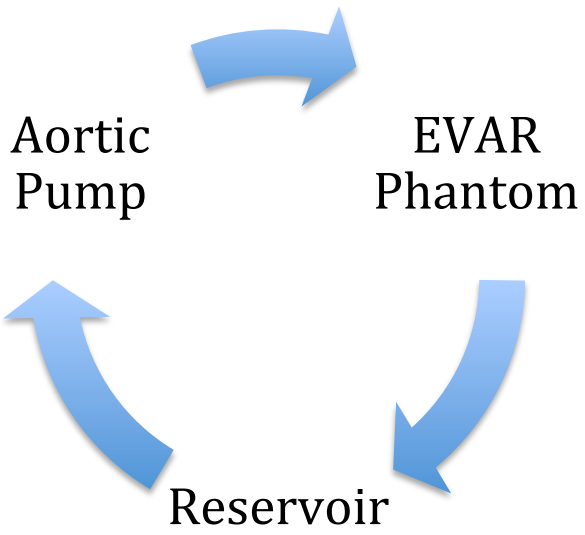

Figure 12: ***Large aortic flow***

The second system simulating the endoleak had a significantly smaller diameter. A C-Flex tube with an internal diameter of 2 mm was used for this system. Blood mimicking fluid from a drop bag was pumped through this tube (inside the phantom) by an infusion pump (IVAC 570) and outflow from the tube collected and re-circulated through the pump (Figures 2 & 8).

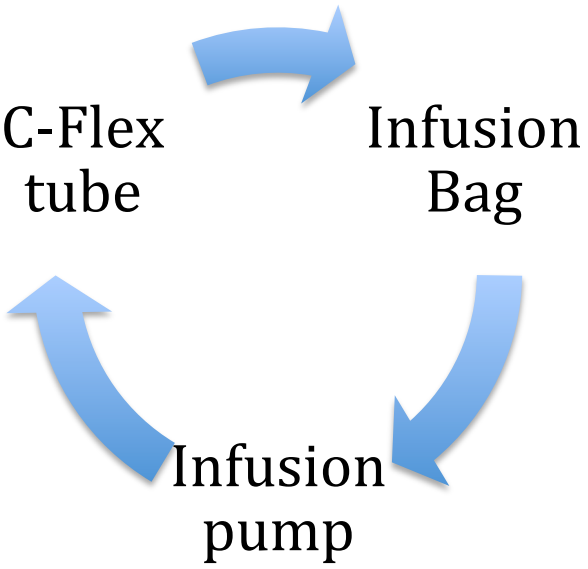

Figure 13: ***Small endoleak flow***

Phantom validation

Our phantom was developed in conjunction with ultrasound physicists and sonographers who helped with the design of the phantom. These physicists and sonographers were also part of the team who carried out surveillance for the clinical arm of the study. The tissue mimicking material used for the phantom was agar based; the recipe had been developed by Teirlinck et al (Teirlinck, Bezemer et al. 1998). Browne et al (Browne, Ramnarine et al. 2003) assessed the acoustic properties of this agar based tissue mimicking material and found acoustic velocity to remain relatively constant despite increasing frequency of ultrasound. The attenuation demonstrated a liner response to increase in frequency. These characteristics were in line with recommendations made by the IEC 1390 standard (International Electrochemical Commission 1996).

The acoustic properties of this tissue mimicking material at the frequencies used in our laboratory project had been determined by Brewin et al (Brewin, Pike et al. 2008). They demonstrated good agreement with expected values of the attenuation coefficient and speed of sound, with two independent laboratories confirming agreement. The spectral slope of the backscatter power also compared favourably with theoretical spectral slope values. The TMM retained its acoustic properties over a three-year period. We therefore decided on using this particular TMM as it had been tested and validated for use in an ultrasound phantom. Its properties were consistent and showed minimal degradation over time.

Ultrasound flow models using TMM have been used and evaluated for recreating events within the human body. Browne et al (Browne, Watson et al. 2004) assessed and validated a sensitivity performance index test protocol, evaluating a range of

ultrasound scanners. The material that we used for our small flow system (C-Flex) was validated by the same group and has been proven to resist collapse despite being embedded in TMM.

The flow systems and the general design of our phantom was developed in conjunction with ultrasonographers who were involved in the clinical part of our project and were familiar with the ultrasonic appearance endoleaks associated with the post EVAR aorta. The phantom was designed as a realistic physical interpretation of acoustic events within the human aorta post endovascular repair of aortic aneurysms.

The validation of this phantom lay in its construction and design. The various components including the TMM and C-Flex had been chosen through previous research. Valuable input from the sonographers and physicists had helped with the designing of the flow systems specifically the concept of two independent flow systems, providing a non-anthropomorphic phantom that allowed for experimental control of our test variables.

Test design and setup

Once assembled, the phantom was evaluated to ensure its compliance with the basic specifications of Doppler flow phantoms (Teirlinck, Bezemer et al. 1998, Browne, Watson et al. 2004). The phantom was also evaluated to assess whether it was able to provide the functionality required for assessing the limitations of DUS in the post EVAR setting.

A number of different flow and geometrical configurations were assessed to establish the limits of flow in the small endoleak system that could be visualised by duplex (Browne, Watson et al. 2004). A test protocol was formulated in collaboration with ultrasound physicists, consisting of different geometrical and flow rate combinations (Table 11). The flow rates were established keeping in mind reported rates for slow and fast type II endoleaks (Arko, Filis et al. 2003)

Prior to the phantom being assessed by the test operators, the phantom was evaluated by the ultrasound physicists to ensure that our experimental setup was a realistic representation of the ultrasonic appearance of events in the post EVAR aorta. After developing the test protocol (Table 11, Appendix 3 & 4), the phantom was bench tested with all the various flow and geometrical configurations (Table 11) and two sets of expected observations were derived 30 days apart. These expected observations were graded on a scale of 0-3

0 = no visualisation of flow

1 = Possible visualisation of flow

2 = Probable visualisation of flow

3 = Definite visualisation of flow

Doppler ultrasound diagnosis of the presence of an endoleak essentially depends upon detection of a smaller, second flow outside of the stent-graft, but within the native aneurysm sac. We extrapolated this concept to the visualisation of a small flow adjacent to a large stent-graft flow. Type 2 endoleaks are a result of back flow into the aneurysm sac from native branches of the aorta. These are typically small arteries such as the lumbar arteries or the inferior mesenteric artery. Back flow through these arteries is usually slow. Type 1 endoleaks are from the stent-graft attachment sites and have typically faster flow rates. Type 3 endoleaks are a result of modular disruption of the stent-graft and behave in a similar fashion to type 1 endoleaks tending to be faster. Several flow rates in the smaller 'endoleak' system were therefore assessed to ascertain the impact of flow rates on Doppler ultrasound detection of flow.

Some endoleaks could be difficult to visualise due to their proximity and geometrical relationship with the main aortic flow. The phantom was designed keeping this in mind. The geometry of the phantom and the ability to rotate the phantom along the larger flows' axis, allowed for assessment of several geometrical combinations of the small and large flows. The test protocol therefore consisted of assessments in three planes, with the smaller system running tangential, proximal and distal to the main aortic flow. The impact of proximity and the spatial relationships of the smaller and larger flows on visualisation of the small flow by DUS could thus be assessed.

Another criticism of DUS as a surveillance modality has been its operator dependant nature. Several studies have reported varied success using DUS as a surveillance modality post EVAR, the variability being partly blamed on the operator dependant nature of DUS (Heilberger, Schunn et al. 1997, Sato, Goff et al. 1998, McWilliams,

Martin et al. 1999, Wolf, Johnson et al. 2000, Zannetti, De Rango et al. 2000, d'Audiffret, Desgranges et al. 2001, McWilliams, Martin et al. 2002, Giannoni, Palombo et al. 2003, Raman, Missig-Carrol et al. 2003, Elkouri, Panneton et al. 2004, Napoli, Bargellini et al. 2004, Henao, Hodge et al. 2006, Sandford, Bown et al. 2006). We attempted to assess whether the level of technical expertise of the DUS operator plays a part in detection of complications post EVAR. To ascertain this and to assess reproducibility of results by different operators, our study group consisted of three operators with varying levels of experience in performing vascular ultrasound (specifically post EVAR ultrasound).

All our test operators were experienced in vascular ultrasound and were also part of the clinical arm carrying out surveillance Duplex scans for patients post endovascular aneurysm repair. However, their level of experience in performing post EVAR duplex surveillance varied from 1 year to 10 years. Two sets of observations were recorded for every operator 30 – 45 days apart. For the purposes of interpretation these two sets of observations recorded for each operator were treated as independent observations. Observers were asked to rate flow visualisation on a scale of 0-3

All evaluations were preformed with an ATL HDI 5000 (Royal Philips Electronics, Amsterdam, Netherlands) ultrasound scanner. The Curvilinear C5-2 abdominal transducer was used for the assessments. This probe generates 2-5 MHz ultrasound signals, is curved and is typically used for assessments of the abdomen. The ultrasound scanner was pre-set to Abdominal EVAR protocol (Table 10) with similar settings as used to scan patients post EVAR, however the operators had freedom to vary the gain and Pulse repetition frequencies (PRF's). During clinical ultrasonography, sonographers usually adjust gain and PRF's to obtain the best

possible views and minimize blooming of colour. Figure 14 depicts typical Doppler images of the phantom.

The small vessel infusion bag was filled with blood mimicking fluid (ATS model 707) and attached to the infusion pump (IVAC 750). Prior to initiating the test, the flow systems were cleared of any air bubbles. The outflow of the large 'aortic' flow automatically re-circulated through the priming tank. However, for the small 'endoleak' flow system the outflow had to be manually collected and re-circulated through the phantom.

Table 10: ***Pre-set ultrasound settings for scanning the phantom***

Probe	C5-2
Dynamic range	170 dB
Compression Curve	2
Persistence	Med
2D Optimisation	General
Thermal index	0.4
Mechanical Index	1.1

The large vessel flow was connected to the aortic pump (Watson-Marlow 620U IP31 NEMA 2 pump) that was set at a fixed rate of 45 rpm to simulate the heart beating at 90 beats per minute. Prior to the test being initiated, the system was primed with the aortic pump running at 100 rpm for about 30-45 minutes with a wire mesh filter, placed over the reservoir outlet / pump inlet pipe, ensuring that any circulating residue remained within the priming tank and did not interfere with evaluations.

Table 11: ***Test protocol (Viewing positions correspond to figures 4 & 5. 10 observations per observer per plane, total of 180 observations were obtained)***

Distal plane	Viewing position	5	5	4	4	1	1	2	2	3	3
	Flow rate in small vessel (ml/hr)	500	300	300	700	300	700	300	500	300	500
Tangential	Viewing position	1	5	2	4	3	1	4	4	5	2
	Flow rate in small vessel (ml/hr)	300	300	500	500	700	700	700	900	900	900
Proximal	Viewing position	5	5	4	4	1	1	2	2	3	4
	Flow rate in small vessel (ml/hr)	500	300	300	700	300	500	300	500	300	300

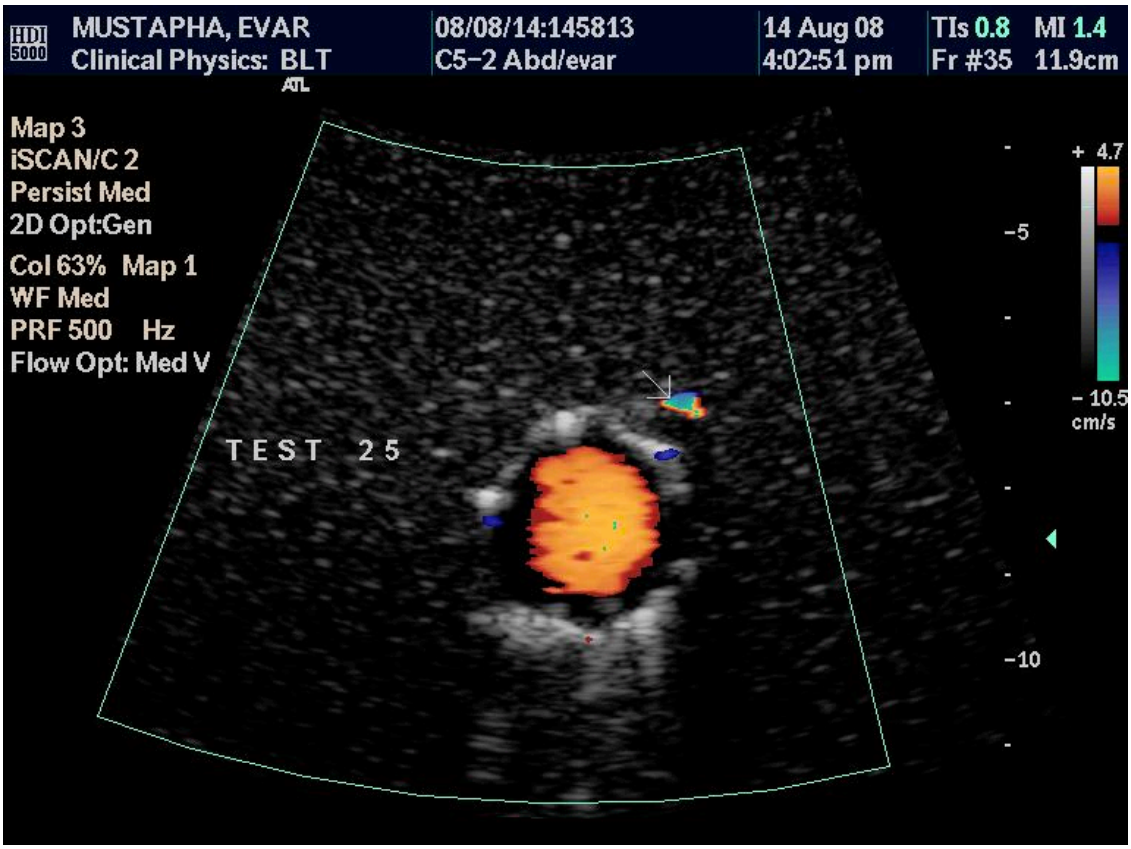

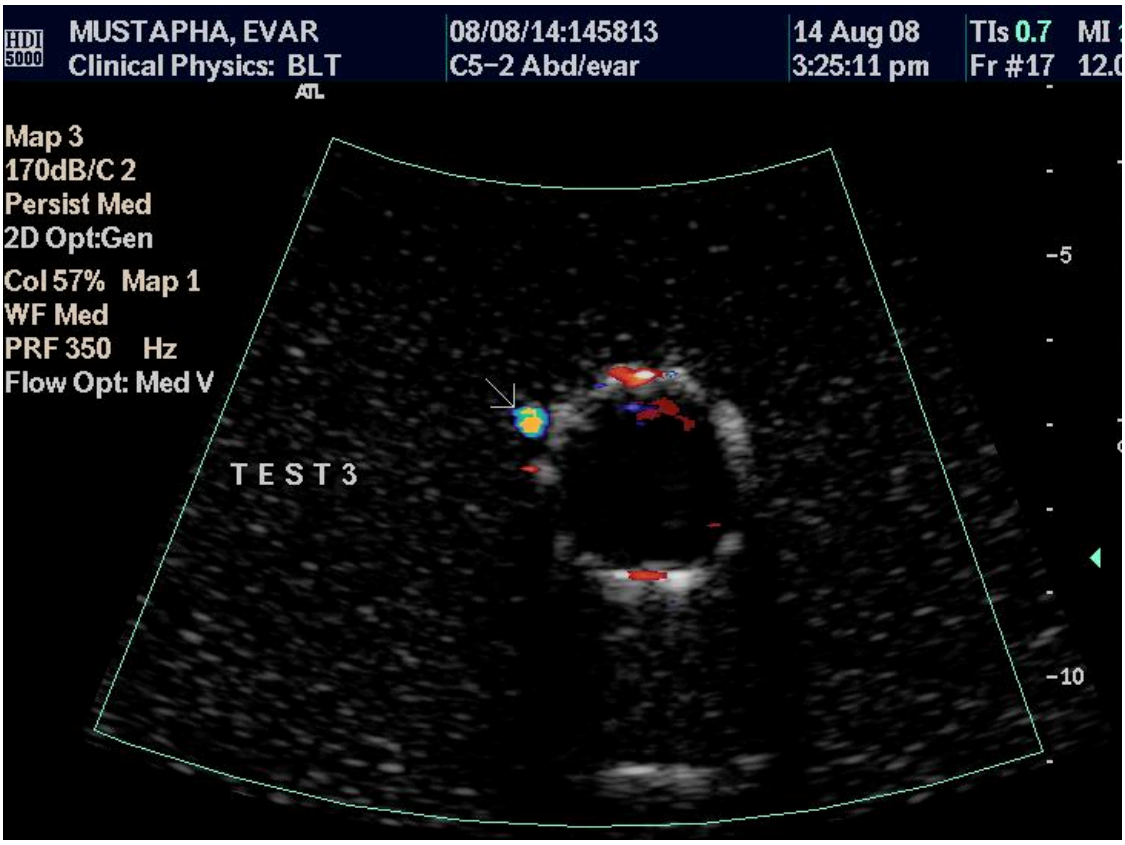

Figure 14: ***Duplex appearance of the flow phantom***

The clinical arm

The clinical arm of our project aimed at identifying the limitations of duplex ultrasound for the detection of endoleaks in patients post EVAR. EVAR has been performed at Barts and The London NHS Trust since August 2000. Traditionally, similar to other centres throughout the world, surveillance for these patients was carried out with CT scans that were performed pre-discharge, at 6 weeks, 3 months, 6 months, 12 months post procedure and then annually thereafter.

Duplex ultrasound scanning was introduced into the protocol for surveillance of patients post EVAR for this study. A new surveillance protocol was designed that included both CT and duplex scans, ideally both scans being performed on the same day. As part of this new protocol, patients would undergo a CT scan and duplex scan on the same day at 6 weeks, 3 months, 12 months and annually after endovascular repair of their aneurysms.

One hundred and thirteen patients underwent EVAR between August 2000 and August 2008 and were entered into our prospective trust-wide registry. Eighty-nine patients were male, with a mean age of 76.6 years (Table 12). The predominant device used for EVAR was the Cook Zenith endograft. This endograft is made of stainless steel stents that provide the exoskeleton for a woven polyester graft. The endograft employs supra-renal fixation, achieving proximal sealing with radial force and barbs that attach to the aortic wall. One hundred patients underwent elective repair of their aneurysms, thirteen were emergencies (2 symptomatic, 11 ruptures).

Patients were followed up for an average of 18.5 months (range 3-91 months). 13 patients died during the study period. Another 7 patients were either lost to follow up or had their follow up scans at their local hospitals that were unavailable to us.

Table 12: ***Patient demographics***

Patients, n	113
Demographics	
Mean age (range) years Gender, male (%)	75.06 (51-91) 84 (74.33)
Device used (%)	
Cook Medtronic Gore Lemaitre Endologix	74 (65.4) 30 (26.5) 7 (6.1) 1 (0.8) 1 (0.8)
Timing of EVAR	
Elective	100
Emergency Symptomatic Ruptures	13 2 11

Compliance with instructions for use of these devices was compared with their anatomy as seen on their pre-operative CT scans (Table 13). Seven patients (6.1%) had anatomy that was outside the instructions for use for the corresponding endograft deployed.

Table 13: ***Non compliance with device instructions for use***

Non-compliance with instructions for use (n=7)	
Neck length	2
Angulation	4
Neck diameter	1

Two patients had short proximal neck lengths. One of these patients had been treated with the Cook Zenith endograft (neck length 10 mm) and the other with the Endologix Powerlink device (neck length 11 mm). 4 patients had proximal neck angulation that was more than specified by the respective instructions for use. 3 of these had been treated with the Cook zenith device (angle with the long axis of the aneurysm 64, 61 and 75) and one with the Gore device (angle with the long axis of the aneurysm 75). One patient treated with the Medtronic device had a proximal neck diameter measuring 33 mm.

Up to January 2006, patients had been followed up with regular CT scans as described above. Pre-discharge and 3 month post discharge, patients underwent either CT or DUS. These scans was performed depending upon the findings from the intra-operative post-procedure angiogram or surgeon preference. Since January 2006, all patients in our EVAR registry underwent surveillance with both CT and DUS; scans being performed at 3, 6, 12 months post discharge and annually thereafter. It was

attempted to perform both the CT and duplex scans on the same day, however this was not always possible. Duplex and CT scans performed within 8 weeks of each were considered as paired scans for our study. All patients post EVAR also routinely underwent a pre-discharge duplex scan, CT being performed only if complications were detected on the duplex or at the completion angiogram. A 6-week scan was done at the discretion of the operating clinician, usually performed if the completion angiogram or pre-discharge scan revealed complications that warranted further follow up prior to the 3 month scan. Pre-discharge scans were included in our study if both the imaging modalities were performed within a week of each other. Similarly 6 week scans were included if the CT and DUS scans occurred within 3 weeks of each other.

Endoleaks were defined as areas of persistent flow outside the stent but within the aneurysm sac and were classified as types 1-5 (Table 2) (Veith, Baum et al. 2002).

All operators performing the duplex scans were blinded to the results of the corresponding CT scan. However, it was not always possible to blind the radiologists reporting the CT scans to the results of the duplex scans. This was especially the case when CT scans were performed as a result of findings of the duplex scans. Pre-discharge CT scans were only performed when duplex scans reported complications.

Scans that had been performed outside of the above surveillance protocol but were paired with corresponding CT or DUS scan as defined (Pre-discharge scan within 1 week of each other, 6 week scan within 3 weeks of each other and for the other scans – within 8 weeks of each other). For the purposes of this study, unpaired scans were excluded from analysis. DUS scans that had been reported as suboptimal/inadequate were also excluded from analysis.

All endoleaks detected on either CT or DUS were discussed in a multi-disciplinary setting. Patients with endoleaks associated with aneurysm sac size enlargement were considered for further intervention. Sac size increase of more than 5mm were considered significant and decisions were made regarding further management depending on patient characteristics. Both the CT, DUS scans and reports were made available to the clinicians deciding on further management.

Interventions performed included diagnostic catheter angiography, proximal or distal stent-graft extensions, embolisation, realignment, explantation and conversion. Patients that required interventions due to complications being detected on surveillance were re-entered into our surveillance protocol. All paired scans that had been performed between January 2006 and August 2008 were included in the study.

CT protocol

The CT scan protocol traditionally favoured for post EVAR surveillance has been the triphasic protocol. This includes an initial non-contrast scan, an arterial first pass scan and a delayed phase scan (Rozenblit, Patlas et al. 2003). At our institution, to minimise radiation exposure for patients, routine surveillance scans were performed with only an arterial first pass scan. An initial non-contrast scan was performed for every patient prior to undergoing EVAR; this was used as a baseline for confirming areas of calcification on subsequent scans. A delayed phase scan was only performed if there was a suspicion of complications on the first pass scan.

All scans were performed on a 64 slice multi-row detector CT scanner (Siemens Somatom). The protocol for abdominal aortic imaging was 0.6 mm slice collimation, 5mm slice width, pitch factor of 1.2 and feed/rotation of 23.0 mm. there was a 10 -15 sec delay for contrast injection for the arterial phase. Contrast was injected at a 3 – 3.5 ml/s, and a total contrast dose of 100 – 120 ml was used.

Post procedure surveillance CT scans were reviewed by one of four interventional radiologists who were part of the team performing endovascular aneurysm repairs at our institution. All scans were reviewed on a workstation with capabilities for multi-planar reconstruction (MPR). Scans were reported to a standard protocol including the maximal aneurysm sac diameter, integrity and anatomical location of the sent graft, endoleaks and their source; and any other complications, if present. Endoleaks were classified as previously described (Table 2). Accurate endoleak classification was achieved by assessing the anatomical location of the endoleak, density of the endoleak and patency of the IMA, lumbar arteries. Comparisons were made with the non-

contrast images and particular attention was paid to the sealing, overlap zones of the endograft (Gorich, Rilinger et al. 1999, Stavropoulos, Clark et al. 2005). Endoleaks related the proximal and distal attachment sites were classified as type 1, those related to the lumbar and inferior mesenteric arteries as type 2, whilst those originating adjacent to modular stent attachment sites were classified as type 3.

All CT scans were also externally reviewed and validated to ascertain the origin of the endoleaks and adherence to reporting protocols. The external validator was blinded to the results reported by the vascular radiologists and the Duplex ultrasound results. There was agreement with the reported results in all but one case of a potential type 2 endoleak that had resolved on subsequent scans. Figure 15 depicts a typical post EVAR CT angiogram with the arrow pointing to an endoleak.

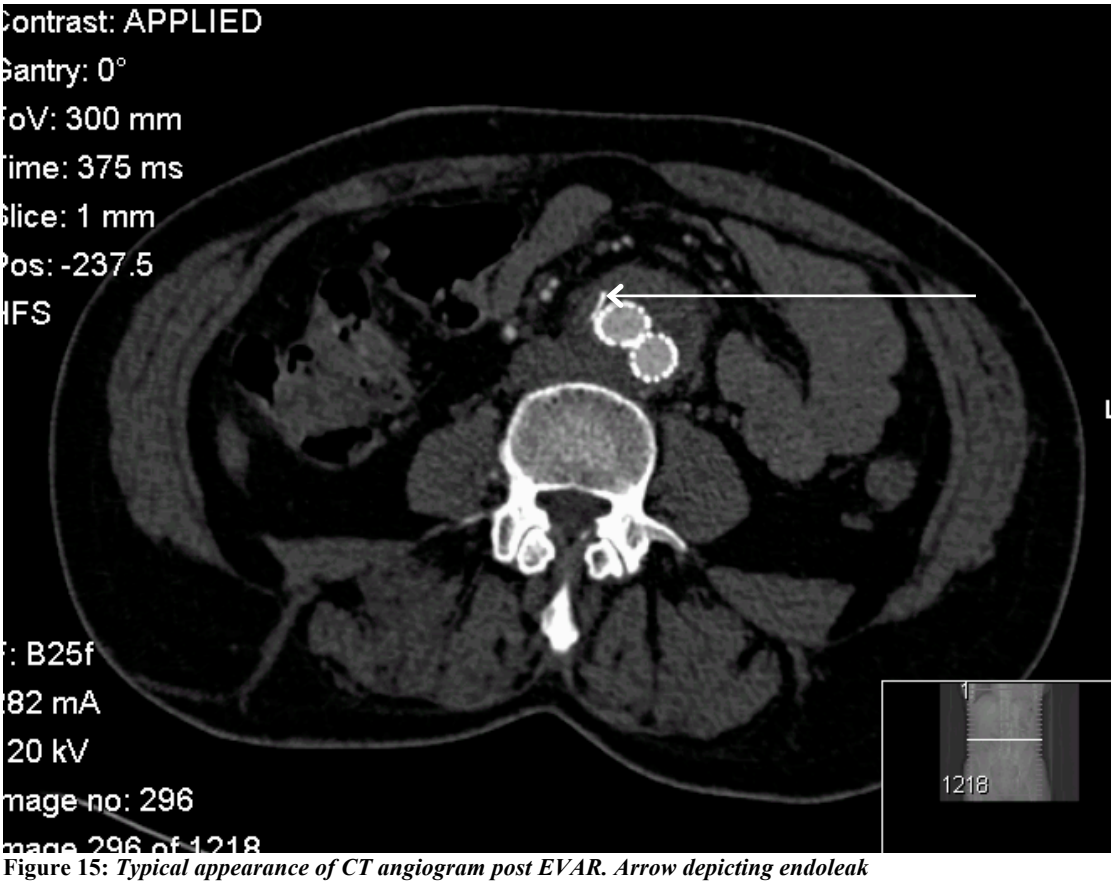

Figure 15: ***Typical appearance of CT angiogram post EVAR. Arrow depicting endoleak***

Duplex protocol

All duplex scans were performed at our dedicated vascular laboratory by a team of 4 vascular ultrasound technologists. The scans were performed on an HDI 5000 Philips scanner till September 2007, since then the Philips iU22 scanner has also been used. Scans were performed using the 5-2 curvilinear abdominal probes.

All post EVAR evaluations were performed to a pre-agreed protocol (Appendix 1, 2). This protocol was designed specifically for the purpose of this study in collaboration with the DUS operators and introduced as part of routine surveillance for patients post EVAR.

The aorta was initially scanned using B-mode imaging from the diaphragm down to the femoral arteries in both the transverse and longitudinal planes, to determine the proximal and distal limits of the stent graft. The maximum aortic diameter during peak systole was recorded in this mode.

Colour Doppler mode was then used to identify the renal arteries. The entire stent-graft was visualised in colour Doppler mode, identifying any endoleaks, occlusions, kinking, significant stenosis of the stent and distal flow characteristics. Particular attention was paid to the proximal and distal stent attachment sites, the origins of the inferior mesenteric, lumbar and internal iliac arteries. Any flow visualised outside the stent, but within the aneurysm sac, was analysed using pulsed wave Doppler, to determine pulsatility of flow.

For any endoleaks that were identified, attempts were made to trace them back to their source to enable classification. Endoleaks were classified as previously described

(Table 2). Scans were classed as being adequate, if the entire aneurysm sac was visualised and colour images of flow within the stent were obtained. In cases of inadequate scans, patients were asked to return to the vascular laboratory for a repeat scan in a few days. Figure 16 depicts a typical post EVAR Doppler image with an arrow pointing to the endoleak.

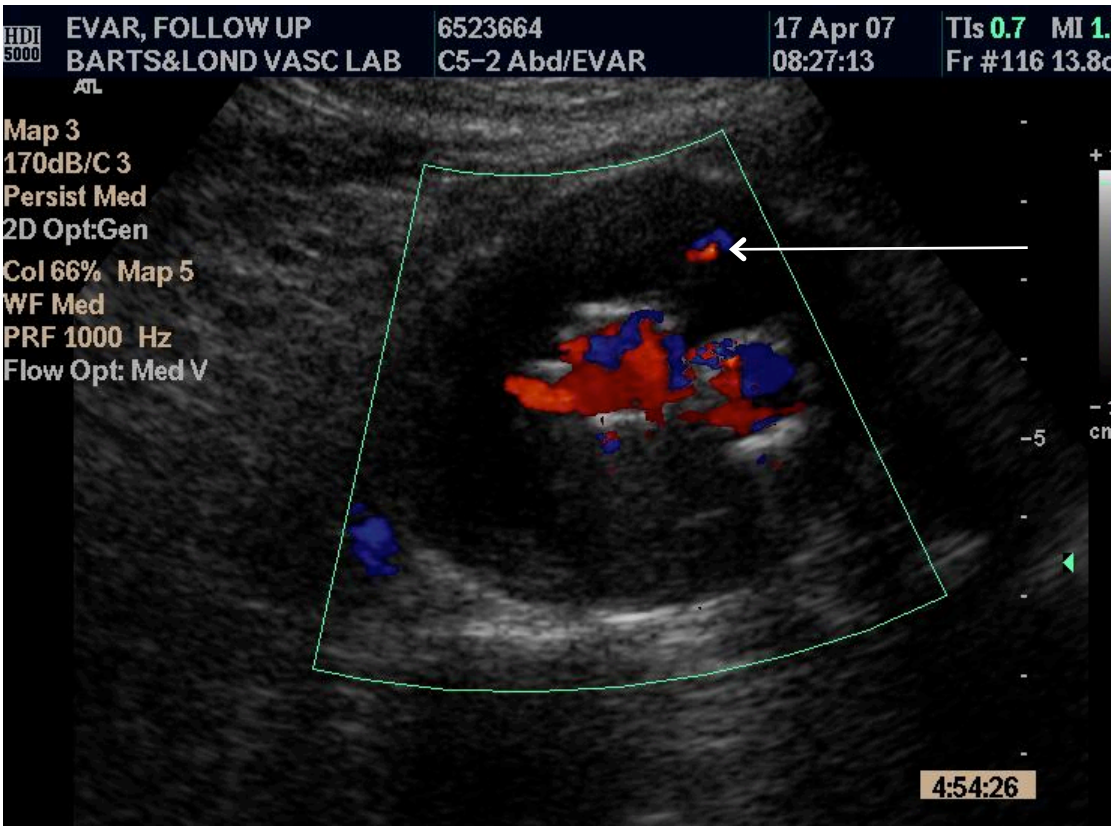

Figure 16: ***Typical appearance of post EVAR Doppler. Arrow pointing to endoleak***

Statistical evaluation

Laboratory arm

The Doppler flow phantom was designed to enable manipulation of the geometrical and flow characteristics of the small and large flow systems such that their impact on the reliable detection of flow in the small system could be assessed. The phantom could be rotated along the axis of the large flow enabling the small system to be effectively moved. The endoleak system could thus run proximal, distal or tangential to the large flow.

For the purposes of statistical evaluation, one of the variables considered was the relative plane of the small flow to the large flow. This was categorised as small flow being proximal, distal or in the same horizontal plane as the large flow. When vertical planes were considered, the corresponding categories were small flow in the same plane as the large flow or in a different plane to the large flow. When considered in context of viewing positions and cross sectional schematics (Figures 5 & 6), the proximal and distal planes correspond to the proximal and distal planes used for the analysis; however, for the tangential plane, position 1 would be proximal, position 5 would be distal and positions 2, 3 & 4 would be in the same plane as the large flow. Similarly for the vertical assessment planes, positions 1, 2 & 4 of the proximal and distal planes would be in the same plane as the large flow, positions 3 and 5 being in a different plane. Also, all the viewing positions for the tangential plane would be in a different vertical plane to the large flow. Thus the categories considered for the relative geometrical plane of the two flows were

1) Endoleak system proximal to the aortic flow
2) Endoleak system distal to the aortic flow.
3) Endoleak system in the same horizontal plane as the aortic flow,

4) Endoleak system in the same vertical plane as the aortic flow,
5) Endoleak flow in a different vertical plane to the aortic flow

Univariate analysis

The following parameters were considered whilst assessing the limitations of duplex ultrasound for the Doppler flow phantom.

1. Flow rate in the second endoleak flow system
2. Depth of the endoleak from the viewing window
3. Distance of the endoleak from the main aortic flow
4. Spatial relationships of the aortic and endoleak flows
5. Operators

As part of the clinical arm of our study, if any suspected endoleaks were detected on Doppler ultrasound, a further assessment was performed to confirm or refute findings if appropriate. The laboratory arm of the study intended to assess the limits of Doppler ultrasound in diagnosing endoleaks. Therefore, for the purposes of statistical evaluation, any flow visualisation in the small system was treated as flow being detected, even if the operator rated the flow as being possible or probable. Thus, endoleak detection scores of 1-3 were considered to represent endoleak flow being visualised and scores of 0 was regarded as absent endoleak flow. Statistical tests employed to determine significance of results were the chi-squared test and Fischer's exact test.

Multivariate analysis

The univariate analysis was employed to identify the variables that had a significant impact on the visualisation of flow in the small system. Multivariate analysis was performed using binary logistic regression analysis to understand the inter-relationships between the variables and their impact on flow detection in the endoleak system.

Clinical arm

CT was considered to be the gold-standard imaging modality for our study. Endoleaks detected on CT were classified as true endoleaks and those detected only on duplex as false endoleaks. The sensitivity, specificity, positive and negative predictive value of duplex was calculated assuming independence between individual paired scans. Kappa statistics were used to assess agreement between the two modalities for detecting endoleaks.

Statistical analysis for comparing sac size estimation and agreement between the two modalities was performed using the Pearson correlation coefficient, Bland and Altman's method and the paired Students t-test.

RESULTS

Laboratory results

A total of 180 observations were obtained for the 30 different flow and geometrical configurations assessed by the test operators. These flow and geometrical combinations were designed to assess the limitations of duplex in the clinical setting of post EVAR surveillance. As described previously, the test protocol had been designed in consultation with ultrasound physicists who had also generated a set of expected results.

Of the thirty combinations, flow detection was thought to be likely in 26 combinations, making it possible for flow to be detected in 156 instances. The test operators detected flow in 133 of these (Table 14). For the remaining 24 instances where flow detection was thought to be difficult, the test operators could detect flow in 10 instances.

Table 14: ***Expected and actual visualisation of second flow***

	Expected visualisation of small flow	Actual visualisation of small flow
Flow seen	156	143
No Flow seen	24	37

Kappa statistic was found to be 0.36. A breakdown of these results according to the different variables assessed is expressed in Tables 11, 12, 13 & 14.

Table 15: ***Expected and actual visualisation for the different assessment planes***

Assessment plane	Instances (n)	Expected visualisation	Actual visualisation
Proximal	72	72	67 (93%)
Distal	72	48	44 (92%)
Same horizontal	36	36	32 (89%)
Same vertical	78	60	60 (100%)
Different vertical	102	96	86 (90%)

Table 16: ***Expected and actual visualisation at different endoleak flow rates***

Rate of endoleak flow (ml/hr)	Instances (n)	Expected visualisation	Actual visualisation
300	78	60	59 (98%)
500	48	48	39 (82%)
700	36	30	29 (97%)
900	18	18	16 (94%)

Table 17: ***Expected and actual visualisation at different depths from the viewing windows***

Depth from viewing window (mm)	Instances (n)	Expected visualisation	Actual visualisation
63	12	12	11 (92%)
67	60	60	56 (93)
72	12	12	12 (100%)
81	6	6	5 (83%)
90	18	18	15 (67%)
95	60	42	37 88%
99	12	6	7 (116%)

Table 18: ***Expected and actual visualisation at different distances of small flow from large flow***

Distance from aortic flow (mm)	Instances (n)	Expected visualisation	Actual visualisation
14	6	6	5 (83%)
14.8	12	12	11 (92%)
15.9	12	0	7 *
16.6	30	30	27 (90%)
18.4	12	12	10 (83%)
19.8	18	18	17 (94%)
22.8	24	18	18 (100%)
24.4	18	18	16 (89%)
26.9	12	6	5 (83%)
34.9	12	12	9 (75%)
37.7	24	24	18 (75%)

* Incalculable; higher than predicted

Visualisation of flow at different flow rates of the endoleak

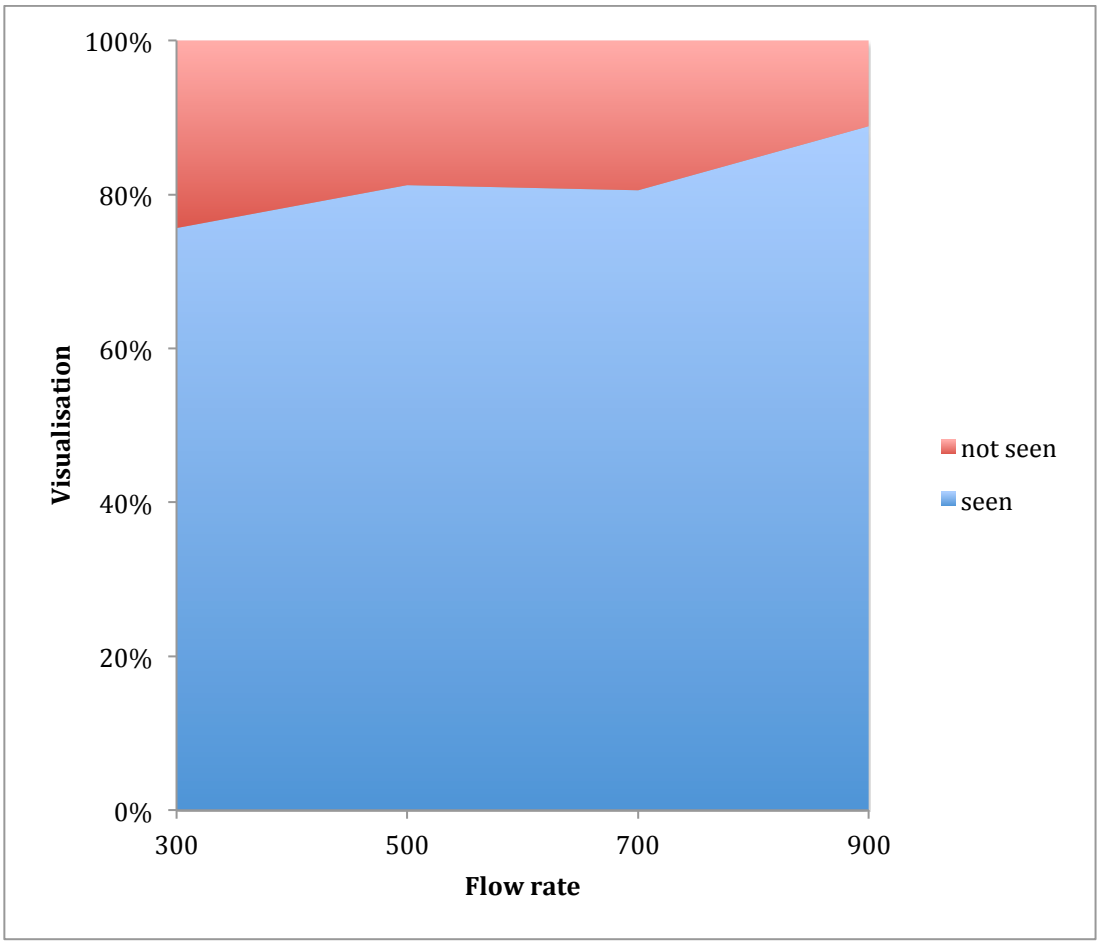

Figure 17: ***Graph depicting endoleak visualisation as a function of endoleak rate of flow.***

Table 19 & Figure 17 demonstrate the visualisation of small flow at the flow rates depicted independent of the other variables. Tables 16, 17, 18 & 19 demonstrate flow detection in the small system for different small system flow rates, when considered in the context of the other variables i.e. operators, depth of the small system from the viewing window, distance between the two flow systems and the relative geometrical planes of the two flows.

Table 19: ***Flow detection based on flow rates in the small system***

Flow rate in the small system (ml/hr)	Instances	Detected	% Detection
300	78	59	75
500	48	39	81
700	36	29	81
900	18	16	89

Chi square statistics, p=0.616

Table 20: ***Breakdown of endoleak detection rates with varying endoleak flow speeds when considering the spatial arrangement of the large and small flows***

	Endoleak flow rate (ml/hr)	Instances	Detected	% Detection
Distal Plane	300	36	21	58
	500	18	11	61
	700	12	7	58
	900	6	5	83
Proximal Plane	300	42	38	90
	500	18	17	94
	700	12	12	100
Same Horizontal Plane	500	12	11	92
	700	12	10	83
	900	12	11	92
Same Vertical Plane	300	42	31	74
	500	18	16	89
	700	18	13	72
Different Vertical Plane	300	36	28	77
	500	30	23	77
	700	18	16	89
	900	18	16	89

Table 21: ***Endoleak detection as a function of flow rates and depth from the viewing window***

Depth of small flow from viewing window (mm)	Endoleak flow rate (ml/hr)	Instances	Detected	% Detection
63	300	6	5	83
	700	6	6	100
67	300	36	33	92
	500	18	17	94
	700	6	6	100
72	500	6	6	100
	900	6	6	100
81	700	6	5	83
90	500	6	5	83
	700	6	5	83
	900	6	5	83
95	300	30	19	63
	500	18	11	61
	700	12	7	58
99	300	6	2	33
	900	6	5	83

Table 22: ***Breakdown of flow detection by flow rate and operator***

Operator	Small system flow rate (ml/hr)	Instances	Detected	% Detection
1	300	26	18	69
	500	16	13	81
	700	12	10	83
	900	6	6	100
2	300	26	21	81
	500	16	12	75
	700	12	9	75
	900	6	4	67
3	300	26	20	77
	500	16	14	88
	700	12	10	83
	900	6	6	100

Table 23: ***Endoleak detection as function of small system flow rate and distance between small and large flows***

Distance of small flow from large flow (mm)	Small system flow rate (ml/hr)	Instances	Detected	% Detection
14	700	6	5	83
14.8	300	6	5	83
	500	6	6	100
15.9	300	6	4	67
	700	6	3	50
16.6	500	12	11	92
	700	6	5	83
	900	12	11	92
18.4	300	6	5	83
	500	6	5	83
19.8	300	12	11	92
	700	6	6	100
22.8	300	12	7	58
	700	6	6	100
	900	6	5	83
24.4	300	12	11	92
	500	6	5	83
26.9	300	6	1	17
	700	6	4	67
34.9	300	6	6	100
	500	6	3	50
37.7	300	12	9	75
	500	12	9	75

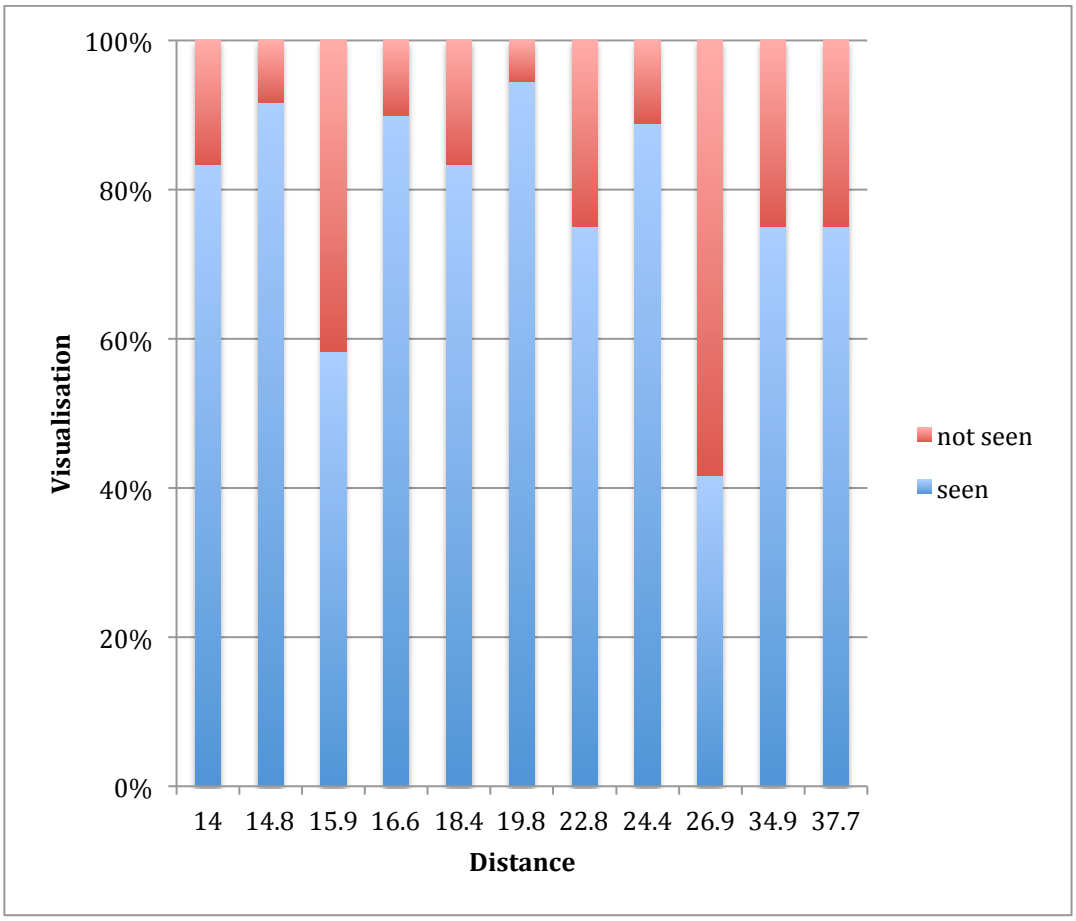

Figure 18: ***Relationship between endoleak detection and distance between the large and small flows.***

Figure 18 depicts the relationship between flow detection in the small endoleak system and the distance between the small and large flows for all operators irrespective of the rate of flow in the endoleak system. Fishers exact test statistic was calculated and revealed a p value of 0.026. Table 23 also depicts the relationships between detection and distance between the flows, when small system flow rate is also factored in.

Visualisation of endoleak at different depths from the viewing window

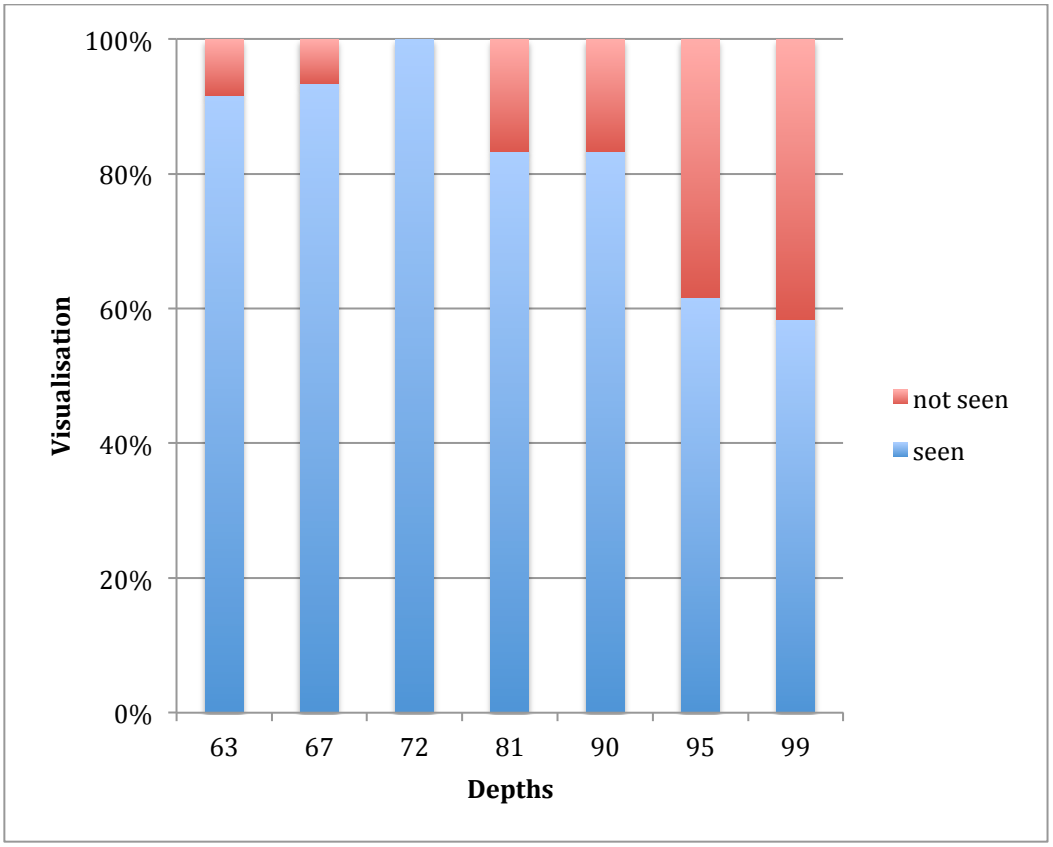

Figure 19: ***Relationship between depth of the endoleak flow from the viewing window and detection rates***

Detection of flow in the small system was assessed at different depths of the small system. The results, when flow detection was considered secondary to depth from the viewing window, independent of the other variables, are graphically depicted in Figure 19. Fisher's exact test was used to assess the relationship between flow detection and depth of the small flow from the viewing window ($p = 0.0002$).

Visualisation at relative horizontal planes of endoleak and aortic flow

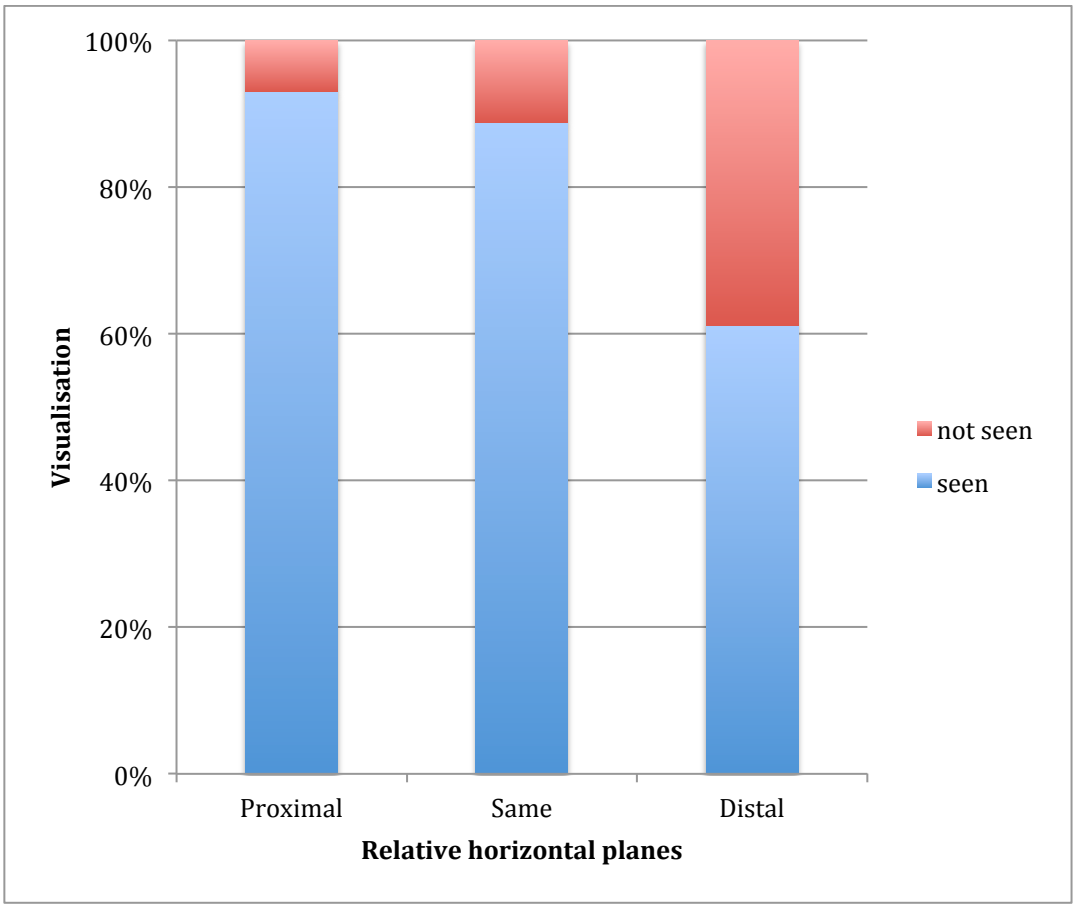

Figure 20: ***Relationship between relative horizontal planes of small and large flow and detection of flow in the endoleak system***

Visualisation by relative vertical planes of aortic and endoleak flows

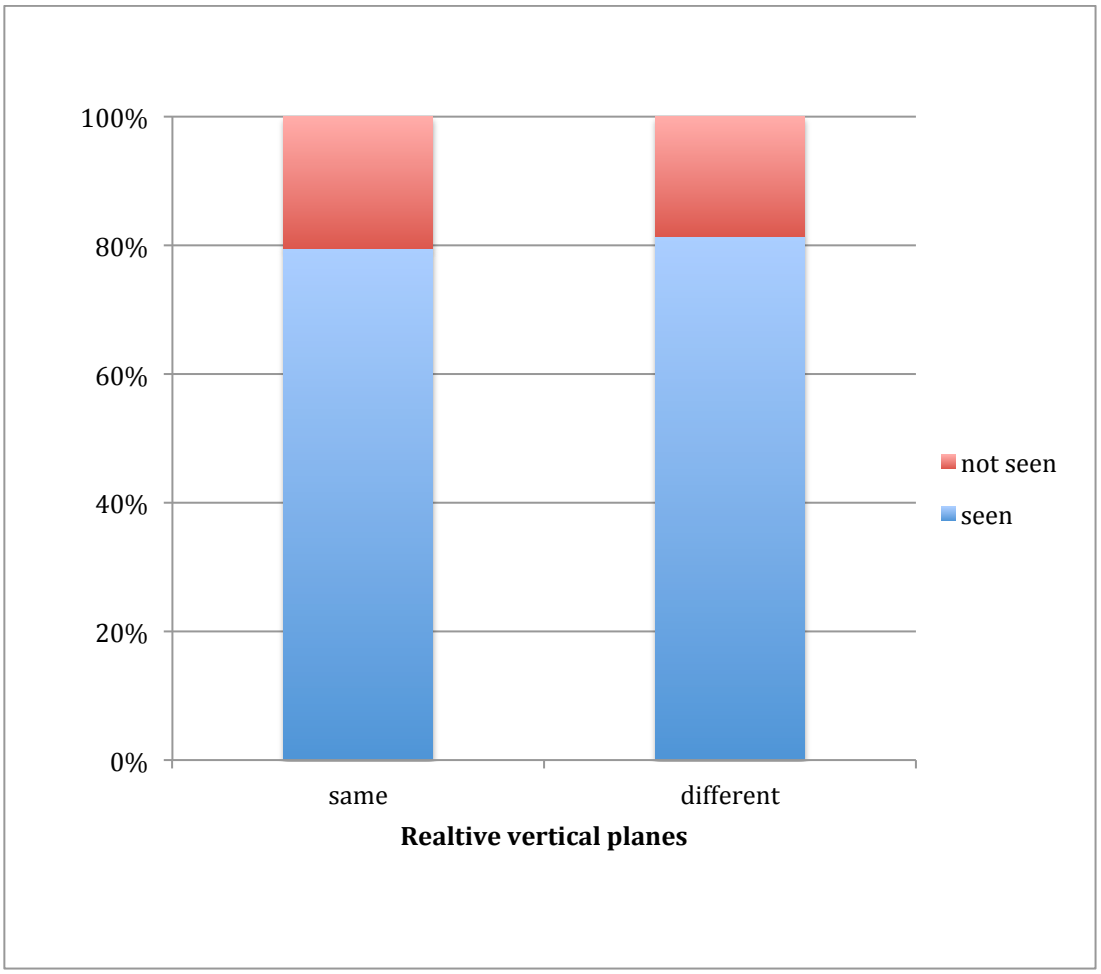

Figure 21: ***Relationship between relative vertical planes of small and large flows and detection of flow in the small system***

Figures 15 & 16 depict the relationship between detection of flow in the small system and the relative horizontal and vertical planes of the small and large flows at all small system flow rates. For the purposes of analysis, the spatial relationships between the two flows were assessed in the horizontal and vertical planes. Chi square test was performed and revealed a p value of 0.000003 for the horizontal plane assessment and >0.05 for the vertical plane assessment.

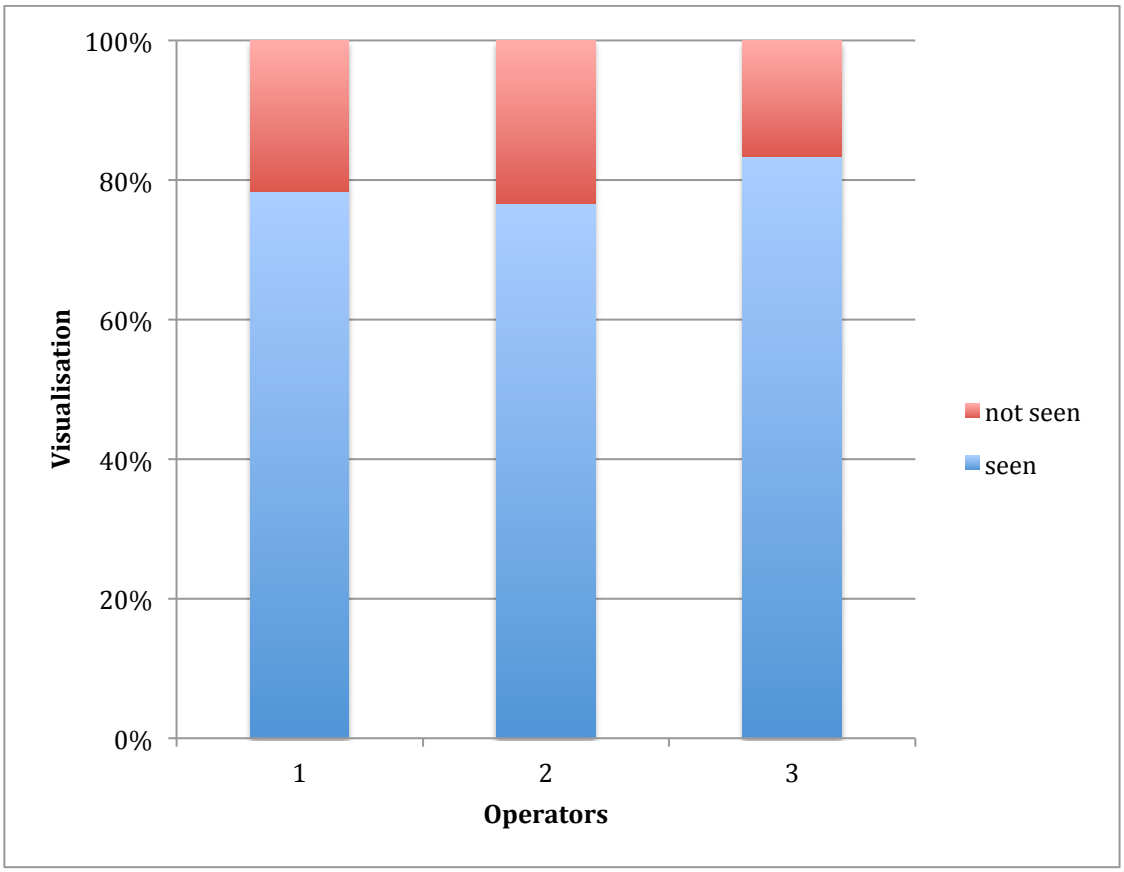

Figure 22: ***Effect of operator experience on detection of flow in the small system***

The effect of operator experience on the detection of flow in the small system was studied. Figure 22 depicts this relationship for all flow rates in the small system and across all geometrical configurations. Chi square test revealed the p value to be >0.05.

Detection of flow in the second system by the operators irrespective of the small system flow rates whilst altering the geometrical configurations of the two flows are tabulated in Tables 20, 21 & 22.

Table 24: ***Detection of small flow by operators categorised by relative planes of the two flows***

Operator	Plane	Instances	Detected	% Detection
1	Proximal	24	21	88
	Distal	24	14	58
	Same horizontal	12	14	100
	Same vertical	26	18	69
	Different vertical	34	29	85
2	Proximal	24	23	96
	Distal	24	15	63
	Same horizontal	12	8	67
	Same vertical	26	21	81
	Different vertical	34	25	74
3	Proximal	24	23	88
	Distal	24	15	63
	Same horizontal	12	12	100
	Same vertical	26	21	81
	Different vertical	34	29	85

Table 25: ***Detection of small flow by operators at various depths of the small flow***

Operators	Depth from viewing window (mm)	Instances	Detected	% Detection
1	63	4	3	75
	67	20	18	90
	72	4	4	100
	81	2	2	100
	90	6	4	67
	95	20	11	56
	99	4	3	75
2	63	4	4	100
	67	20	19	95
	72	4	4	100
	81	2	1	50
	90	6	3	50
	95	20	13	65
	99	4	2	50
3	63	4	4	100
	67	20	19	95
	72	4	4	100
	81	2	2	100
	90	6	6	100
	95	20	13	65
	99	4	2	50

Table 26: ***Detection of flow by the operators at various distances between the two flows***

Operators	Distance of small from large flow (mm)	Instances	Detected	% Detection
1	14	2	2	100
	14.8	4	3	75
	15.9	4	3	75
	16.6	10	10	100
	18.4	4	4	100
	19.8	6	5	83
	22.8	8	6	75
	24.4	6	4	67
	26.9	4	3	75
	34.9	4	3	75
	37.7	8	6	75
2	14	2	1	50
	14.8	4	4	100
	15.9	4	2	100
	16.6	10	7	70
	18.4	4	3	75
	19.8	6	6	100
	22.8	8	6	75
	24.4	6	6	100
	26.9	4	2	50
	34.9	4	3	75
	37.7	8	6	75
3	14	2	2	100
	14.8	4	4	100
	15.9	4	2	50
	16.6	10	10	100
	18.4	4	3	75
	19.8	6	6	100
	22.8	8	6	75
	24.4	6	6	100
	26.9	4	2	50
	34.9	4	3	75
	37.7	8	6	75

Inter-observer agreement was studied using Cohen's kappa statistic and was found to show $\kappa = 0.21$-0.4. Intra-observer variation was also studied comparing the two sets of observations for each operator. ($\kappa = 0.21 – 0.4$)

Clinical Results

One hundred and thirteen patients underwent EVAR at our institution between August 2000 and August 2008. A total of 305 CT and 296 Duplex scans were performed during follow up. Paired CT and DUS scans, defined as performed within 8 weeks of each other, were obtained in 190 instances (Figure 23) within a period of 11.2 days of each other (range 0 – 49 days).

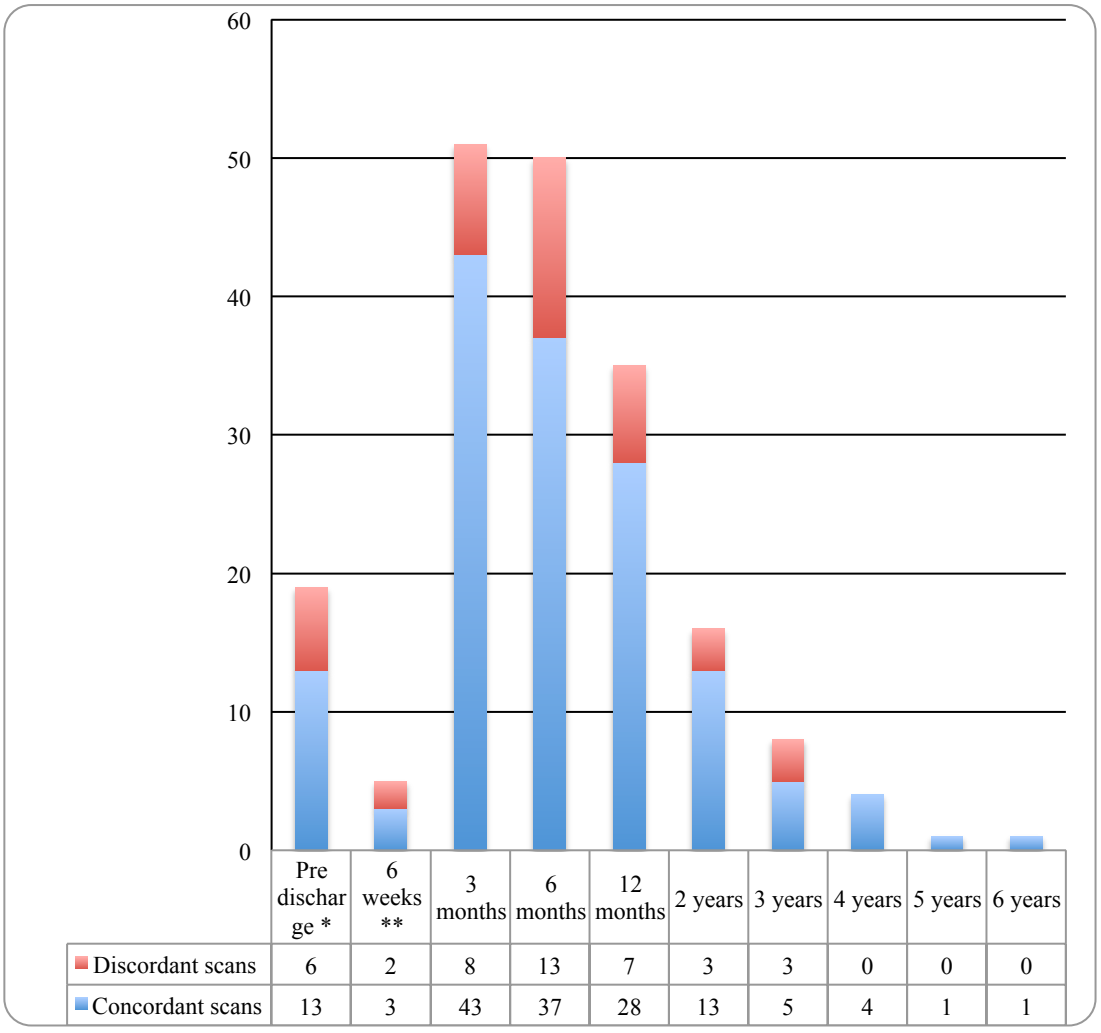

	Pre discharge *	6 weeks **	3 months	6 months	12 months	2 years	3 years	4 years	5 years	6 years
Discordant scans	6	2	8	13	7	3	3	0	0	0
Concordant scans	13	3	43	37	28	13	5	4	1	1

Figure 23: ***Distribution of paired CT and DUS scans***

Table 27*: Distribution of endoleaks, associated sac size change and need for intervention in our study population*

Patient	Leak	Seen on CT	Seen on DUS	Change in sac size	Intervention
1	Unclassified	Yes	No	↔	No
2	Unclassified	No	Yes	↑	Yes *
3	II	No	Yes	↓	No
4	II	Yes	Yes	↔	No
5	II	No	Yes	↔	No
6	II	No	Yes	↔	No
7	II	Yes	Yes	↔	No
8	II	No	Yes	↓	No
9	II	No	Yes	↓	No
10	II	Yes	Yes	↓	No
11	I	No	Yes	↔	No
	II	No	Yes	↔	No
12	II	No	Yes	↔	No
13	I	No	Yes	↓	No
14	Unclassified	Yes	No	↓	No
15	Unclassified	No	Yes	↔	Yes **
16	II	Yes	Yes	↓	No
17	II	Yes	No	↓	No
18	I	Yes	Yes	↔	Yes
19	II	Yes	No	↔	No
20	II	Yes	No	↓	No
21	I	Yes	Yes	↔	Yes
22	II	Yes	Yes	↔	No
23	I	Yes	Yes	↔	No
24	II	No	Yes	↓	No
25	I	Yes	Yes	↔	Yes
26	II	No	Yes	↓	No
27	I	No	Yes	↔	No
28	I	Yes	Yes	↔	Yes
29	II	Yes	No	↔	No
30	Unclassified	Yes	Yes	↔	No
	II	Yes	Yes	↔	No
31	II	No	Yes	↔	No
32	I	Yes	No	↑	Yes ***
33	II	No	Yes	↔	No
34	I	Yes	Yes	↔	Yes
35	Unclassified	Yes	Yes	↓	No
36	II	Yes	Yes	↔	No
37	I	Yes	Yes	↔	No
38	I	Yes	Yes	↔	Yes
39	II	Yes	Yes	↔	No
40	II	Yes	Yes	↔	No
41	II	Yes	Yes	↔	No
42	II	Yes	Yes	↔	No

↔, ↓, ↑ - Indicates stable, decreasing and increasing sac sizes respectively

** Unclassified endoleak seen on DUS, increasing sac size seen on both CT and DUS. Patient underwent realignment procedure for suspected endotension.*

*** Unclassified leak seen on DUS, CT reported spontaneous thrombosis of this endoleak that had been previously visualised on an unpaired CT scan. Patient underwent device explantation after two failed endovascular interventions.*

**** Small type 1a endoleak of uncertain significance, associated with a 0.3 cm increase in sac size. Treated with a proximal extension cuff.*

A total of 28 endoleaks were identified on CT in 27 patients. 9 were type 1, 15 were type 2 and in 4 cases CT could not adequately classify the endoleak. Of these, DUS identified 21 endoleaks, 8 were type 1, 11 were type 2 and 2 were of uncertain origin. An additional 16 endoleaks were identified by DUS in 15 patients, 3 were classified as type 1, 11 as type 2 and 2 of uncertain origin (Tables 23 & 24).

Table 28: ***Distribution of endoleaks and agreement by modality***

Endoleaks visualised on both CT and DUS		Endoleaks visualised only on CT		Endoleaks visualised only on DUS	
21	*8 Type 1*	7	*1 Type 1*	16	*3 Type 1*
	11 Type 2		*4 Type 2*		*11 type 2*
	2 Unclassified		*2 Unclassified*		*2 Unclassified*

Eight out of 9 type 1 endoleaks identified on CT were detected on DUS. One type 1 endoleak seen on CT but not on DUS was a small type 1a endoleak associated with a 0.3 cm increase in diameter (Figures 19 & 20).

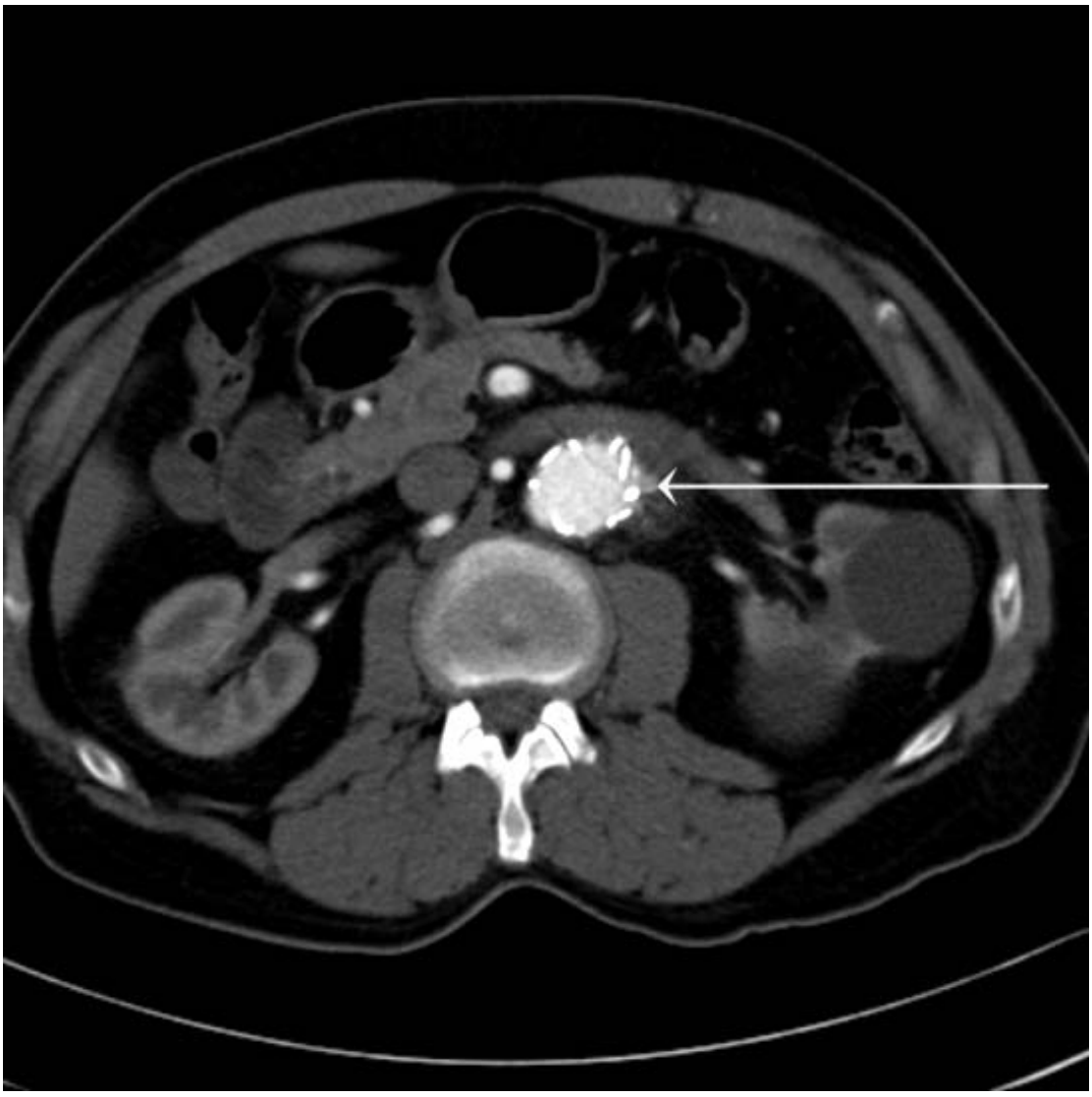

Figure 24: ***CT angiogram image for small leak seen only on CT (Arrow pointing to suspected endoleak)***

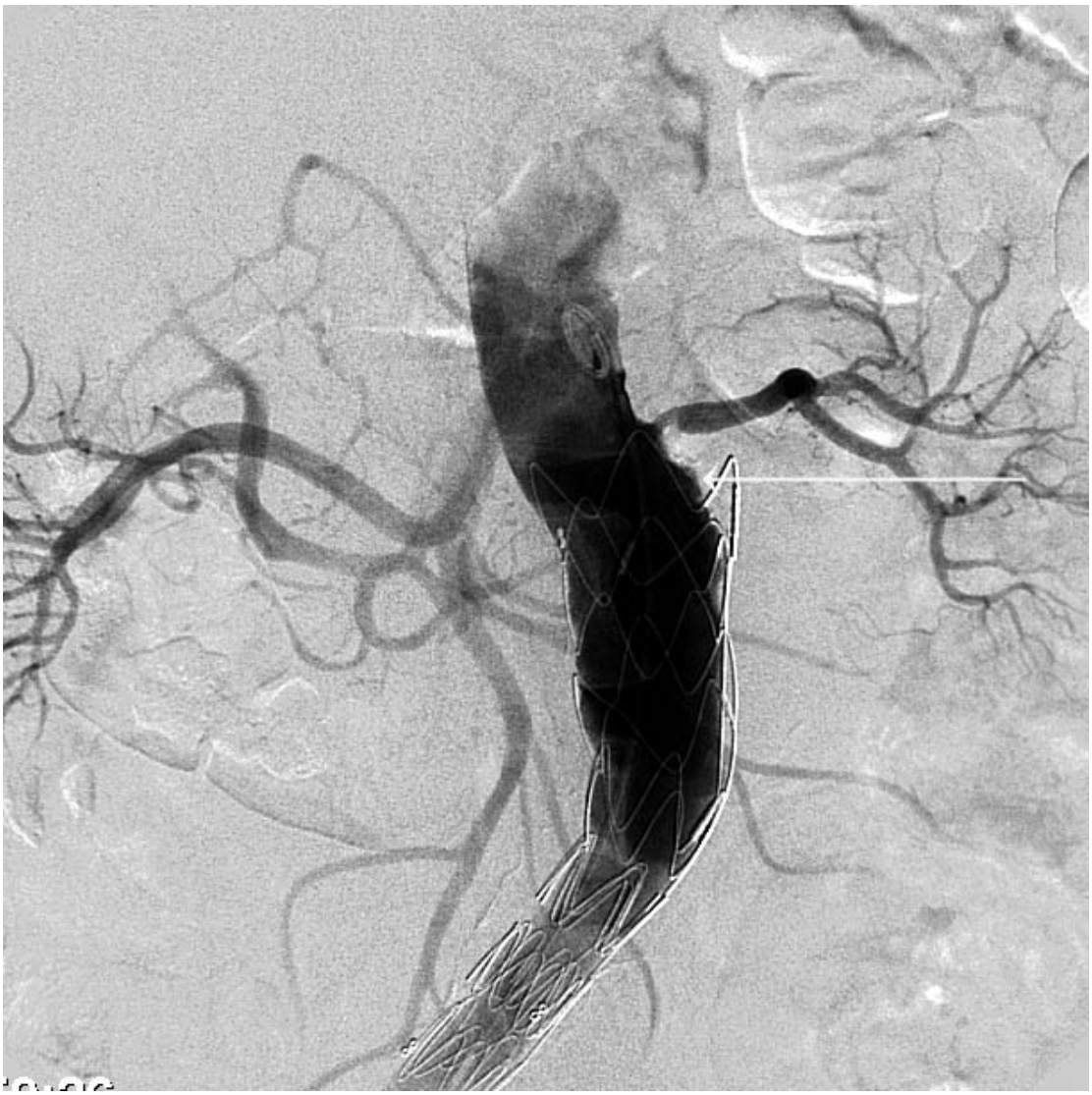

Figure 25: ***Conventional catheter angiographic image (Arrow pointing to suspected endoleak)***

Sensitivity, Specificity, Positive and Negative Predictive Value

148/190 (77.9%) DUS and CT scans were concordant in terms of endoleak detection and 42/190 (22.1%) were discordant (Table 29) (Unweighted κ statistic 0.475)

Table 29: ***Correlation between CT and DUS for diagnosis of endoleaks***

	CT	
DUS	*Endoleak*	*No Endoleak*
Endoleak	35	31
No Endoleak	11	113

Using CT as the gold standard imaging modality EVAR surveillance and assuming independence between individual paired scans, we found DUS, in our practice, to have a sensitivity of 72.1%, specificity of 80.4%, positive predictive value of 50% and a negative predictive value of 91.4%.

Aneurysm size

As part of the clinical arm of the study we compared CT and DUS assessment of the AAA sac sizes. Maximal aneurysm diameter was measured using both CT and DUS at every patient attendance. CT sac size estimation varied from 31 – 120 mm (mean 55.32) as compared to DUS 36 – 105 (mean 50.31) (Figures 21 & 22)

Sac size estimations were also carried out for serial paired scans that were obtained for 62 patients between 3 to 6 months apart. This varied from 0 to 18 for CT and 0 to 11 mm for DUS (Figure 28). The change in sac size estimation in the time interval between the serial scans as assessed by both modalities was compared. ($p = 0.9$)

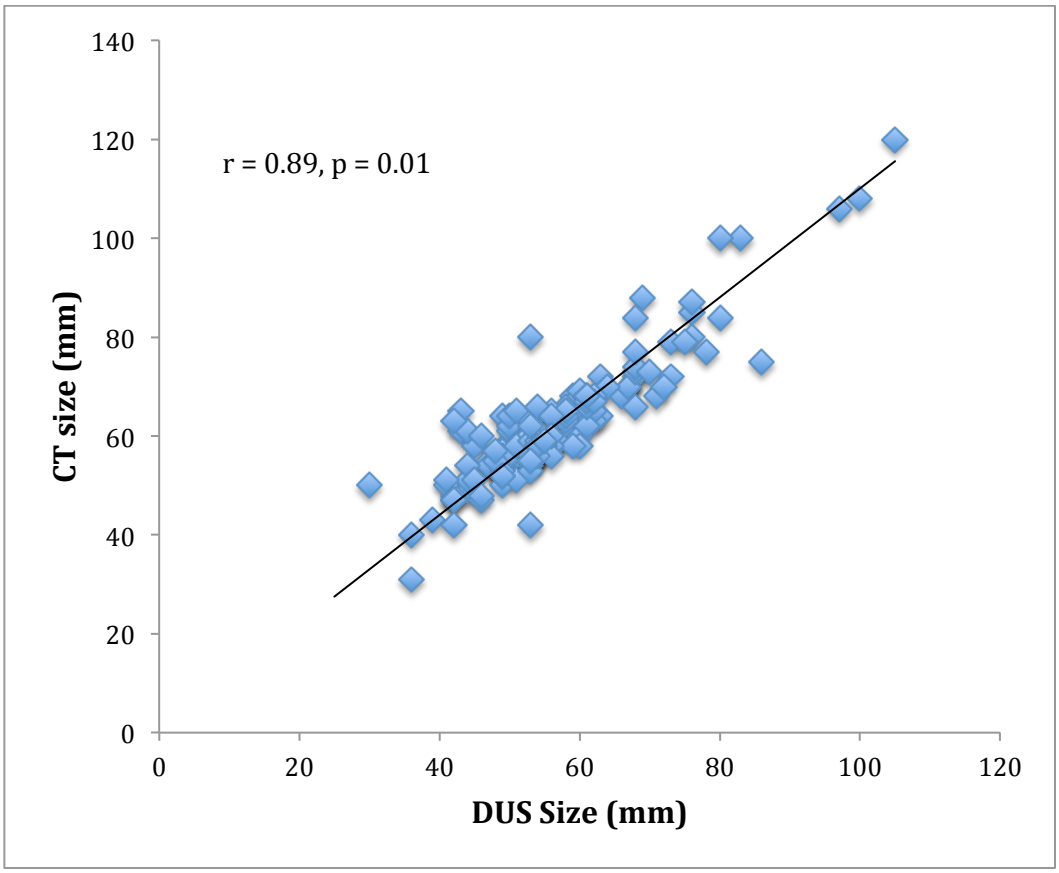

Figure 26: ***Correlation plot for absolute sac size estimation by DUS and CT***

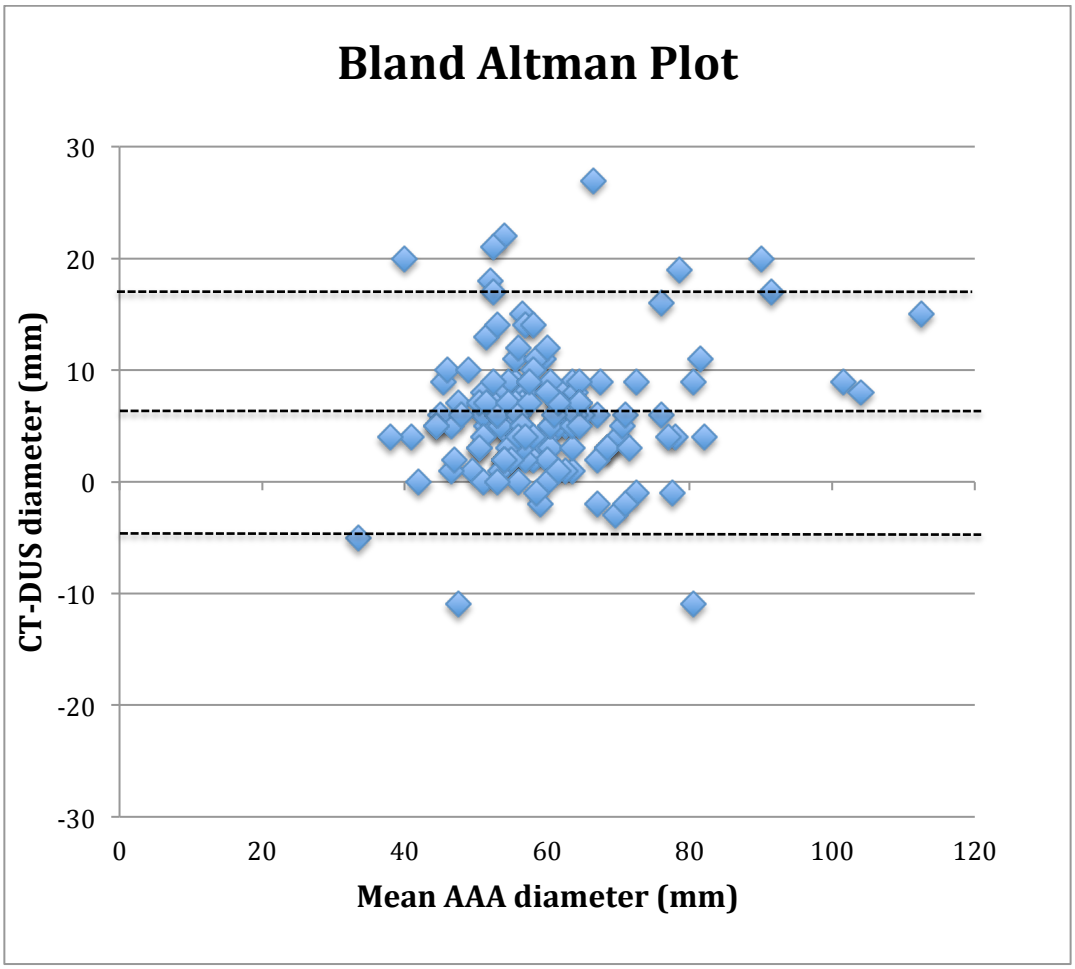

Figure 27: ***Bland Altman plot for CT – DUS size measurement (Dotted lines - 2 standard deviations)***

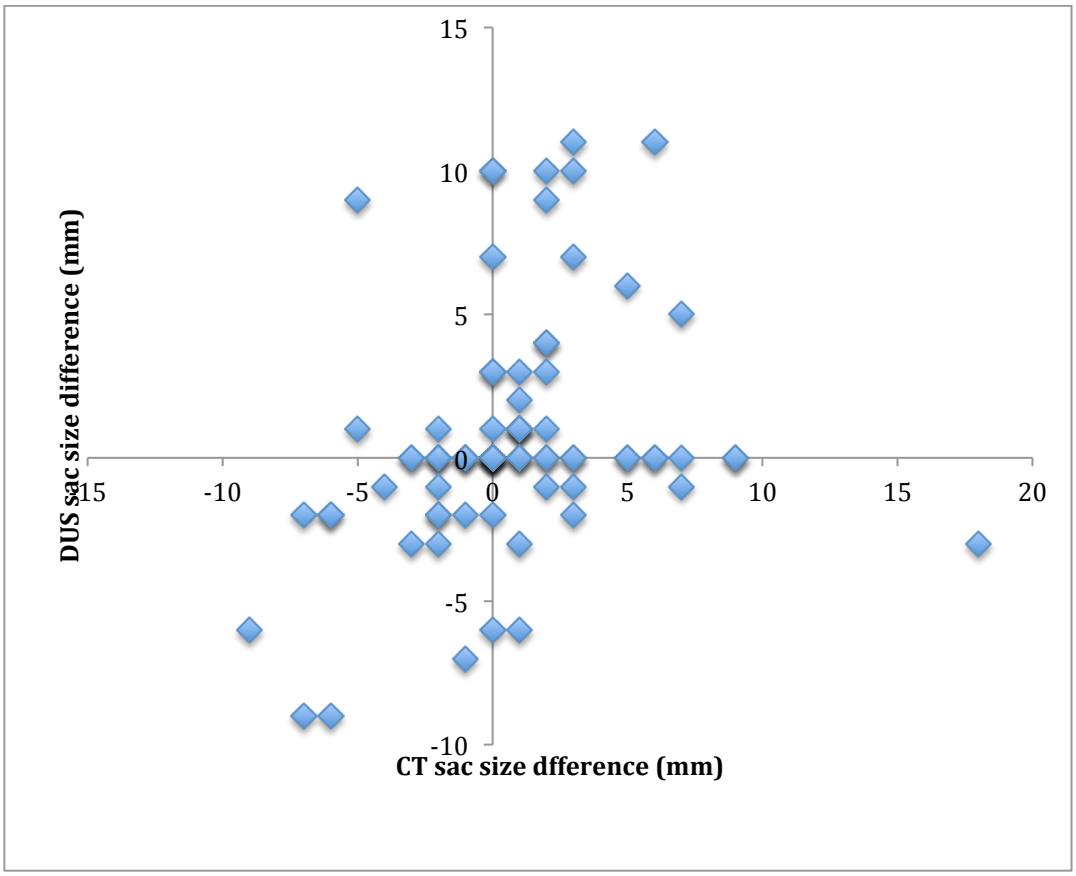

Figure 28: ***Correlation plot for change in sac size with CT and DUS, p<0.05 (Serial paired scans obtained for 62 patients, negative change indicates increase in size of sac)***

DISCUSSION

At Barts and The London NHS Trust, we have had the benefit of a dedicated vascular ultrasound laboratory with 4 experienced vascular ultrasonographers who perform all our vascular scans. From the EVAR surveillance point of view, our study found DUS to be 72.1% sensitive and 80.4% specific, a positive predictive value of 50% and a negative predictive value of 91.4% for the detection of endoleaks considering CT to the gold standard imaging modality.

Fate of endoleaks in our study population

The clinical arm of the study found a total of 28 endoleaks in 27 patients detected with CT. Twenty-one of these endoleaks were seen on both CT and DUS, 7 were seen on CT alone. A further 16 endoleaks were visualised on DUS alone.

Endoleaks detected on both CT and DUS

Twenty-one endoleaks were detected and accurately classified on both CT and DUS. Eight of these were type 1 endoleaks, 7 type 1a and 1 type 1b. Six type 1a endoleaks required intervention whilst 1 type 1a and 1 type 1b had resolved spontaneously on subsequent follow up. Eleven endoleaks were classified as type 2 on both CT and DUS. Of these, 10 were still present on the last paired scan. Two endoleaks of uncertain origin have resolved.

Endoleaks detected solely on CT

One type 1 endoleak, 4 type 2 endoleaks and 2 leaks of uncertain origin were diagnosed solely on CT. The type 1 endoleak was detected on a 6 month follow up CT scan and had not been visualised on the paired DUS scan performed on the same day. This endoleak had also not been detected on any previous paired or unpaired CT or DUS scans. It was classified as a type 1a endoleak (Figure 24) and was associated with a slight increase in sac size. After discussion in our multi-disciplinary meeting, a decision was made to treat this endoleak. At catheter angiography there was continuing ambiguity about the significance of this small endoleak (Figure 25), but as it was associated with a 0.3 cm increase in sac size, a decision was made to treat this and a proximal extension cuff was deployed.

Of the 4 type 2 and 2 uncertain origin leaks also detected only on CT, all except 1 type 2 endoleak have resolved spontaneously or have been classified as artefacts on subsequent scans.

Endoleaks detected solely on DUS

Three type 1 endoleaks were detected solely on DUS. All of these were visualised on pre-discharge scans and had resolved on subsequent follow up. Of the 11 type 2 endoleaks, 7 were still present on the last surveillance scan, 4 have resolved. Both the 2 uncertain origin endoleaks required intervention. One patient underwent a realignment procedure and the second patient underwent an explantation procedure following two failed endovascular interventions. For both these patients, increasing

sac size was identified by both modalities and the leaks had been visualised at other out of protocol, unpaired CT scans.

For our study population, we were able to accurately detect all endoleaks that required intervention by DUS, except one endoleak. For this patient, there was ambiguity about the significance of this small type 1 endoleak that had been detected only on CT. There is a possibility that this endoleak was in fact an artefact visualised on both CT and catheter angiography. An increase in the aneurysm sac size increase of 0.3 cm could be regarded as an acceptable variation in aneurysm size measurements.

Endoleaks detected only on one imaging modality

Table 30: ***Endoleak anatomy for leaks detected only on one modality***

Leak	Visualised	Leak anatomy	Change in sac size	Intervention
Unclassified	CT	Posterior to graft (artefact)	↔	No
Unclassified	DUS	Unclear (modular/type 3)	↑	Yes
II	DUS	Lumbar	↓	No
II	DUS	Lumbar	↔	No
II	DUS	IMA	↔	No
II	DUS	Lumbar	↓	No
II	DUS	Lumbar	↓	No
I	DUS	Type 1 a	↔	No
II	DUS	IMA	↔	No
II	DUS	Lumbar	↔	No
I	DUS	Type 1 a	↓	No
Unclassified	CT	Posterior on pre-discharge scan (lumbar)	↓	No
Unclassified	DUS	Posterior (type 2 lumbar or type 3)	↔	Yes
II	CT	Lumbar	↓	No
II	CT	Lumbar	↔	No
II	CT	Lumbar	↓	No
II	DUS	Lumbar	↓	No
II	DUS	Lumbar	↓	No
I	DUS	Type 1 a	↔	No
II	CT	Lumbar	↔	No
II	DUS	Lumbar	↔	No
I	CT	Type 1 a	↑	Yes
II	DUS	IMA	↔	No

Seven endoleaks were visualised only on CT and a further 16 endoleaks were visualised only on DUS (Table 30). All CT scans for these 23 patients with endoleaks detected only on one modality were reviewed. For patients with endoleaks diagnosed only on CT, the scans were analysed to ascertain the possible reasons behind failed detection on DUS. The one type 1 endoleak, detected only on CT, was found to be a small perigraft leak both on CT and at catheter angiography. However, continuation of the leak into the aneurysm sac could not be demonstrated on either the CT scan or

at catheter angiography. As this leak was associated with a small increase in sac size, and as there was a theoretical risk of this endoleak causing failure of the proximal seal, intervention was performed. The likely explanation for non-detection of this leak on DUS could be its relatively small size and the absence of communication with the aneurysm sac.

4 type II leaks were missed on DUS. CT scan reviews for these patients demonstrated these type II leaks to be originating from lumbar arteries and to be in direct apposition with the stent-graft. All of these type II endoleaks were also small flow endoleaks on CT scans. The close proximity of the main aortic flow (stent-graft) to the endoleak and the relatively small size of these endoleaks could be the possible reasons behind their non-detection on DUS. One of these type 2 endoleaks was still present on the last follow up CT scan, others had all resolved at the last follow up scan.

An additional 16 endoleaks were visualised on DUS alone. Two of these patients required intervention for increasing sac size identified on both modalities. For both these patients, the increasing sac size had been identified on both CT and DUS and the endoleaks had been visualised at other instances on CT, but these CT scans had either been performed out of protocol or were not paired with a DUS scan and were thus not included in the study. DUS operators had been unable to classify these endoleaks. On retrospective review of the paired CT scans the leaks were not visible but comparison of sac sizes with the previous CT scans did confirm enlargement of aneurysm sac size.

3 type I endoleaks had been identified on DUS alone. All of these had been visualised on pre-discharge DUS scans. On review of the corresponding CT scans, these endoleaks could not be visualised. These leaks could also not be visualised on

subsequent paired DUS scans. In all these 3 cases, the DUS had preceded the CT scan by a few days. It is possible that these endoleaks had resolved by the time of the CT scan.

A further 11 type II endoleaks were visualised on DUS alone. Paired CT scan review of all these endoleaks confirmed their absence on the scan. DUS reports of all these type II endoleaks revealed them to be relatively small flow endoleaks. Both IMA and lumbar endoleaks had been identified on DUS. 4 of these endoleaks had resolved on subsequent scans, 7 were sill present on the last scan.

Duplex ultrasound is a dynamic imaging modality. DUS provides real time information as opposed to CT that provides static imaging albeit with excellent anatomic detail. The aorta/aneurysm interface is a dynamic area that responds to changes in the cardiac cycle and aortic wall compliance. It is possible that these slow flow endoleaks were not visualised on CT as the CT scan was out of phase with the endoleak. However, this remains an interesting area where further research is required.

In all 14 type II endoleaks were detected only on one imaging modality. 3 of these endoleaks were a result of back perfusion of the sac from the inferior mesenteric artery, 11 (78.5%) resulted from lumbar artery back perfusion. Flow from lumbar arteries results in back perfusion of the sac and is likely to be posterior to the endograft with the patient in the supine position. All of these endoleaks were also reported to be slowly flowing or small endoleaks on DUS and CT scans respectively.

Reinterventions

For our study population of 113 patients who underwent EVAR between August 2000 and August 2008, 19 underwent re-interventions (Table 31). 9 of these were for endoleaks detected on either or both CT and DUS during our study period (Table 29). 7 of these endoleaks were type 1a endoleaks that were treated with proximal extension cuffs.

One patient underwent explantation of his endograft. This patient had a bifurcated endograft inserted originally but had presented with an increasing sac size 6 months post procedure. A diagnostic angiogram performed revealed a type 3 endoleak (previously unclassified on duplex, not visualised on CT) and underwent a bridging stent to cover the disruption of the original stent graft. A repeat scan a month later revealed a type 1a endoleak and proximal extension cuff was deployed. However a further emergency admission necessitated a laparotomy with explantation of the endograft.

Another patient underwent a realignment procedure. This patient had an increasing sac size on both CT and DUS with an unclassified endoleak seen on DUS. The original EVAR had been performed 3 years prior to us instituting our study and the increasing sac size had been thought to be secondary to graft porosity, the patient subsequently undergoing a realignment procedure.

Table 31: ***Reinterventions***

Proximal cuff	9
Iliac limb extension	4
Embolisation of endoleak	1 (IMA)
Realignment	1
Endograft explantation	1
Fem-fem cross over grafting	1
Pseudoaneurysm repair	2

2 patients had proximal cuff extensions that had been performed prior to our study period. 4 patients underwent iliac limb extensions but did not have any endoleaks detected by either modality. One patient underwent embolisation of his IMA. This patient had an emergency aorto-uni-iliac device inserted originally as an emergency for rupture. The surveillance CT and DUS scans had not detected any endoleaks. However, 6 months post procedure he underwent an out of protocol emergency CT for abdominal pain and was found to have an intra peritoneal thrombus with contrast extravasation into the abdomen that was in communication with the IMA. This was embolised.

1 patient had to undergo a femoro-femoral crossover graft procedure for iliac limb thrombosis. Another 2 patients who had had aorto-uni-iliac devices with femoro-femoral cross over grafts as their initial procedure had to have revisions of their femoral anastomoses for pseudoaneurysms.

IFU and complications post procedure

7 of our patients had aneurysm anatomy outside of instructions for use for the device deployed (Table 13). 2 patients with short neck lengths had been treated outside instructions for use. Both these patients developed type 1a endoleaks that required proximal cuff extensions. One patient with neck angulation outside instructions for use (75°) also developed a type 1a endoleak that required a proximal cuff extension.

The EUROSTAR investigators evaluated the importance of neck lengths on clinical outcomes (Leurs, Kievit et al. 2006) and found that neck lengths of less than 10 mm were associated with an increased incidence of type 1a endoleaks within 30 days of the procedure, also those with neck lengths less than 15 mm had a higher risk of being diagnosed with proximal endoleaks within 48 months of follow up.

Schanzer et al (Schanzer, Greenberg et al. 2011) reviewed pre and post procedure scans of 10228 patients using the M2S database over a 10-year period and found that only 42% of their patients had anatomy that met the most conservative device instructions for use. Anatomy for 69% of their patients met the most liberal instructions for use. Their study end-point was aneurysm sac enlargement; that has been previously shown to correlate with the likelihood of developing complications (Fairman, Nolte et al. 2006, Lalka, Greenberg et al. 2009, Schanzer, Greenberg et al. 2011). Although they did not present specific data for patients undergoing EVAR outside IFU and their rate of developing complications, 41% of their patients had aneurysm sac size enlargement.

Other authors have argued that patients with unfavourable anatomy, specifically those with excessive proximal neck angulation, perform better with endografts that employ

supra-renal fixation (Robbins, Kritpracha et al. 2005). They evaluated 289 EVAR procedures performed using the Medtronic Talent endograft and categorized patients into four groups depending on their proximal neck angulation. Although they did find that device kinking was associated with proximal neck angulation, they did not report any significant difference between the groups in terms of increased incidence of complications such as endoleaks or migration.

Lee et al (Lee, Ullery et al. 2013) evaluated 218 patients undergoing EVAR at a single academic centre. For 143 patients, anatomical characteristics met the device specific instructions for use. However, for 75 patients, that had been preferentially treated with the Cook Zenith device employing supra-renal fixation, anatomical characteristics were outside of the device specific IFU. They evaluated outcomes for these two groups and found that the latter group was more likely to be treated with proximal cuff extensions and needed increased fluoroscopy time intra-procedure. However, for their study, rates of complications such as migration, endoleaks and freedom from aneurysm related mortality were similar between the two groups.

For our study we found that 3 of 7 patients that had been treated outside the device specific instructions for use required reinterventions (**Table 32**). All these patients had developed type 1a endoleaks that required proximal extensions with either cuffs or Palmaz stents® (Cordis Inc, Bridgewater Township, NJ, USA). 2 of these patients had been treated with devices that employ supra-renal fixation, whilst the patient with an angulated but of an adequate length neck had been treated with a device utilising infra-renal fixation.

Table 32: ***Reinterventions for procedures outside IFU***

Characteristic outside IFU	**Device**	**Fixation**	**Reintervention**
Short neck length (10 mm)	Cook	Supra-renal	Proximal extension
Short neck length (11 mm)	Endologix	Supra-renal	Proximal extension
Angulated proximal neck (70)	Gore	Infra-renal	Proximal extension
Angulated proximal neck (68)	Cook	Supra-renal	None
Angulated proximal neck (64)	Cook	Supra-renal	None
Angulated proximal neck (64)	Cook	Supra-renal	None
Neck diameter (33 mm)	Medtronic	Supra-renal	None

Overall for our study 19 (16%) patients underwent interventions. 7 patients were lost to follow up and 13 patients died during the course of the study. Cause of death could be determined for 7 cases, 5 patients died secondary to cardiac events, 2 patients succumbed on ITU having been admitted with graft related sepsis.

Paired CT and DUS scans

Previous reports comparing CT and DUS for follow up of patients post EVAR have defined paired scans as those that have taken place from within the same day of each other to up-to six months apart (McWilliams, Martin et al. 1999, Wolf, Johnson et al. 2000, McWilliams, Martin et al. 2002, Raman, Missig-Carrol et al. 2003, Elkouri, Panneton et al. 2004, Sandford, Bown et al. 2006). There has been some criticism of the time delay between the CT and DUS scans, as this could be responsible for discordant and unreliable results. Ideally, both the CT and DUS scans should be performed on the same day, but this is not always feasible. Even though our study defines paired scans as instances where both scans had been performed within 8 weeks of each other, 140/190 (73.7%) of our paired CT and DUS scans were performed within 2 weeks of each other with the majority 111/190 (58.4%) being performed less than a week apart. Only 25/190 (13.2%) paired scans were performed more than 4 weeks apart.

For our study, of the total 190 sets of paired scans, similar results were reported for both the CT and the paired DUS scan in 77.9% (148/190) of cases. For the remaining 22.1% (42/190) discordant results were obtained between the CT and paired DUS scan. Nine of these 42 discordant scans had been performed at an interval of more than 4 weeks, twenty-five being performed within 2 weeks of each other.

31 of the 42 discordant scans were actually DUS scans that had reported endoleaks. These were classified as false positives as for our study we had considered CT as the gold standard imaging modality. It is possible that these false positives could have actually been true endoleaks that have only been detected on duplex.

Aneurysm sac size estimation

Similar to previous reports comparing aneurysm sac size estimation between CT and DUS, we found a statistically significant difference between the two investigative modalities ($p<0.05$) (Sprouse, Meier et al. 2003, Elkouri, Panneton et al. 2004). Although we found good correlation between CT and DUS for sac size estimation, the agreement between CT and DUS was poor ($r=0.9$, $p<0.01$) (Figure 26). Bland-Altman plot demonstrated that there was difference between the two modalities at all aneurysm diameters (Figure 27). The average difference between CT and DUS measurements for sac size for our sample was 6 mm, which is comparable with other studies assessing the two modalities for aneurysm sac size measurements (Sprouse, Meier et al. 2003, Manning, Kristmundsson et al. 2009).

When patients undergo surveillance post endovascular repair, it is the change in sac size rather than the absolute sac size that determines the requirement for re-intervention. Several authors have reported on predictors of sac size change post endovascular repair of abdominal aortic aneurysms. There is agreement that thrombus burden in the neck, adherence to IFU and the presence of an endoleak are important predictors of sac size change post EVAR. Types 1 and 3 endoleaks usually require urgent intervention. However, for type 2 endoleaks, the decision to intervene usually rests on sac size change, with intervention likely if sac size is increasing. Therefore, change in sac size rather than absolute sac size is an important predictor of the requirement for intervention.

We attempted to assess the change in sac sizes between the two modalities. For our study population, we were able to assess change in sac sizes for 62 patients with serial paired scans. These paired serial differences were normally distributed, statistical analysis with the paired students t test revealed no significant difference between CT and DUS measurements (p=0.9) (Figure 28).

For our clinical study, 19 patients underwent reinterventions. 9 of these were for endoleaks detected on either CT or DUS during our study period. For 2 of these patients, an increasing sac size was detected by both modalities. The other 7 patients had no significant increase in sac size that had been detected on either modality. However, sac sizes had continued to remain similar to the last values.

It is well recognised that endoleaks are a predictor of increasing sac size and as a consequence predict the risk of reintervention post EVAR. Intuitively, an increase in sac size usually warrants further investigations or close surveillance to enable assessment and intervention for the potentially life threatening complication of late aneurysm rupture post EVAR. Change in aneurysm sac size by inference is an equally important predictor for endoleaks. Our study found no significant difference between DUS and CT for the assessment of sac size change for serial paired scans obtained for 62 patients. DUS surveillance

Assessment of the ultrasound phantom

Univariate analysis

Effect of varying endoleak flow rate

The phantom allowed for assessment of flow detection in the small system whilst altering its flow rate. When evaluating visualisation as a function of flow rate in the endoleak system independent of the other parameters, the test operators were able to detect flow in 88.9% of all endoleaks at a flow rate of 900 ml/hr compared to 75.6% of endoleaks at 300 ml/hr (Figure 17). These results did not achieve statistical significance (p= 0.616) but were similar to those reported by other patient studies (Mirza, Karthikesalingam et al. 2010).

A trend towards easier detection of high flow endoleaks was also demonstrable. This trend was also followed when breaking down results according to the relative planes of the large aortic flow and the small endoleak flow systems (Table 20). Evaluating flow detection in the subgroup where the small system is distal to the main aortic flow, the test operators achieved detection rates of 58.3% for endoleaks at 300 ml/hr, 61.1% at 500 ml/hr, 58.3% at 700 ml/hr and 83.3% at 900 ml/hr.

Effect of varying geometry

The phantom allowed us to manipulate the geometrical and spatial relationship of the two flow systems. Our results demonstrated statistical significance between two of these geometrical parameters namely, the distance between the two flow systems and

the relative horizontal plane of the small flow compared to the large flow; and flow detection in the small system. Fisher's exact test and Pearson's chi square tests revealed statistical significance ($p = 0.026$, 0.0002 respectively).

When assessing detection of flow in the small system relative to its distance from the large flow, it was noted that at distances 15.9 mm, 26.9 mm of the endoleak flow from the aortic flow, detection of flow in the small system was difficult (Figure 18). This corresponded with the predicted results generated by the ultrasound physicists prior to the phantom being assessed by the test operators (Table 18). At these two distances of the small and large flows, the second system was distal to the large flow. This also corresponds with the results obtained by assessing the relative horizontal planes of the small and large flows where it was found that flow detection was difficult in the distal plane especially in the presence of a small flow rate in the second system. We also found a significant relationship between the depth of the second system and detection of flow in the small system ($p = 0.0002$) (Figure 19) with detection of flow becoming difficult with increasing depth of the second flow system.

The third variable assessed to evaluate the effect of altering the geometrical relationship on flow detection was the relative vertical plane of the small flow to the large flow (Figure 21). Analysis of this variable did not reveal any statistically significant difference in small flow detection whether the small flow was in the same or a different vertical plane to the large flow.

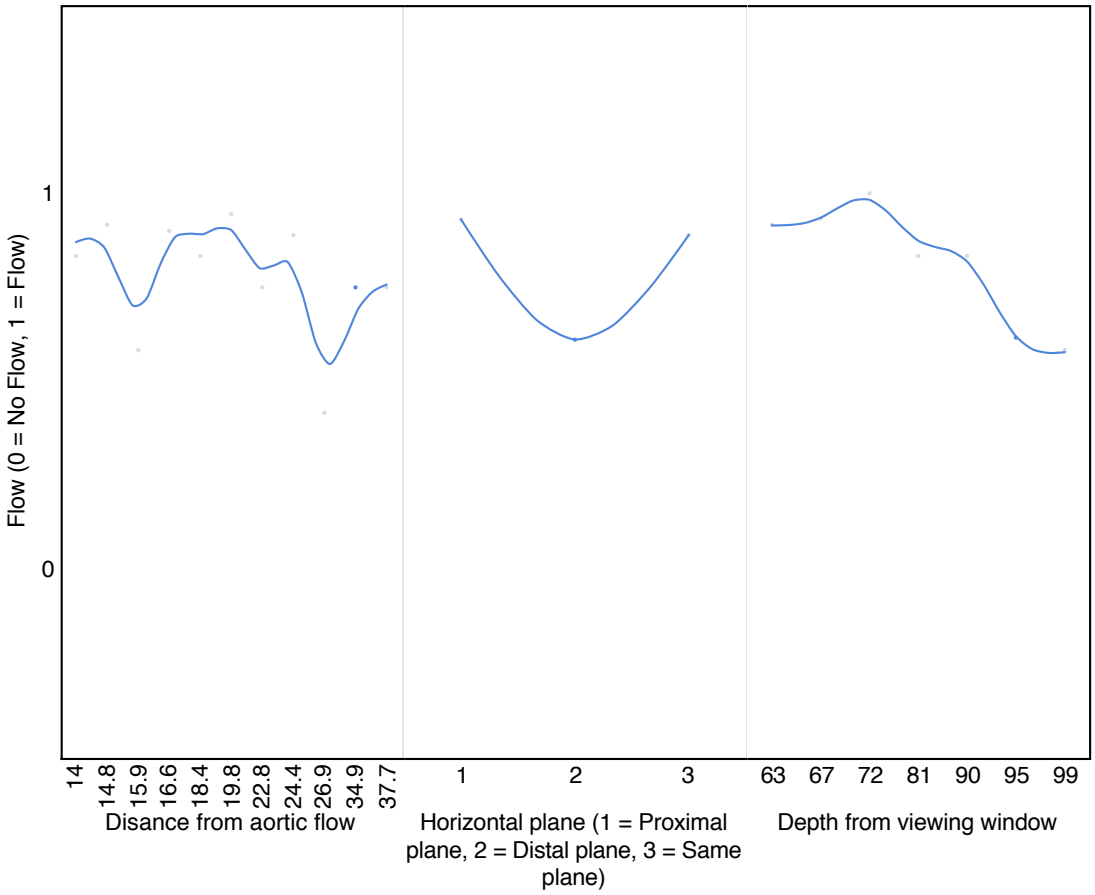

Figure 29: ***Scatter plot depicting the relationships of the significant variables and flow detection in the small flow (mean detection, smooth curve through data)***

Figure 29 is a visual representation of the effect of varying geometrical and endoleak flow rates on detection of flow by the operator. It depicts the relationships of the three significant geometrical variables affecting flow detection in the second system, with flow detection becoming increasingly difficult with increasing depth and distance of the endoleak flow from the viewing window and from the large flow respectively. The vertical axis represents flow detection. The horizontal axis represents the changes in the independent variables affecting flow detection. Detection of the endoleak flow also becomes difficult when the second system is in a plane distal to the large flow.

Effect of operator experience

The comparative data obtained from the study of the phantom, evaluating the same geometrical and flow rate combinations (Figure 22), for the three test operators did not reveal any statistically significant difference for flow detection ($p=0.6$). Despite the considerable difference in experience for the test operators and contrary to published research, our results did not reveal any significant difference in detecting complications between different operators for the post EVAR aorta.

However, assessing for intra and inter observer agreement, we could only demonstrate fair agreement. Cohen's kappa analysis was performed to assess this agreement between the operators. K values ranged from 0.21-0.4 when assessing both inter and intra-observer agreement. We also assessed for agreement between the operators and predicted results that were achieved by the clinical physicists. Again, kappa analysis demonstrated fair agreement ($\kappa=0.36$).

Our results are reflective of what has been reported in terms of the operator dependant nature of ultrasound (**Table 5**). The clinical physicists involved with the project had limited clinical experience compared with our test operators who had regular clinical contact and substantial experience in vascular ultrasonography. This might explain the failure to achieve higher levels of agreement with the predicted results. However, even when assessing inter-observer and intra-observer agreement, our results indicate only fair agreement for detection of flow.

Multivariate analysis

Univariate analysis was performed to identify the variables that had a statistically significant impact on flow detection in the small system. Pearson's chi square and Fishers exact tests were employed to identify depth of small flow from viewing window, distance between the large, small flows; and the relative horizontal planes of the small and large flows as the statistically significant variables impacting flow detection.

Table 33: ***Multivariate analysis performed using binary logistic regression analysis using significant variable identified through univariate analysis***

	B	S.E.	Wald	df	Sig.	Exp(B)	95% C.I. for Exp (B)	
							Lower	Upper
Horizontal plane	.660	.474	1.936	1	.164	1.935	.764	4.901
Distance from aortic flow	.010	.029	.127	1	.722	1.010	.955	1.069
Depth from viewing window	-.097	.024	16.621	1	.000	.908	.866	.951
Constant	8.137	1.590	26.182	1	.000	3418.361		

Multivariate analysis was performed using binary logistic regression. The model was statistically significant and was able to explain 22% of the variance observed (Nagelkerke R^2). The whole model fit test proved that there was statistical dependence between the above variables and prediction of flow detection ($p = 0.0002$, $U = 0.2$). The lack of fit test did not reveal statistical significance supporting the view that adding more variables would be unlikely to make a difference to the predictive model. The likelihood ratio tests confirmed the statistical significance of depth of the

endoleak from the viewing window as the variable predicting flow detection (Table 33).

CONCLUSIONS

The results from our assessment of the Doppler flow phantom have demonstrated that depth of the endoleak from the viewing window has a significant impact on flow detection. We also established that endoleaks that are present in a plane distal to the large artic flow are more difficult to diagnose.

Clinical research has suggested that slow flowing endoleaks are difficult to diagnose (Mirza, Karthikesalingam et al. 2010). Our test protocol was designed with a higher number of assessments at slower flow rates of the endoleak system. Even though our results analysing the impact of endoleak flow rates on detection did not reveal statistical significance, we did demonstrate a trend toward detection of flow in the second system being difficult with reduced flow in the endoleak system. It is possible that with increasing the number of test scenarios or operators, we might have been able to demonstrate statistical significance. Multivariate analysis, however, does suggest that increasing the number of variables would be unlikely to have any significant impact on the predictive model.

The clinical arm of our study demonstrates that DUS can be effective in diagnosing complications post EVAR. It has value in detecting a change in aneurysm sac size, although as reported by several other authors, it tends to underestimate aneurysm sac sizes as compared to CT (Sprouse, Meier et al. 2003, Elkouri, Panneton et al. 2004). For the clinical part of or study we were able to diagnose all complications requiring intervention and our results for sac size estimation are also in keeping with previous published reports. The results from our clinical arm, therefore, support the use of Duplex ultrasound in post EVAR surveillance protocols.

There have been reports of improvements in the sensitivity and specificity of duplex ultrasound with the introduction of contrast (Heilberger, Schunn et al. 1997,

McWilliams, Martin et al. 1999, McWilliams, Martin et al. 2002, Giannoni, Palombo et al. 2003, Napoli, Bargellini et al. 2004, Henao, Hodge et al. 2006). Ultrasound contrast media such as sulphur hexafluoride (Sonovue) and galactose / Peflutren and albumin (Optison) are gas filled, stable micro-bubbles with a high degree of echogenicity, that cause an increase in backscatter. The improvement in complication detection rates with contrast though, has not been uniform. McWilliams et al (McWilliams, Martin et al. 1999) compared contrast-enhanced duplex (CED) with arterial phase CT and reported excellent results, but the same group could not reproduce these results when comparing biphasic CT and CED (McWilliams, Martin et al. 2002). A further recent study, using a continuous contrast infusion technique found CED to be comparable to CT (Henao, Hodge et al. 2006). Our study did not employ contrast enhanced ultrasound, but the Doppler flow phantom provides a good opportunity for further research into whether the addition of ultrasound contrast offers any significant advantages over unenhanced ultrasound in this group of patients.

Management of abdominal aortic aneurysms is a constantly evolving field with technology being constantly updated. Older generation stent grafts such as those used by Parodi et al (Parodi, Palmaz et al. 1991) have been replaced with newer ones. New concepts in devices such as the Nellix system (Endologix inc, Irvine, California, USA) are also being trialled that may revolutionise the endovascular management of aneurysms. With all this advancement major complications post EVAR are rare, but this has also resulted in complex cases, that would previously have not been thought to be amenable for endovascular grafting, being considered for EVAR. Wider exposure and information dissemination has also implied that patients are more inclined towards having minimally invasive surgery and increased the number of such procedures being performed. The need for surveillance of patients post procedure

therefore remains of utmost importance. Endoleaks, originally thought to be a difficult problem has gained better understanding. Type 2 endoleaks that are not associated with an increase in aneurysm size are mostly managed conservatively.

Several centres now routinely perform post EVAR surveillance with Duplex, with CT or catheter angiography being performed in cases of ambiguity or complications (Harrison, Oshin et al. 2011). Another recent study has suggested basing post EVAR surveillance on early results, eliminating the 6 month scan; and yearly surveillance with Duplex ultrasound for patients without initial complications (Sternbergh, Greenberg et al. 2008). A recent survey of post EVAR surveillance practices in the UK has revealed heterogeneity in post EVAR surveillance (Karthikesalingam, Page et al. 2011) indicating a continuing lack of consensus amongst vascular centres.

Screening for abdominal aortic aneurysms has been discussed in detail over the last few years (Kyriakides, Byrne et al. 2000, Ashton, Buxton et al. 2002, Cosford and Leng 2007). It has also been suggested that screening for abdominal aortic aneurysms will be associated with a modest increase in the overall surgical workload of hospitals (Kyriakides, Byrne et al. 2000). Increased aneurysm detection will translate into an increased number of patients undergoing EVAR for their abdominal aortic aneurysms. With abdominal aortic aneurysm screening now being performed in the UK, the time is right for the introduction of a DUS based surveillance protocol of patients post EVAR. Such a protocol may include both CT and DUS for the first year, subsequent surveillance being performed only with DUS. CT scans could be performed in cases where complications are detected on DUS. Contrast enhanced duplex needs to be investigated further and may provide information to help drive down both costs and radiation exposure to patients from EVAR surveillance.

In conclusion the results form our phantom have demonstrated that certain types of endoleaks are more difficult to diagnose on ultrasound. Duplex ultrasound offers advantages over other modalities for post EVAR surveillance, however its role in its current form, is more likely to be complimentary to other imaging modalities such as CT.

Future Work

Our laboratory work has revealed results suggesting that the depth of the endoleak from the viewing window is the most important predictor of the determination of flow in the endoleak system. The next step for the project would be to assess the impact of introduction of ultrasonic contrast media into the flow systems. This may lead to increased detection of endoleaks that have proven elusive to the non-contrast model. For the clinical arm, selected patients with endoleaks that were missed on Duplex could be evaluated further by means of contrast-enhanced duplex to ascertain if these endoleaks were to become apparent.

These investigations could prove a definitive increase in sensitivity of DUS for the detection of endoleaks and other complications in the post EVAR setting. Another area of future development could be the assessment of the ultrasound phantom as a training modality for vascular ultrasonographers. The phantom could be developed further with this in mind and may become a useful training tool.

REFERENCES

AbuRahma, A. F., C. A. Welch, B. B. Mullins and B. Dyer (2005). "Computed tomography versus color duplex ultrasound for surveillance of abdominal aortic stent-grafts." J Endovasc Ther **12**(5): 568-573.

Anjum, A., R. von Allmen, R. Greenhalgh and J. T. Powell (2012). "Explaining the decrease in mortality from abdominal aortic aneurysm rupture." Br J Surg **99**(5): 637-645.

Arko, F. R., K. A. Filis, S. A. Siedel, B. L. Johnson, A. R. Drake, T. J. Fogarty and C. K. Zarins (2003). "Intrasac flow velocities predict sealing of type II endoleaks after endovascular abdominal aortic aneurysm repair." J Vasc Surg **37**(1): 8-15.

Armerding, M. D., G. D. Rubin, C. F. Beaulieu, S. M. Slonim, E. W. Olcott, S. L. Samuels, M. J. Jorgensen, C. P. Semba, R. B. Jeffrey, Jr. and M. D. Dake (2000). "Aortic aneurysmal disease: assessment of stent-graft treatment-CT versus conventional angiography." Radiology **215**(1): 138-146.

Ashton, H. A., M. J. Buxton, N. E. Day, L. G. Kim, T. M. Marteau, R. A. Scott, S. G. Thompson and N. M. Walker (2002). "The Multicentre Aneurysm Screening Study (MASS) into the effect of abdominal aortic aneurysm screening on mortality in men: a randomised controlled trial." Lancet **360**(9345): 1531-1539.

Ayuso, J. R., T. M. de Caralt, M. Pages, V. Riambau, C. Ayuso, M. Sanchez, M. I. Real and X. Montana (2004). "MRA is useful as a follow-up technique after endovascular repair of aortic aneurysms with nitinol endoprostheses." J Magn Reson Imaging **20**(5): 803-810.

Bastos Goncalves, F., H. J. Verhagen, K. Chinsakchai, J. W. van Keulen, M. T. Voute, H. J. Zandvoort, F. L. Moll and J. A. van Herwaarden (2012). "The influence of neck thrombus on clinical outcome and aneurysm morphology after endovascular aneurysm repair." J Vasc Surg **56**(1): 36-44.

Bendick, P. J., P. G. Bove, G. W. Long, G. B. Zelenock, O. W. Brown and C. J. Shanley (2003). "Efficacy of ultrasound scan contrast agents in the noninvasive follow-up of aortic stent grafts." J Vasc Surg **37**(2): 381-385.

Bertges, D. J., K. Chow, M. C. Wyers, D. Landsittel, A. V. Frydrych, W. Stavropoulos, W. A. Tan, R. Y. Rhee, M. F. Fillinger, R. M. Fairman and M. S. Makaroun (2003). "Abdominal aortic aneurysm size regression after endovascular repair is endograft dependent." J Vasc Surg **37**(4): 716-723.

Blanchard, J. F. (1999). "Epidemiology of abdominal aortic aneurysms." Epidemiol Rev **21**(2): 207-221.

Bown, M. J., A. J. Sutton, P. R. Bell and R. D. Sayers (2002). "A meta-analysis of 50 years of ruptured abdominal aortic aneurysm repair." Br J Surg **89**(6): 714-730.

Brewin, M. P., L. C. Pike, D. E. Rowland and M. J. Birch (2008). "The acoustic properties, centered on 20 MHZ, of an IEC agar-based tissue-mimicking material and its temperature, frequency and age dependence." Ultrasound Med Biol **34**(8): 1292-1306.

Browne, J. E., K. V. Ramnarine, A. J. Watson and P. R. Hoskins (2003). "Assessment of the acoustic properties of common tissue-mimicking test phantoms." Ultrasound Med Biol **29**(7): 1053-1060.

Browne, J. E., A. J. Watson, P. R. Hoskins and A. T. Elliott (2004). "Validation of a sensitivity performance index test protocol and evaluation of colour Doppler sensitivity for a range of ultrasound scanners." Ultrasound Med Biol **30**(11): 1475-1483.

Chaikof, E. L., M. F. Fillinger, J. S. Matsumura, R. B. Rutherford, G. H. White, J. D. Blankensteijn, V. M. Bernhard, P. L. Harris, K. C. Kent, J. May, F. J. Veith and C. K. Zarins (2002). "Identifying and grading factors that modify the outcome of endovascular aortic aneurysm repair." Journal of Vascular Surgery **35**(5): 1061-1066.

Chandran, K. B. (1993). "Flow dynamics in the human aorta." J Biomech Eng **115**(4B): 611-616.

Chuter, T., K. Ivancev, M. Malina, T. Resch, J. Brunkwall, B. Lindblad and B. Risberg (1997). "Aneurysm pressure following endovascular exclusion." Eur J Vasc Endovasc Surg **13**(1): 85-87.

Cohan, R. H. and J. H. Ellis (1997). "Iodinated contrast material in uroradiology. Choice of agent and management of complications." Urol Clin North Am **24**(3): 471-491.

Cook Inc. Cook Zenith - Instructions for use. http://www.cookmedical.com/ai/resources.do?id=2152.

Cosford, P. A. and G. C. Leng (2007). "Screening for abdominal aortic aneurysm." Cochrane Database Syst Rev(2): CD002945.

Curci, J. A. and R. W. Thompson (2004). "Adaptive cellular immunity in aortic aneurysms: cause, consequence, or context?" J Clin Invest **114**(2): 168-171.

d'Audiffret, A., P. Desgranges, D. H. Kobeiter and J. P. Becquemin (2001). "Follow-up evaluation of endoluminally treated abdominal aortic aneurysms with duplex ultrasonography: validation with computed tomography." J Vasc Surg **33**(1): 42-50.

Dawson, P. (1996). "The non-ionic isotonic contrast agents. Perspectives and controversies." European Radiology **6 Suppl 2**: S20-24.

De Bruin, J. L., A. F. Baas, J. Buth, M. Prinssen, E. L. Verhoeven, P. W. Cuypers, M. R. van Sambeek, R. Balm, D. E. Grobbee, J. D. Blankensteijn and D. S. Group (2010). "Long-term outcome of open or endovascular repair of abdominal aortic aneurysm." N Engl J Med **362**(20): 1881-1889.

Dias, N. V., K. Ivancev, M. Malina, T. Resch, B. Lindblad and B. Sonesson (2004). "Intra-aneurysm sac pressure measurements after endovascular aneurysm repair: differences between shrinking, unchanged, and expanding aneurysms with and without endoleaks." J Vasc Surg **39**(6): 1229-1235.

Dias, N. V., K. Ivancev, T. A. Resch, M. Malina and B. Sonesson (2007). "Endoleaks after endovascular aneurysm repair lead to nonuniform intra-aneurysm sac pressure." J Vasc Surg **46**(2): 197-203.

Dobrin, P. B. and R. Mrkvicka (1994). "Failure of elastin or collagen as possible critical connective tissue alterations underlying aneurysmal dilatation." Cardiovascular surgery **2**(4): 484-488.

Elkouri, S., J. M. Panneton, J. C. Andrews, B. D. Lewis, M. A. McKusick, A. A. Noel, C. M. Rowland, T. C. Bower, K. J. Cherry, Jr. and P. Gloviczki (2004). "Computed tomography and ultrasound in follow-up of patients after endovascular repair of abdominal aortic aneurysm." Ann Vasc Surg **18**(3): 271-279.

Endologix Inc. Endologix - Instructions for use. http://endologix.com/pdf/Endologix_IFU_English.pdf.

EVAR trial participants (2005). "Endovascular aneurysm repair and outcome in patients unfit for open repair of abdominal aortic aneurysm (EVAR trial 2): randomised controlled trial." Lancet **365**: 2187-2192.

EVAR trial participants (2005). "Endovascular aneurysm repair versus open repair in patients with abdominal aortic aneurysm (EVAR trial 1): randomised controlled trial." Lancet **365**: 2179 - 2186.

EVAR trial participants (2010). "Endovascular versus open repair of abdominal aortic aneurysms." N Engl J Med **362**(20): 1863-1871.

Fairman, R. M., L. Nolte, S. A. Snyder, T. A. Chuter, R. K. Greenberg and I. Zenith (2006). "Factors predictive of early or late aneurysm sac size change following endovascular repair." J Vasc Surg **43**(4): 649-656.

Giannoni, M. F., G. Palombo, E. Sbarigia, F. Speziale, A. Zaccaria and P. Fiorani (2003). "Contrast-enhanced ultrasound imaging for aortic stent-graft surveillance." J Endovasc Ther **10**(2): 208-217.

Golledge, J. and P. E. Norman (2010). "Atherosclerosis and abdominal aortic aneurysm: cause, response, or common risk factors?" Arterioscler Thromb Vasc Biol **30**(6): 1075-1077.

Golzarian, J., L. Dussaussois, H. T. Abada, P. A. Gevenois, D. Van Gansbeke, J. Ferreira and J. Struyven (1998). "Helical CT of aorta after endoluminal stent-graft therapy: value of biphasic acquisition." AJR Am J Roentgenol **171**(2): 329-331.

Golzarian, J., S. Murgo, L. Dussaussois, S. Guyot, K. A. Said, J. C. Wautrecht and J. Struyven (2002). "Evaluation of abdominal aortic aneurysm after endoluminal treatment: comparison of color Doppler sonography with biphasic helical CT." AJR Am J Roentgenol **178**(3): 623-628.

Gorich, J., N. Rilinger, R. Sokiranski, K. Orend, C. Ermis, S. C. Kramer, H. Brambs, L. Sunder-Plassman and R. Pamler (1999). "Leakages after endovascular repair of aortic aneurysms: Classification based on findings at CT, angiography and radiography." Radiology **213**(3): 767-772.

Greenfield, A. L., E. J. Halpern, J. Bonn, R. J. Wechsler and M. B. Kahn (2002). "Application of duplex US for characterization of endoleaks in abdominal aortic stent-grafts: report of five cases." Radiology **225**(3): 845-851.

Hager, E. S., J. S. Cho, M. S. Makaroun, S. C. Park, R. Chaer, L. Marone and R. Y. Rhee (2012). "Endografts with suprarenal fixation do not perform better than those with infrarenal fixation in the treatment of patients with short straight proximal aortic necks." J Vasc Surg **55**(5): 1242-1246.

Haider, S. E., S. F. Najjar, J. S. Cho, R. Y. Rhee, M. K. Eskandari, J. S. Matsumura, M. S. Makaroun and M. D. Morasch (2006). "Sac behavior after aneurysm treatment with the Gore Excluder low-permeability aortic endoprosthesis: 12-month comparison to the original Excluder device." J Vasc Surg **44**(4): 694-700.

Harrison, G. J., O. A. Oshin, S. R. Vallabhaneni, J. A. Brennan, R. K. Fisher and R. G. McWilliams (2011). "Surveillance after EVAR based on duplex ultrasound and abdominal radiography." Eur J Vasc Endovasc Surg **42**(2): 187-192.

Heilberger, P., C. Schunn, W. Ritter, S. Weber and D. Raithel (1997). "Postoperative color flow duplex scanning in aortic endografting." J Endovasc Surg **4**(3): 262-271.

Hellinger, J. C. (2005). "Endovascular repair of thoracic and abdominal aortic aneurysms: pre- and postprocedural imaging." Tech Vasc Interv Radiol **8**(1): 2-15.

Hellmann, D. B., D. J. Grand and J. A. Freischlag (2007). "Inflammatory abdominal aortic aneurysm." JAMA **297**(4): 395-400.

Henao, E. A., M. D. Hodge and D. D. Felkai (2006). "Contrast-enhanced Duplex surveillance after endovascular abdominal aortic aneurysm repair: Improved efficacy using a continuous infusion technique." J Vasc Surg **43**: 259 - 264.

Hirose, H. and M. D. Tilson (2001). "Abdominal Aortic Aneurysm As an Autoimmune Disease." Annals of the New York Academy of Science **947**: 416-418.

Iezzi, R., A. Cotroneo and A. Fillippone (2006). "Multidetector CT in abdominal aortic aneurysm treated with endovascular repair: are unenhanced and delayed phase enhanced images effective for endoleak detection? ." Radiology **241**(3): 915-921.

International Commission on Radiological Protection (2000). Managing Patient Dose in Computed Tomography.

International Electrochemical Commission (1996). IEC 1390 Real-time pulse-echo systems - Guide for test procedures to determine performance specifications. Publication number 130. Ultrasonics, IEC. **1390**.

International Electrotechnical Commission (2001). IEC 61685 ed 1.0: Ultrasonics - Flow measurment systems - Flow test object. Geneva, IEC. **1685**.

Ivanov, V. N., P. Lopez Bergami, G. Maulit, T. A. Sato, D. Sassoon and Z. Ronai (2003). "FAP-1 association with Fas (Apo-1) inhibits Fas expression on the cell surface." Mol Cell Biol **23**(10): 3623-3635.

Johnsen, S. H., S. H. Forsdahl, K. Singh and B. K. Jacobsen (2010). "Atherosclerosis in abdominal aortic aneurysms: a causal event or a process running in parallel? The Tromso study." Arterioscler Thromb Vasc Biol **30**(6): 1263-1268.

Karthikesalingam, A., A. A. Page, C. Pettengell, R. J. Hinchliffe, I. M. Loftus, M. M. Thompson and P. J. Holt (2011). "Heterogeneity in surveillance after endovascular aneurysm repair in the UK." Eur J Vasc Endovasc Surg **42**(5): 585-590.

Kuivaniemi, H., C. D. Platsoucas and M. D. Tilson, 3rd (2008). "Aortic aneurysms: an immune disease with a strong genetic component." Circulation **117**(2): 242-252.

Kyriakides, C., J. Byrne, S. Green and N. R. Hulton (2000). "Screening of abdominal aortic aneurysm: a pragmatic approach." Ann R Coll Surg Engl **82**(1): 59-63.

Lalka, S. G., R. K. Greenberg, T. Chuter and L. A. Nolte (2009). Prediction of long-term change in post-EVAR aneurysm sac size. Southern association for vascular surgery. Arizona.

Lau, L. L., A. G. Hakaim, W. A. Oldenburg, B. Neuhauser, J. M. McKinney, R. Paz-Fumagalli and A. Stockland (2003). "Effect of suprarenal versus infrarenal aortic endograft fixation on renal function and renal artery patency: a comparative study with intermediate follow-up." J Vasc Surg **37**(6): 1162-1168.

Lederle, F. A., J. A. Freischalag, T. C. Kyriakides, F. T. Padberg, J. S. Matsumara, T. R. Kohler, P. H. Lin, J. M. Jean-Claude, D. F. Cikrit, K. M. Swanson and P. N.

Peduzzi (2009). "Outcomes following open vs endovascular repair of abdominal aortic aneurysm: a randomised trial." JAMA **302**(14).

Lederle, F. A., J. A. Freischlag, T. C. Kyriakides, J. S. Matsumura, F. T. Padberg, Jr., T. R. Kohler, P. Kougias, J. M. Jean-Claude, D. F. Cikrit, K. M. Swanson and O. V. A. C. S. Group (2012). "Long-term comparison of endovascular and open repair of abdominal aortic aneurysm." N Engl J Med **367**(21): 1988-1997.

Lederle, F. A., D. B. Nelson and A. M. Joseph (2003). "Smokers' relative risk for aortic aneurysm compared with other smoking-related diseases: a systematic review." J Vasc Surg **38**(2): 329-334.

Lederle, F. A., S. E. Wilson, G. R. Johnson, D. B. Reinke, F. N. Littooy, C. Acher, D. J. Ballard, L. Messina, I. L. Gordon, E. P. Chute, W. C. Krupski and D. Bandyk (2002). "Immediate repair compared with surveillance of small abdominal aortic aneurysms." N Engl J Med **346**(19): 1437-1444.

Lederle, F. A., S. E. Wilson, G. R. Johnson, D. B. Reinke, F. N. Littooy, C. W. Acher, L. M. Messina, D. J. Ballard and H. J. Ansel (1995). "Variability in measurement of abdominal aortic aneurysms. Abdominal Aortic Aneurysm Detection and Management Veterans Administration Cooperative Study Group." J Vasc Surg **21**(6): 945-952.

Lee, J. T., B. W. Ullery, C. K. Zarins, C. t. Olcott, E. J. Harris, Jr. and R. L. Dalman (2013). "EVAR deployment in anatomically challenging necks outside the IFU." Eur J Vasc Endovasc Surg **46**(1): 65-73.

Leurs, L. J., J. Kievit, P. C. Dagnelie, P. J. Nelemans, J. Buth and E. Collaborators (2006). "Influence of infrarenal neck length on outcome of endovascular abdominal aortic aneurysm repair." J Endovasc Ther **13**(5): 640-648.

Lin, K. K., J. A. Kratzberg and M. L. Raghavan (2012). "Role of aortic stent graft oversizing and barb characteristics on folding." J Vasc Surg **55**(5): 1401-1409.

Lindholt, J. S. and G. P. Shi (2006). "Chronic inflammation, immune response, and infection in abdominal aortic aneurysms." Eur J Vasc Endovasc Surg **31**(5): 453-463.

Madsen, E. L., F. Dong, G. R. Frank, B. S. Garra, K. A. Wear, T. Wilson, J. A. Zagzebski, H. L. Miller, K. K. Shung, S. H. Wang, E. J. Feleppa, T. Liu, W. D. O'Brien, Jr., K. A. Topp, N. T. Sanghvi, A. V. Zaitsev, T. J. Hall, J. B. Fowlkes, O. D. Kripfgans and J. G. Miller (1999). "Interlaboratory comparison of ultrasonic backscatter, attenuation, and speed measurements." J Ultrasound Med **18**(9): 615-631.

Malina, M., T. Resch and B. Sonesson (2008). "EVAR and complex anatomy: an update on fenestrated and branched stent grafts." Scand J Surg **97**(2): 195-204.

Manning, B. J., T. Kristmundsson, B. Sonesson and T. Resch (2009). "Abdominal aortic aneurysm diameter: a comparison of ultrasound measurements with those from standard and three-dimensional computed tomography reconstruction." J Vasc Surg **50**(2): 263-268.

McClennan, B. L. (1987). "Low-osmolality contrast media: premises and promises." Radiology **162**(1 Pt 1): 1-8.

McClennan, B. L. (1990). "Preston M. Hickey memorial lecture. Ionic and nonionic iodinated contrast media: evolution and strategies for use." AJR Am J Roentgenol **155**(2): 225-233.

McDonnell, C. O., M. Halak, A. Bartlett and S. R. Baker (2006). "Abdominal aortic aneurysm neck morphology: proposed classification system." Ir J Med Sci **175**(3): 4-8.

McLafferty, R. B., B. S. McCrary, M. A. Mattos, L. A. Karch, D. E. Ramsey, M. M. Solis and K. J. Hodgson (2002). "The use of color-flow duplex scan for the detection of endoleaks." J Vasc Surg **36**(1): 100-104.

McWilliams, R. G., J. Martin, D. White, D. A. Gould, P. L. Harris, S. C. Fear, J. Brennan, G. L. Gilling-Smith, A. Bakran and P. C. Rowlands (1999). "Use of contrast-enhanced ultrasound in follow-up after endovascular aortic aneurysm repair." J Vasc Interv Radiol **10**(8): 1107-1114.

McWilliams, R. G., J. Martin, D. White, D. A. Gould, P. C. Rowlands, A. Haycox, J. Brennan, G. L. Gilling-Smith and P. L. Harris (2002). "Detection of endoleak with enhanced ultrasound imaging: comparison with biphasic computed tomography." J Endovasc Ther **9**(2): 170-179.

Medicines and Healthcare products regulatory Agency (2007). Nephrogenic Systemic Fibrosis (NSF) and gadolinium containing MR contrast agents: Public Assessment Report**:**

.

Medtronic Inc. Endurant - Instructions for use.

Mirza, T. A., A. Karthikesalingam, D. Jackson, S. R. Walsh, P. J. Holt, P. D. Hayes and J. R. Boyle (2010). "Duplex ultrasound and contrast-enhanced ultrasound versus computed tomography for the detection of endoleak after EVAR: systematic review and bivariate meta-analysis." Eur J Vasc Endovasc Surg **39**(4): 418-428.

Napoli, V., I. Bargellini and S. Sardella (2004). "Abdominal Aortic Aneurysm: Contrast-enhanced US for Missed Endoleaks after Endoluminal Repair." Radiology **233**: 217 - 225.

Norman S Williams, C. J. K. Bulstrode and P. R. O'Connell (2008). Bailey & Love's Short Practice of Surgery, Hodder Arnold.

Ohki, T., K. Ouriel, P. G. Silveira, B. Katzen, R. White, F. Criado and E. Diethrich (2007). "Initial results of wireless pressure sensing for endovascular aneurysm repair: the APEX Trial--Acute Pressure Measurement to Confirm Aneurysm Sac EXclusion." J Vasc Surg **45**(2): 236-242.

Ouriel, K., D. G. Clair, R. K. Greenberg, S. P. Lyden, P. J. O'Hara, T. P. Sarac, S. D. Srivastava, B. Butler and E. S. Sampram (2003). "Endovascular repair of abdominal aortic aneurysms: device-specific outcome." J Vasc Surg **37**(5): 991-998.

Pages, S., J. P. Favre, A. Cerisier, S. Pyneeandee, C. Boissier and C. Veyret (2001). "Comparison of color duplex ultrasound and computed tomography scan for surveillance after aortic endografting." Ann Vasc Surg **15**(2): 155-162.

Palmisano, A. and A. Vaglio (2009). "Chronic periaortitis: a fibro-inflammatory disorder." Best Pract Res Clin Rheumatol **23**(3): 339-353.

Parent, F. N., G. H. Meier, V. Godziachvili, C. J. LeSar, F. M. Parker, K. A. Carter, R. G. Gayle, R. J. DeMasi, M. J. Marcinczyk and R. T. Gregory (2002). "The incidence and natural history of type I and II endoleak: a 5-year follow-up assessment with color duplex ultrasound scan." J Vasc Surg **35**(3): 474-481.

Parmer, S. S., J. P. Carpenter and I. Endologix (2006). "Endovascular aneurysm repair with suprarenal vs infrarenal fixation: a study of renal effects." J Vasc Surg **43**(1): 19-25.

Parodi, J. C., J. C. Palmaz and H. D. Barone (1991). "Transfemoral intraluminal graft implantation for abdominal aortic aneurysms." Ann Vasc Surg **5**(6): 491-499.

Pennell, R. C., L. H. Hollier, J. T. Lie, P. E. Bernatz, J. W. Joyce, P. C. Pairolero, K. J. Cherry and J. W. Hallett (1985). "Inflammatory abdominal aortic aneurysms: a thirty-year review." J Vasc Surg **2**(6): 859-869.

Prinissen, M., E. L. G. Verhoeven, J. Buth, P. W. M. Cuypers, M. R. H. M. van Sambeek, R. Balm, E. Buskens, D. E. Grobbee and J. D. Blankensteijn (2004). "A randomised trial comparing conventional and endovascular repair of abdominal aortic aneurysms." N Engl J Med **351**(16): 1607-1618.

Raman, K. G., N. Missig-Carrol, T. Richardson, S. C. Muluk and M. S. Makaroun (2003). "Colour-flow duplex ultrasound scan versus computed tomographic scan in the surveillance of endovascular aneurysm repair." J Vasc Surg **38**(4): 645 -651.

Ramnarine, K. V., T. Anderson and P. R. Hoskins (2001). "Construction and geometric stability of physiological flow rate wall-less stenosis phantoms." Ultrasound Med Biol **27**(2): 245-250.

Ramnarine, K. V., D. K. Nassiri, P. R. Hoskins and J. Lubbers (1998). "Validation of a new blood-mimicking fluid for use in doppler test objects." Ultrasound Med Biol **24**(3): 451-459.

Robbins, M., B. Kritpracha, H. G. Beebe, F. J. Criado, Y. Daoud and A. J. Comerota (2005). "Suprarenal endograft fixation avoids adverse outcomes associated with aortic neck angulation." Ann Vasc Surg **19**(2): 172-177.

Rozenblit, A., M. Patlas and A. Rosenbaum (2003). "Detection of Endoleaks after Endovascular Repair of Abdominal Aortic Aneurysm: Value of Unenhanced and Delayed Helical CT Acquisitions." Radiology **227**: 426-433.

Sakalihasan, N., R. Limet and O. D. Defawe (2005). "Abdominal aortic aneurysm." Lancet **365**(9470): 1577-1589.

Sandford, R., M. Bown and G. Fishwick (2006). "Duplex Ultrasound Scanning is Reliable in the Detection of Endoleak Following Endovascular Aneurysm Repair." Eur J Vasc Endovasc Surg **32**(5): 537 - 541.

Sato, D. T., C. D. Goff, R. T. Gregory, K. D. Robinson, K. A. Carter, B. R. Herts, H. B. Vilsack, R. G. Gayle, F. N. Parent, 3rd, R. J. DeMasi and G. H. Meier (1998). "Endoleak after aortic stent graft repair: diagnosis by color duplex ultrasound scan versus computed tomography scan." J Vasc Surg **28**(4): 657-663.

Schanzer, A., R. K. Greenberg, N. Hevelone, W. P. Robinson, M. H. Eslami, R. J. Goldberg and L. Messina (2011). "Predictors of abdominal aortic aneurysm sac enlargement after endovascular repair." Circulation **123**(24): 2848-2855.

Sonesson, B., N. Dias, M. Malina, P. Olofsson, D. Griffin, B. Lindblad and K. Ivancev (2003). "Intra-aneurysm pressure measurements in successfully excluded abdominal aortic aneurysm after endovascular repair." J Vasc Surg **37**(4): 733-738.

Sovak, M. (1994). "Contrast media: a journey almost sentimental." Investigative Radiology **29 Suppl 1**: S4-14.

Spring, D. B. and C. P. Quesenberry, Jr. (1991). "Costs of low-osmolar contrast media." JAMA **266**(8): 1081-1082.

Sprouse, L. R., G. H. Meier, C. J. LeSar, R. J. DeMasi, J. Sood, F. N. Parent, M. J. Marcinzyck and R. G. Gayle (2003). "Comparison of abdominal aortic aneurysm diameter measurements obtained with ultrasound and computed tomography: is there a difference?" J Vasc Surg **38**(3): 466-471.

Stavropoulos, S. W., T. W. Clark, J. P. Carpenter, R. M. Fairman, H. Litt, O. C. Velazquez, E. Insko, M. Farner and R. A. Baum (2005). "Use of CT angiography to

classify endoleaks after endovascular repair of abdominal aortic aneurysms." J Vasc Interv Radiol **16**(5): 663-667.

Sternbergh, W. C., 3rd, S. R. Money, R. K. Greenberg and T. Chuter (2004). "Influence of endograft oversizing on device migration, endoleak, aneurysm shrinkage, and aortic neck dilatation: Results from the Zenith multicenter trial." J Vasc Surg **39**(1): 20-26.

Sternbergh, W. C., R. K. Greenberg, T. Chuter and B. H. Tonnessen (2008). "Redefining postoperative surveillance after endovascular aneurysm repair: Recommendations based on 5-year follow-up in the US Zenith multicenter trial." J Vasc Surg **48**(2): 278-285.

Surry, K. J. M., H. J. B. Austin, A. Fenster and T. M. Peters (2004). "Poly(vinyl alcohol) cryogel phantoms for use in ultrasound and MR imaging." Physics in Medicine and Biology **49**(24): 5529 - 5546.

Teirlinck, C. J., R. A. Bezemer, C. Kollmann, J. Lubbers, P. R. Hoskins, K. V. Ramnarine, P. Fish, K. E. Fredeldt and U. G. Schaarschmidt (1998). "Development of an example flow test object and comparison of five of these test objects, constructed in various laboratories." Ultrasonics **36**(1-5): 653-660.

The UK small aneurysm trial participants (1998). "Mortality results for randomised controlled trial of early elective surgery or ultrasonographic surveillance for small abdominal aortic aneurysms." The Lancet **352**(9141): 1649-1655.

Thompson, M. M., J. R. Boyle, t. Hartshorn, C. Maltezos, A. Nasim, R. D. Sayers, G. Fishwick and P. R. Bell (1998). "Comparison of computed tomography and duplex imaging in assessing

aortic morphology following endovascular aneurysm repair." Br J Surg **85**: 346-350.

United Kingdom small aneurysm trial participants (2002). "Long-Term Outcomes Of Immediate Repair Compared With Surveillance Of Small Abdominal Aortic Aneurysms." New England Journal of Medicine **346**(19): 1445-1452.

van der Laan, M. J., L. W. Bartels, M. A. Viergever and J. D. Blankensteijn (2006). "Computed tomography versus magnetic resonance imaging of endoleaks after EVAR." Eur J Vasc Endovasc Surg **32**(4): 361-365.

van Marrewijk, C., J. Buth, P. L. Harris, L. Norgren, A. Nevelsteen and M. G. Wyatt (2002). "Significance of endoleaks after endovascular repair of abdominal aortic aneurysms: The EUROSTAR experience." J Vasc Surg **35**(3): 461-473.

van Prehn, J., F. J. Schlosser, B. E. Muhs, H. J. Verhagen, F. L. Moll and J. A. van Herwaarden (2009). "Oversizing of aortic stent grafts for abdominal aneurysm repair: a systematic review of the benefits and risks." Eur J Vasc Endovasc Surg **38**(1): 42-53.

Vascutek Inc. Anaconda - Instructions for use.

Veith, F. J., R. A. Baum, T. Ohki, M. Amor, M. Adiseshiah, J. D. Blankensteijn, J. Buth, T. A. Chuter, R. M. Fairman, G. Gilling-Smith, P. L. Harris, K. J. Hodgson, B. R. Hopkinson, K. Ivancev, B. T. Katzen, M. Lawrence-Brown, G. H. Meier, M.

Malina, M. S. Makaroun, J. C. Parodi, G. M. Richter, G. D. Rubin, W. J. Stelter, G. H. White, R. A. White, W. Wisselink and C. K. Zarins (2002). "Nature and significance of endoleaks and endotension: summary of opinions expressed at an international conference." J Vasc Surg **35**(5): 1029-1035.

W L Gore Inc. "Gore Excluder - Instructions for use."

Walker, D. I., K. Bloor, G. Williams and I. Gillie (1972). "Inflammatory aneurysms of the abdominal aorta." British Journal of Surgery **59**(8): 609-614.

Walker, T. G., S. P. Kalva, K. Yeddula, S. Wicky, S. Kundu, P. Drescher, B. J. d'Othee, S. C. Rose and J. F. Cardella (2010). "Clinical practice guidelines for endovascular abdominal aortic aneurysm repair: written by the Standards of Practice Committee for the Society of Interventional Radiology and endorsed by the Cardiovascular and Interventional Radiological Society of Europe and the Canadian Interventional Radiology Association." J Vasc Interv Radiol **21**(11): 1632-1655.

Wolf, Y. G., B. L. Johnson, B. B. Hill, G. D. Rubin, T. J. Fogarty and C. K. Zarins (2000). "Duplex ultrasound scanning versus computed tomographic angiography for postoperative evaluation of endovascular abdominal aortic aneurysm repair." J Vasc Surg **32**(6): 1142-1148.

Xu, C., C. K. Zarins and S. Glagov (2001). "Aneurysmal and occlusive atherosclerosis of the human abdominal aorta." J Vasc Surg **33**(1): 91-96.

Zannetti, S., P. De Rango, B. Parente, G. Parlani, F. Verzini, A. Maselli, L. Nardelli and P. Cao (2000). "Role of duplex scan in endoleak detection after endoluminal abdominal aortic aneurysm repair." Eur J Vasc Endovasc Surg **19**(5): 531-535.

APPENDICES

Appendix 1: Protocol for Ultrasonographers

Surveillance Scan of Endovascular Abdominal Aortic Aneurysm Repair Stents

---

Important Note:

-The previous duplex reports and CT scans should not be referred to for any patient

-All scans should be videotaped with ONLY the patient number displayed on the screen. Do not enter the patient's name onto the new patient screen at the beginning of the scan

B-Mode:

-Using B-mode, image the aorta in longitudinal and transverse planes to determine the proximal and distal limits of the graft.

-Using B-mode, image the aorta in several different planes (transverse, longitudinal), and take several diameter measurements of the aortic sac during peak systole. Note and report the *maximum* aortic sac diameter seen at peak systole.

Colour and Pulsed-Wave (PW) Doppler:

-Using colour Doppler try to image the renal arteries and make a note of how many renal arteries are visualised, and on which side.

-Using colour Doppler set at PRFs appropriate to eliminate aliasing or confirm occlusion where necessary, image the stent, the common iliac arteries and the external iliac arteries down to the level of the inguinal ligament.

-Note any occlusion, significant stenosis or kinking of the stent and iliac arteries.

-Using colour Doppler set at a PRF of approx. 13cm/sec and colour gain set just below the level where background noise appears as colour on the screen, image the entire length of the stent in longitudinal and transverse planes.

-Pay particular attention to the posterior aspect of the sac for lumbar artery origins, and pay particular attention to the anterior aspect of the distal sac for the IMA.

-If any colour is displayed outside the stent, within the aneurysm sac, use PW Doppler to determine if this colour represents artefactual noise, or if it is pulsatile.

-Take thermal images of any suspected endoleak in colour and with its PW spectrum.

-Try to determine source of endoleak (proximal or distal end of graft, IMA or lumbar branch, defect in graft).

-Once the source of endoleak has been identified the endoleak can be classified and reported as Type I (failure of the graft to attach properly at either end, resulting in flow back into the sac from the proximal or distal end of the graft), Type II (retrograde flow into the sac from an aortic branch, i.e. lumbar or IMA) or Type III (defect in graft, i.e. a tear in the graft material).

Adequacy and Quality of Scan:

-Determine and note whether or not the scan was adequate: an adequate scan will yield views of the entire aneurysm sac and colour images of flow within the stent. If either of these are not seen, the scan is inadequate.

- Note the quality of the scan:

1- All views poor

2- Most views poor

3- Half views clear

4- Most views clear

5- All views adequate.

- Complete the Post-EVAR surveillance Duplex report worksheet

Appendix 2: Duplex report worksheet

Barts and The London NHS
NHS Trust

Post EVAR Surveillance Duplex

Patient Name: Date:

Hospital Number:

DOB:

Adequacy of scan: Adequate

(Adequate scan: Entire sac and flow within graft visualised)

Reason for inadequate scan:

Maximum sac diameter (cm):

(Peak systolic, in any direction, in any plane)

Renal arteries visualised: Both

Endoleak seen: No

Description of Endoleak:

(Include Type and Origin)

Graft Patency: Patent

Stenosis/Kinking:

Quality of scan (1-5): 5

(1 – All views poor, 2 – Most views poor, 3 – Half views clear,

4 – Most views clear, 5 – All views adequate)

Appendix 3: Phantom setup

EVAR test object protocol (Tester/Controller)

Set up

ATL HDI 5000 – Power up scanner. Press “scan head” and select correct probe (C5-2) and protocol “Abdominal – EVAR”.

SMALL VESSEL – Fill the small vessel drop bag with blood mimicking fluid (ATS Model 707). Ensure that there are no air bubbles in the line by releasing it from the infusion pump and undoing pipe clamp. Also ensure that there are no kinks in the line. Fluid should flow into the blood mimic beaker. Once flow is seen tighten pipe clamp. Re-attach the line into the infusion pump and close. Turn on the infusion pump. Set the rate to 300 ml/hr. In order to start the pump, press “run/hold” 5 times. Should alarm sound, this could be because of air in the tube or the drip monitor is not in position.

LARGE VESSEL – Turn on the aorta pump. Set the rate to 45 rpm. Press start. Ensure that there are no air bubbles or visible particulates in the vessel. In order to rid the system of these anomalies, release the pipe join in reservoir an run peristaltic pump at 100 rpm with wire gauze held over reservoir outlet/pump inlet pipe. Once blood mimic has been cleared, re-attach the pipe join whilst ensuring not to introduce further air into the system.

Plane 2:

Set up in following order: position, small flow (ml/hr)

1. 1,300; 2. 5,300; 3. 2,500; 4. 4,500; 5. 3,700; 6. 1,700; 7. 4,700; 8. 4,900; 9. 5,900; 10. 2,900

Plane 1:

Set up in following order: position, small flow (ml/hr)

1. 5,500; 2. 5,300; 3. 4,300; 4. 4,700; 5. 1,300; 6. 1,700; 7. 2,300; 8. 2,500; 9. 3,300; 10. 3,500

Plane 3:

Set up in following order: position, small flow (ml/hr)

1. 5,500; 2. 5,300; 3. 4,300; 4. 4,700; 5. 1,300; 6. 1,500; 7. 2,300; 8. 2,500; 9. 3,300; 10. 4,300

Appendix 4: EVAR test (Operator protocol)

EVAR test – observer protocol

Position oneself comfortably in seat and ensure that the controls are handy. Select the curvilinear probe (C5-2) and rotate the phantom so that scan plane 2 is on top. Fill well with distilled water. Place probe at scan position 3 with probe perpendicular to phantom. Set 2D gain so that tissue background corresponds to middle of greyscale bar. When image is maximised for greyscale, the HD zoom should be used to focus on the area surrounding the stent. It may be necessary to revert to full screen at times in order to check the angling of the probe.

Once the test begins, the colour flow should be switched on and positioned over the aorta stent vessel with edges of box approx. 2 cm away from it in all directions. The colour should then be optimised so that the small flow can be visualised using the two controls: colour gain and colour PRF. Start each test with the PRF set high and the colour gain set low. Increase the gain until the point where the colour in that large vessel is not leaking outside its perimeter. Adjust/reduce PRF until small flow can (or cannot) be seen.

One will be asked to assess how well the small vessel is visualised in relation to the big vessel. This should be scored: 0 = no visualisation, 1 = possible visualisation, 2 = probable visualisation, 3 = definite visualisation. One should also note down the gain and PRF settings, which can be altered for each position.

Plane 2:

This test is performed with the probe at right angles to the acoustic window. Use probe guide at pinned positions in order to set the angle and position.

“PERFORM TESTS”

Empty the well using the large syringe. Wipe excess water with paper towels. Rotate the phantom to scan plane 1. Fill well with distilled water.

Plane 1:

This test is performed with the probe at 70° angle to the acoustic window. Use angle guide at pinned rail positions to set the transducer angle to 70°.

“PERFORM TESTS”

Rotate the phantom to scan plane 3. Use angle guide at pinned rail positions to set the transducer angle to 70° and set transverse position.

Plane 3:

This test is performed with the probe at 70° angle to the acoustic window. Use angled edge of probe guide at pinned positions in order to set the angle and position.

“PERFORM TESTS”

Empty the well using the large syringe. Wipe excess water with paper towels.